Novel Optical Phenomena Induced by External Control Lasers

A THESIS

submitted for the Award of Ph.D degree of

Mohan Lal Sukhadia University

in the

Faculty of Science

BY

Anil K. Patnaik

Under the Supervision of

Professor G. S. Agarwal
Director, Physical Research Laboratory

DEPARTMENT OF LASER PHYSICS AND QUANTUM OPTICS
PHYSICAL RESEARCH LABORATORY, AHMEDABAD.

MOHANLAL SUKHADIA UNIVERSITY, UDAIPUR

Year of submission: 2001

CERTIFIED that the work incorporated in the thesis

Novel Optical Phenomena Induced by External Control Lasers

submitted by Shri. **Anil K. Patnaik** was carried out by the candidate under my guidance at the Physical Research Laboratory, Ahmedabad. The work presented in this thesis is original and has not formed basis for the award of any degree or diploma by any university or institution.

Professor G. S. Agarwal
(Supervisor)

to

Maa, Baba and Bou

Contents

Acknowledgement

I would like to express my sincere gratitude to Professor G. S. Agarwal for his excellent guidance and valuable suggestions in last five years. It was a great opportunity to learn from his deep insight in the subject, excitement in new findings, working out everything from first principle and over all his organized and sharp working style. I am greatly benefited from the discussions with him and his encouraging and inspiring words, for which I will always be indebted to him. I also thank Mrs. Agarwal for being cordial and cooperative, at times, even in odd hours.

I would like to thank Prof. K. Hakuta (Tokyo, Japan) for his encouragements in the last part of my thesis.

I take this opportunity to thank all my teachers, right from my early school days who laid the foundation in me to step into this venture. In particular I thank Drs. and Profs. P. Khare, K. Malla, K. C. Mohapatra, N. C. Mishra, K. Moharana, L. P. Singh and R. Srianand for their inspirations to persue my present interest.

I thank Drs. and Profs. J. Banerji, B. P. Das, D. P. Dewangan, S. Dutta Gupta, A. Laxminarayan, N. Nayak, J. C. Parikh, V. B. Sheorey for many interesting discussions. I sincerely thank the academic committees and all PRL faculty members who helped me during these five years period. I also thank Anu, R. Arun, S. Arun, Chandan, Harsha, Prasant, RP, Siva, Tarak for the useful discussions and many helps. I specially thank Shubhrangshu for the careful proof reading of this manuscript.

I also thank all staff members of computer center, library, dispensary and administration for rendering their help and cooperation at all stages; to name a few: Babubhai, Dholakia, Ghiya, Leela, Nishtha, Puravi, Ranganathan, Rohini, R. Shukla and Sudheen. I specially thank Baliyan, Ravi, Hiranmay, Mohanty, Ramesh, Varun, J. Trivedi and their families for their encouragements and being extremely helpful at the time of need.

I gratefully thank Gautam bhai and TanujaAppa, Sarira bhai and Neena bhauja, and their little heroes Siddhu and Rushil for making me feel at home.

I am grateful to Drs. Ansujoy, Ravindran and Santhanam for their caring and inspiring company, and their constructive criticisms. It was a good fortune to get entertaining and jovial batch-mates Alam+Khairunisha, Alok, ADShukla, Dipu+Amrita, Jitti, Koushik, Mohit, Pankaj, Rajesh, Rajneesh, Sankar, Sridhar, Sudhir, Sunish, Som, and Vinay. I thank them all for the unforgettable moments I had with them. I thank Ansu, Banibrata, Gautam, Jayendra, Kaushar, Rishi, Rathin, Sagar, Sai, Shajesh, Sarika, Satyavir and Sruba for making the life at 7th floor lively through many activities and discussions on and off the fields. I thank the whole student family of PRL for the wonderful hostel quadrangle time, as well as in PRL both academically

and non-academically viz. the Maniac Club, Volley Ball etc. Just to name a few of them: Alok, Aninda, Anirban, Brajesh, Ghosh, Jyoti, Kunu, Lokesh, Muthu, Nanda, Niraj, Pradeep, Prashant, Prerna, Ratan, Ravindra, Sandeep, Sudeshna, Sanjay, Sanjeev, Tarun. Apart from them I would also like to extend my thanks to the UN school students and many short term visitors who contributed to the excitements of the PRL life. Especially I thank Dipali, Geetu, Giri, JyotiPrakash, Kishor, Mayank, Naresh and Upma for their care and inspirations. I also take this opportunity to thank my excellent M.Sc. batch mates, seniors and some of my old friends Nayan, Palit, Pankaj, Pranab, Sunil, Suraj and their families, for being so nice to make my past so lovely and memorable.

Lastly I thank my near and dear ones for making me what and where I am. I am thankful to my Maa, Baba, Bou, NituAppa, Sanu, Itu and Tutu bhai, our cute hero Tinku and my family members - for their constant and unconditional love, support and numerous sacrifices.

Anil Kumar Patnaik

Thesis in a Nutshell

In Chapter 1, the introductions to the basics of the light-matter interaction and the basics of the subjects of interest in this thesis is presented. In Sec. 1.1, the propagation of classical electro-magnetic wave, quantum statistical treatment of atomic dynamics and semi-classical treatment of the atom-electromagnetic wave interaction are discussed. The key theme of the thesis - *atomic coherence* is introduced in Sec. 1.2, with examples to simplest atomic systems. Many different applications of the coherence are discussed.

In Chapter 2, response of an anisotropic medium to a linearly polarized laser field is discussed. Induced anisotropy in an initially isotropic atomic medium by magnetic field or laser field, giving rise to rotation of plane polarization of a weak probe field, is also discussed.

In Chapter 3, laser field induced birefringence in an initially isotropic medium and its control in a four level cascade system (a model system of ^{40}Ca) is demonstrated using atomic coherence effects. It is also shown that the control laser can be used to obtain large enhancement of magneto-optical rotation (MOR - the polarization rotation induced by a magnetic field) by suitably choosing the control field parameters. Further it is shown that the control field can also produce *new frequency regions* which show very significant magneto-optical rotation.

In Chapter 4, control of MOR in an inhomogeneously broadened medium is analyzed. It shown how control laser can modify the susceptibilities and hence result significantly large MOR in frequency regions, where MOR otherwise is small. Analytical conditions are derived to select the probe frequency regions where one can obtain large MOR. The claims are substantiated by presenting many numerical results for many different parameters at different conditions.

In Chapter 5, coherences in spontaneous emission - a coherence produced by an incoherent (vacuum) field, known as vacuum induced coherence (VIC), is introduced. A master equation formalism for the treatment of spontaneous emission is developed. The origin of VIC and various consequences are discussed. The conditions for VIC to

occur are also discussed with examples.

In Chapter 6, VIC in two radiatively coupled multilevel systems in free space is examined. It is shown that this radiative coupling between the dipoles can produce new interference effects, which are especially important when the distance between two dipoles is less than a wavelength. This possibility is demonstrated by considering two identical V-systems, where the dipole matrix elements are chosen such that they do not meet the condition for VIC to occur. The choice such dipole matrix elements enables to isolate the effects of the VIC in the radiative coupling between multilevel atoms with nearly degenerate transitions. Detailed numerical results are presented to bring out the role of VIC in multi-atom multilevel systems.

In Chapter 7, the possibility of bypassing the stringent requirement, for VIC to occur, is examined. It is demonstrated that preselection of polarization can lead to *new* interference effects in spontaneous emission, which otherwise do not occur unless the transition dipole matrix elements of the atom satisfy the stringent condition. It is shown how the preselection of polarization can be achieved in a *cavity*. This is demonstrated in the context of a four level atomic system in a bimodal cavity in the limit of a bad cavity. As a result of the new coherence, quantum beat is observed in the atomic populations. A clear physical picture is presented for these beat structures.

In Chapter 8, restoration of VIC is examined using a laser field. It is shown that the laser field mixes the atomic energy levels, and thus makes the transition dipole matrix elements dependent on the strength and frequency of the laser field. The modified transition dipole matrix elements are shown to meet the condition for VIC occur in the system. The possibility of laser field induced quantum beats in two-photon correlations in cascade emission is demonstrated. It is also clearly shown that VIC is crucial for the production of quantum beats.

Chapter 1

Introduction

The field of optics is one of the oldest subjects in physical sciences which has consistently contributed to the excitements of physicists working in many different fields. The turn of the twentieth century brought a revolution in this field when Max Plank's postulated to quantize the energy of harmonic oscillator [1], to account for the spectral distribution of electromagnetic energy from a thermal source. It is followed by intuitive phenomenological predictions of Einstein on the rate of absorption and emission of light by an atom [2]. The absorption and emission probabilities of light by the atoms were thought to be the properties of the atomic system, that can not be altered. A new era in the field of interaction of radiation with matter emerged when the coherent sources became available in 1960. The use of coherent radiation sources, its ability to selectively excite atoms, and to prepare atoms in coherent superposition of their energy eigenstates, have found tremendous applications in the field of light-matter interaction and has largely contributed to fundamental understanding of various physical processes and their interactions. In last few decades, pioneering developments have been made, both theoretically and experimentally, to modify and control the optical properties (e.g. dispersion, absorption, refractive index, etc.) of the atoms and the spectral properties of the emitted radiation field. A myriad of new fascinating phenomena have been observed; to name a few - electromagnetically induced transparency (EIT), coherent population trapping (CPT), lasing without inversion (LWI), laser cooling and trapping of neutral atoms, Bose-Einstein condensation, ultra-slow group velocity of light and more recently superluminal light propagation. Of course this list is by no means exhaustive. The key to all these exciting developments is the *atomic coherence*. This thesis addresses atomic coherence effect in two parts and in two different contexts,

namely: (i) laser field induced anisotropy in an isotropic medium, giving rise to coherent control of magneto-optical rotation; (ii) creation of new coherences in spontaneous emission and studying its effects.

1.1 Interaction of Radiation with Matter

From the Newtonian particle description of reflection of light, to present day developments in quantum optics, the understanding of radiation matter interaction has been revolutionized. In the studies of interaction of microscopic (atomic or sub-atomic) entities with the radiation field, the microscopic particle needs to be treated quantum mechanically. But the field could be either classical or fully quantum mechanical, depending on the nature of the problem one is interested in. Many features of light and light-matter interaction could be correctly derived from a classical theory of electromagnetic (EM) field. The Plank's quantization hypothesis is then included in the classical theory as an additional assumption in expressing the energy of the EM field.

In this section we present general methods to the basic interaction processes between EM field and atoms in different formalisms. Without invoking any explicit quantum notion, but only with the assumption that atomic energy levels are discrete, Einstein gave a simple phenomenological rate equations to describe the absorption and emission of light by atoms [2]. He introduced the process of *induced emission* to make his theory consistent with Plank's law. And later, this theory became the basis for the lasers. Subsequently, Einstein's predictions on the atomic absorption and emission probabilities of atom were rigorously proved by complete quantum mechanical treatment [3].

In what follows, we will develop the mathematical framework to bring out the complete description of the atom-laser field interaction. In the following sub-section propagation of a classical field inside an atomic gas medium considered.

1.1.1 Propagation Dynamics of Classical EM Field

We consider propagation of electromagnetic field inside a medium containing neutral gas of atoms, which are non-conducting and non-magnetic. The propagation of the field inside

such a medium is governed by the Maxwell equations [4]

$$\vec{\nabla} \cdot \vec{D} = 0, \tag{1.1a}$$

$$\vec{\nabla} \cdot \vec{B} = 0, \tag{1.1b}$$

$$\vec{\nabla} \times \vec{E} + \frac{1}{c}\frac{\partial \vec{B}}{\partial t} = 0, \tag{1.1c}$$

$$\vec{\nabla} \times \vec{H} - \frac{1}{c}\frac{\partial \vec{D}}{\partial t} = 0. \tag{1.1d}$$

Here $\vec{E}$ and $\vec{B}$ are the macroscopic electric and magnetic field vectors, c is the speed of light in free space. The electric displacement vector $\vec{D}$ and the magnetic field $\vec{H}$ are the derived fields given by

$$\vec{D} = \vec{E} + 4\pi\vec{\mathcal{P}}, \;\; \vec{H} = \vec{B} - 4\pi\vec{M}. \tag{1.2}$$

Here $\vec{\mathcal{P}}$ and $\vec{M}$ represent the macroscopic electric polarization (electric dipole moment per unit volume) and magnetic polarization vectors (magnetic dipole moment per unit volume) which are obtained by spatially averaging over their microscopic counter parts. We note that the contributions from higher order moments (such as electric quadrapole moments), which are negligibly small compared to the dipole contributions, have been neglected in (1.2). Further in this thesis, the systems under consideration are non-magnetic medium, implying $\vec{M} = 0$; hence $\vec{H} = \vec{B}$. Using these conditions in Eqs. (1.1) we get

$$\vec{\nabla} \times \vec{\nabla} \times \vec{E} + \frac{1}{c^2}\frac{\partial^2}{\partial t^2}(\vec{E} + 4\pi\vec{\mathcal{P}}) = 0. \tag{1.3}$$

Further in an isotropic medium $\vec{D} = \varepsilon\vec{E}$, where ε is the permitivity of the medium. Thus from Eq. (1.1a), we get $\vec{\nabla} \cdot \vec{E} = 0$. Using this condition in the vector triple product of Eq. (1.3), one gets

$$\nabla^2\vec{E} - \frac{1}{c^2}\frac{\partial^2\vec{E}}{\partial t^2} = \frac{4\pi}{c^2}\frac{\partial^2\vec{\mathcal{P}}}{\partial t^2}; \tag{1.4}$$

The equation (1.4) is a second order inhomogeneous equation which, in general, is difficult to solve. However, for the class of problems of our interest, one can obtain analytical solutions.

For example, let us consider a plane wave propagating along z-direction in an atomic gas medium

$$\vec{E}(z,t) \equiv \hat{\epsilon}\mathcal{E}(z,t)e^{ikz - i\omega t} + c.c., \tag{1.5}$$

which induces a linear polarization $\vec{\mathcal{P}}$ in the medium

$$\vec{\mathcal{P}}(z,t) \equiv \hat{\epsilon}\mathcal{P}_0(z,t)e^{ikz-i\omega t} + c.c.. \tag{1.6}$$

Here $\mathcal{E}(z)$ is the amplitude of the field with a propagation vector $\vec{k}$ ($k = |\vec{k}|$), central frequency ω and the direction of the electric field is given by $\hat{\epsilon}$. Note that for a continous wave laser, the time dependence of $\mathcal{E}$ can be neglected.

Under the approximation that the bound electrons in an atom experience several orders of magnitude larger electrostatic field ($\sim 10^7$ statvolt/cm) compared to the field produced by the external laser field (~ 0.3 statvolt/cm for a continuous laser with intensity as large as $10\mathrm{W/cm}^2$), the induced polarization can be expanded in a Taylor series in powers of the laser field $\vec{E}$. The α^{th} component of the polarization is

$$\mathcal{P}_\alpha(z,t) \equiv \mathcal{P}_\alpha\Big|_{\mathcal{E}=0} + \sum_\beta \left(\frac{\partial \mathcal{P}_\alpha}{\partial E_\beta}\right)\Big|_{\mathcal{E}=0} E_\beta + \frac{1}{2!}\sum_{\beta,\gamma}\left(\frac{\partial^2 \mathcal{P}_\alpha}{\partial E_\beta \partial E_\gamma}\right)\Big|_{\mathcal{E}=0} E_\beta E_\gamma + \cdots . \tag{1.7}$$

The first term in (1.7) corresponds to the dipole moment per unit volume in the absence of external field, which is identically zero for our system under consideration. Thus the only non-zero contributions to the polarization come from the induced dipole moments by the external laser field. The term in the parenthesis in the second term of Eq. (1.7) represents the linear susceptibility $\chi^{(1)}_{\alpha\beta}$ of the medium to the applied electric field. Similarly, higher order susceptibilities are obtained by the subsequent terms in (1.7). However, the investigations of interest in this thesis is to determine the response of the medium to a weak (*probe*) field. Hence we will deal only with the linear susceptibility, and the corresponding polarization. Note that any physical system requires a finite time to respond to the external field. Thus the polarization observed at time t has contributions due to response of the system to the electric field at all previous times before t. Thus we have the general relation

$$\mathcal{P}_\alpha(z,t) \equiv \sum_\beta \int_{-\infty}^{t} d\tau \chi_{\alpha\beta}(t-\tau)E_\beta(z,\tau). \tag{1.8}$$

We substitute the electric field $\vec{E}$ from (1.5) in the above equation, neglecting the explicit time dependence of $\mathcal{E}$ (which is valid for a continous wave laser), and changing the variable of integration to $t' = t - \tau$ in the above equation, we get

$$\mathcal{P}_\alpha(z,t) \equiv \sum_\beta \chi_{\alpha\beta}(\omega)\mathcal{E}_\beta(z)e^{ikz-i\omega t} + c.c.; \tag{1.9}$$

where

$$\chi_{\alpha\beta}(\omega) \equiv \int_0^\infty dt' \chi_{\alpha\beta}(t') e^{i\omega t'}. \tag{1.10}$$

Here ω is the frequency of the laser field. Note that $\vec{\mathcal{P}}$ can be reduced to the form (1.9) only if field is monochromatic and and has the form in Eq. (1.5). The superscript in χ has been dropped for brevity. Here it may be noted that $\chi_{\alpha\beta}$ is a tensor of rank two. For an isotropic medium $\chi_{\alpha\beta}$ is diagonal, i.e., $\chi_{\alpha\beta} \equiv \delta_{\alpha\beta}\chi$. Thus (1.9) can be written as

$$\vec{\mathcal{P}}(z,t) = \hat{\epsilon}\chi(\omega)\mathcal{E}(z)e^{ikz-i\omega t} + c.c. \tag{1.11}$$

The susceptibility, in principle could be time dependent. But our concern will be the steady state situation where χ is independent of time. If the medium is anisotropic, the response of the medium will be different for different components of the electric field, i.e., $\chi_{\alpha\alpha} \neq \chi_{\beta\beta}$. This asymmetry gives rise to rotation of plane of polarization of the incident probe field (see Chapter 2). In Chapters 3 and 4 we will discuss in detail such polarization rotations and their control by a strong (*control*) field.

Coming back to Eq. (1.4), the propagation equation for the field in (1.5) and corresponding polarization (1.6) becomes

$$\frac{\partial^2 \vec{E}}{\partial z^2} - \frac{1}{c^2}\frac{\partial^2 \vec{E}}{\partial t^2} = \frac{4\pi}{c^2}\frac{\partial^2 \vec{\mathcal{P}}}{\partial t^2}. \tag{1.12}$$

On using Eqs. (1.5) and (1.6) in Eq. (1.12), we get

$$\frac{\partial \mathcal{E}}{\partial z} + \frac{1}{c}\frac{\partial \mathcal{E}}{\partial t} = 2\pi i k \mathcal{P}_0. \tag{1.13}$$

In deriving (1.13), we have made the *slowly varying envelope approximation (SVEA)* [5], i.e., $\mathcal{E}$ and $\mathcal{P}$ are slowly varying functions of position compared to scale of optical wavelength, and also slowly varying functions of time compared to the optical period of the radiation field, i.e.

$$\begin{aligned} \left| k\frac{\partial \mathcal{E}}{\partial z} \right| &\gg \left| \frac{\partial^2 \mathcal{E}}{\partial z^2} \right|, \quad \left| \omega^2 \frac{\partial \mathcal{E}}{\partial t} \right| \gg \left| \frac{\partial^2 \mathcal{E}}{\partial t^2} \right|, \\ \text{and } |\omega^2 \mathcal{P}_0| &\gg \left| \omega \frac{\partial \mathcal{P}_0}{\partial t} \right| \gg \left| \frac{\partial^2 \mathcal{P}_0}{\partial t^2} \right|. \end{aligned} \tag{1.14}$$

In the steady state situation, $\mathcal{P}_0 = \chi(\omega)\mathcal{E}(z)$ [see Eq. (1.11)], Eq. (1.13) reduces to

$$\frac{\partial \mathcal{E}}{\partial z} = 2\pi i k \chi(\omega)\mathcal{E}(z), \tag{1.15}$$

and the solution gives the field at the output

$$\vec{E}_{out}(z=l) = \hat{\epsilon}\mathcal{E}(0)e^{2\pi ikl\chi}e^{ikl-i\omega t} + c.c. \tag{1.16}$$

The measured quantity is $I_{out} \equiv \left|\vec{E}_{out}\right|^2$. Clearly, this macroscopic measurement contains the information of the effects due to the medium via χ. For $\chi \ll 1$, which is the case in the optical frequency domain, the approximate value of linear refractive index $\eta(\omega)$ and absorption coefficient $\alpha(\omega)$ are given by

$$\eta(\omega) \equiv 1 + 2\pi \mathrm{Re}[\chi(\omega)], \tag{1.17a}$$

$$\alpha(\omega) \equiv 4\pi k \mathrm{Im}[\chi(\omega)]. \tag{1.17b}$$

The output intensity is thus given by

$$I_{out}(z=l) \equiv I_{out}(0)e^{-\alpha l}. \tag{1.18}$$

It may be noted that χ would also contain information of any other strong *control* field present in the medium. Evaluation of χ in presence of the control fields and their effects will be discussed in Chapters 3 and 4.

1.1.2 Quantum Statistical Treatment of Atomic Dynamics

A quantum mechanical state of a system is represented by a state vector $|\psi\rangle$ (in Dirac notation [6]). It obeys the Schrödinger equation

$$i\hbar\frac{\partial|\psi\rangle}{\partial t} = \mathcal{H}|\psi\rangle, \tag{1.19}$$

where $\mathcal{H}$ represents the Hamiltonian of the system that governs the time evolution of the system. This equation is useful to derive complete information regarding the system if the initial state of the system is exactly known. However, we often encounter systems where the initial state of the system is not known in a precise manner. For example, an ensemble of atoms at a given temperature in an atomic vapor cell - in which the exact momentum state of each individual atom is impossible to know. But the probability distribution of momentum states inside the cell is known to follow the Maxwell-Boltzmann distribution. In such circumstances, a statistical description of the system is given by density matrix formalism. Further, this formulation can be useful when systems involve many decay and broadening mechanisms.

Any arbitrary state $|\psi\rangle$ of a system (say an atom) can be expressed in terms of a complete set of orthonormal basis states $|i\rangle$, i.e., $|\psi\rangle = \sum_i c_i|i\rangle$; where $|c_i|^2$ represents the probability that the the state $|i\rangle$ and $\sum_i |c_i|^2 = 1$. Often it is useful to take the eigenstates of the free-atomic Hamiltonian as these basis states. Then the density operator ρ for the state $|\psi\rangle$ is defined as

$$\rho = |\psi\rangle\langle\psi| = \sum_{i,j} c_i c_j^* |i\rangle\langle j|. \tag{1.20}$$

It can be represented as a matrix whose elements are

$$\rho_{ij} = \langle i|\rho|j\rangle = c_i c_j^*. \tag{1.21}$$

Therefore

$$\mathrm{Tr}\ \rho = \sum_i c_i c_i^* = 1, \tag{1.22}$$

which is the statement of conservation of probability. Here Tr represents the trace operation defined for an arbitrary matrix M as $\mathrm{Tr}\ M = \sum_n M_{nn}$. Further, the expectation value of any operator A in terms of the density operator can be obtained

$$\langle A\rangle = \langle\psi|A|\psi\rangle = \sum_{i,j} c_i^* c_j A_{ij} = \sum_j \left(\sum_i \rho_{ji} A_{ij}\right) = \sum_j (\rho A)_{jj} \equiv \mathrm{Tr}(\rho A). \tag{1.23}$$

Next we consider an ensemble of such identical systems, where different states of the system are represented by $|\psi_n\rangle$ (say). In many situations the state of the system is not known; however, the probability that the system is in a given state $|\psi_n\rangle$ is known. The density operator for the ensemble is given by

$$\rho = \sum_n p_n |\psi_n\rangle\langle\psi_n|; \quad \sum_n p_n = 1. \tag{1.24}$$

From Schrödinger equation (1.19), it can be shown that

$$\frac{\partial\rho}{\partial t} = -\frac{i}{\hbar}[\mathcal{H}, \rho], \tag{1.25}$$

which is known as Liouville equation of motion for the density matrix. Here the density matrix elements in terms of the $\{|i\rangle\}$ basis are given by

$$\rho_{ij} = \sum_n p_n c_i^n c_j^{n^*}, \tag{1.26}$$

and carrying out similar algebra as in (1.23), one gets the ensemble average of the observable corresponding to the operator

$$\langle A\rangle = \sum_n \langle\psi_n|A|\psi_n\rangle = \mathrm{Tr}(\rho A). \tag{1.27}$$

Thus it is clear from the above equation that evolution of any observable can be determined from the evolution of the density matrix.

From Eq. (1.26), one may note the following properties of the density operator ρ: (a) ρ is Hermitian, (b) ρ is non-negative definite, i.e., $\mathrm{Tr}(\rho U^\dagger U) \geq 0$ for any unitary operator U, (c) $\mathrm{Tr}(\rho^2) \leq 1$, with equality sign holding for pure states. The density matrix elements (1.26) have the following physical interpretation: The diagonal element ρ_{ii} $(\sum_n p_n |c_i^n|^2)$ represents the ensemble averaged probability for the system to be in energy eigenstate $|i\rangle$ - often referred as *population* in state $|i\rangle$. The off-diagonal terms ρ_{ij} give the ensemble average of the cross terms $c_i^n c_j^{n^*}$ that represent the coherence between states $|i\rangle$ and $|j\rangle$. This is non-zero if the system exists in a coherent superposition of the states $|i\rangle$ and $|j\rangle$. Since these terms are complex, ρ_{ij} can also become zero by cancellation of interference terms in Eq. (1.26), while a non-zero value of ρ_{ij} would mean a coherent addition of the cross terms. In the context of atomic states, these matrix elements ρ_{ij} are referred to *atomic coherences* which is the emphasize of this thesis. Explicit evaluation of ρ in presence of external laser field(s) will be presented with examples in the following section.

Note that the Liouville equation (1.25) is a more general equation compared to the Schrödinger equation. Because in addition to the quantum mechanical evolution, it also derives the statistical information of the system. Further, evolution of systems involving many broadening and decay mechanisms (e.g. collisional broadening, spontaneous emission etc.) can be conveniently determined using this density matrix formalism. The equation (1.25) in such cases is modified to

$$\frac{\partial\rho}{\partial t} = -\frac{i}{\hbar}[\mathcal{H},\rho] + \mathcal{L}\rho; \tag{1.28}$$

where $\mathcal{L}$ is the matrix containing the decay terms. The explicit form of $\mathcal{L}$ can be obtained by rigorous calculation using the master equation formulation [7], where the system interacts with a reservoir (could be a background EM field) to decay. In Chapter 5 (Sec. 5.2), we derive a master equation for the spontaneous emission, which occurs due to interaction of atom with the vacuum of the EM field.

1.1.3 Semi-classical Analysis of Laser-Atom interaction

In this section we present the general mathematical framework to describe the interaction of laser with atom. In *semi-classical* treatment, the laser field is treated as a classical monochromatic field (given by (1.5)) and the atom is considered to have quantized energy levels.

The Hamiltonian corresponding to an electron of charge e and mass m_e interacting with an external EM field is given by

$$\mathcal{H} = \frac{1}{2m_e}\left[\vec{p}_e - \frac{e}{c}\vec{A}(\vec{r},t)\right]^2 + \frac{e}{c}\phi(\vec{r},t) + V(r), \tag{1.29}$$

where $\vec{p}_e$ represents the momentum operator corresponding to the electron. $V(r)$ is the atomic binding potential. Here $\vec{A}(\vec{r},t)$ ($\phi(\vec{r},t)$) represents the vector (scalar) potential for the external field, where the electric field ($\vec{E}$) and magnetic field ($\vec{B}$) are given in terms of $\vec{A}$ and ϕ as

$$\vec{E} = -\vec{\nabla}\phi - \frac{1}{c}\frac{\partial \vec{A}}{\partial t}, \tag{1.30a}$$

$$\text{and} \quad \vec{B} = \vec{\nabla} \times \vec{A}. \tag{1.30b}$$

In writing above Eq. (1.29), we have already neglected the interaction of magnetic field part of the external laser field with the spin magnetic moment of the electron. Further we consider the electron is bound to a nucleus (assumed to be static) which is located at $\vec{r}_0$, by a central force potential $V(r)$. Thus the entire atom is immersed in a plane EM wave, which can be described by the vector potential $\vec{A}(\vec{r}_0 + \vec{r}, t)$. Here we make *electric dipole approximation* [9] $\vec{k} \cdot \vec{r} \ll 1$ to get

$$\begin{aligned} \vec{A}(\vec{r}_0 + \vec{r}, t) &= \vec{A}(t) \exp\{i\vec{k} \cdot (\vec{r}_0 + \vec{r})\} \\ &\simeq \vec{A}(t) \exp(i\vec{k} \cdot \vec{r}_0) \end{aligned} \tag{1.31}$$

Thus the dipole approximation amounts to neglecting $\vec{k} \cdot \vec{r}$ ($\simeq a_0/\lambda \ll 1$ in optical domain; a_0 is the Bohr radius of the atom and λ is the wavelength of the external field) in the expansion of the exponential compared to unity. Physically this approximation would mean that the wave function of the electron is too localized about the nucleus and thus the spatial variation of the field of the incident plane wave over the position of the electron can be ignored. If $|\psi_e(\vec{r},t)\rangle$ is the electron wave function, under this approximation, it will

satisfy the Schrödinger Eq. (1.19)

$$i\hbar\frac{\partial}{\partial t}|\psi_e(\vec{r},t)\rangle = \left\{\frac{1}{2m_e}\left[\vec{p}_e - \frac{e}{c}\vec{A}(\vec{r},t)\right]^2 + \frac{e}{c}\phi(\vec{r},t) + V(r)\right\}|\psi_e(\vec{r},t)\rangle. \tag{1.32}$$

Note that we are working in radiation gauge, i.e.,

$$\phi(\vec{r},t) = 0, \text{ and } \vec{\nabla}\cdot\vec{A} = 0. \tag{1.33}$$

To simplify the above Eq. (1.32) we make a transformation [8] on the electron state vector to define a new state vector $|\varphi(\vec{r},t)\rangle$ such that

$$|\psi_e(\vec{r},t)\rangle = \exp\left[\frac{ie}{c\hbar}\vec{A}(\vec{r}_0,t)\cdot\vec{r}\right]|\varphi(\vec{r},t)\rangle. \tag{1.34}$$

Substituting this in Eq. (1.32) and with a small algebra Eq. (1.32) takes a simple form

$$\begin{aligned} i\hbar\frac{\partial}{\partial t}|\varphi(\vec{r},t)\rangle &= \left(\frac{p_e^2}{2m_e} + V(r) - \vec{d}\cdot\vec{E}\right)|\varphi(\vec{r},t)\rangle \\ &= (\mathcal{H}_0 + \mathcal{H}_I)\,|\varphi(\vec{r},t)\rangle, \end{aligned} \tag{1.35}$$

where $\mathcal{H}_0 = p_e^2/2m_e + V(r)$ is the unperturbed Hamiltonian corresponding to the bound electron, $\mathcal{H}_I = -\vec{d}\cdot\vec{E}$ is the interaction Hamiltonian given in terms of gauge independent field $\vec{E}$ - which we will use in our subsequent studies. Here $\vec{d} = e\vec{r}$ is the induced dipole moment and $\vec{E}$ is the applied laser field given in (1.5). In deriving (1.35), we have used the fact that $\vec{p}_e = -i\hbar\vec{\nabla}$ and in radiation gauge $\vec{E} = -\partial\vec{A}/\partial t$. Note that the atomic variables in Eq. (1.35) (e.g. p_e, $\vec{d}$) are to be replaced by the corresponding quantum mechanical operators to get the semi-classical Hamiltonian for radiation-matter interaction. And the state vector $|\varphi(\vec{r},t)\rangle$ can be used in place of $|\psi(\vec{r},t)\rangle$ to evaluate the expectation values of any (gauge-invariant) operators.

In next section we will present an explicit example using semi-classical analysis. The classical treatment of the laser field is quite reliable in such analysis due to the fact that, lasers have large number of photons per mode. On the other hand, for atom interacting with fields having very small photon mode density would require a complete quantum mechanical treatment - e.g., atom interacting with free space vacuum (see Chapter 5), with the dipole radiation from a neighboring atom (see Chapter 6) or vacuum of cavity field (discussed in Chapter 7).

Electric Dipole Transition Selection Rule:

From the interaction Hamiltonian $\mathcal{H}_I$, one can obtain the dipole transition selection rules [11] for the atomic states that would interact with the external electric field. A transition from an initial state $|\psi_i\rangle$ to a final state $|\psi_f\rangle$ is given by the transition matrix element

$$T_{i\to f} \equiv \langle\psi_f|\mathcal{H}_I|\psi_i\rangle \equiv -\langle\psi_f|\vec{d}\cdot\vec{E}|\psi_i\rangle. \tag{1.36}$$

Further $\vec{d}\cdot\vec{E} \propto \vec{r}\cdot\vec{\epsilon} \equiv r_\alpha$ (say), i.e., polarization of the external electric field decides which component of the transition dipole moment will contribute to $\mathcal{H}_I$. The angular part of $T_{i\to f}$ is

$$\int d\varphi \int d\theta \sin\theta Y_{l_f}^{m_f^*}(\theta,\phi)\; r_\alpha\; Y_{l_i}^{m_i}(\theta,\phi); \tag{1.37}$$

where $l_i,\ m_i$ ($l_f,\ m_f$) are the angular and magnetic quantum number of $|\psi_i\rangle$ ($|\psi_f\rangle$) respectively, $Y_{l_i}^{m_i}(\theta,\phi)$ ($Y_{l_f}^{m_f}(\theta,\phi)$) is the spherical harmonic corresponding to $|\psi_i\rangle$ ($|\psi_f\rangle$). The above integral can be calculated for different α values and will give non-zero value only if,

$$\begin{aligned} l_f - l_i &= \pm 1, \\ \text{and}\ \ m_f - m_i &= 0, \pm 1; \end{aligned} \tag{1.38}$$

i.e., the dipole transitions are allowed only between the states of different parity and satisfy Eq. (1.38). Further if spin-orbit coupling is there in the system, then one has to look for non-zero matrix elements of $\mathcal{H}_I$ in $\{|l,s,j,m_j\rangle\}$ basis instead of $\{|l,m\rangle\}$ basis. Here $\vec{J} = \vec{L} + \vec{S}$ is the total angular momentum, and $j = l+s,\ l+s-1,\cdots|l-s|,\ m_j = -j,\ -j+1,\cdots j$. The transition matrix element (1.36) for this can be shown to give non-zero value only if

$$\begin{aligned} j_f - j_i &= 0, \pm 1\ \ (\text{except for } j_i = j_f = 0), \\ l_f - l_i &= \pm 1, \\ \text{and}\ \ m_f - m_i &= 0, \pm 1. \end{aligned} \tag{1.39}$$

This is known as the *electric dipole transition selection rule*. Eq. (1.39) is the guiding rule to select the suitable atomic states and the polarizations of the external fields for the investigations of our interest; e.g., in $j = 1 \to j = 0$ transitions, the states $|j=1, m=1\rangle$ ($|j=1, m=-1\rangle$) $\leftrightarrow |j=0, m=0\rangle$ can be coupled only by left (right) circularly polarized light.

1.2 Atomic Coherences

In Sec. 1.1.2, we have already introduced atomic coherences. In this section we will describe how coherence can be created in an atom by the external laser field, considering

simple atomic schemes. We will discuss how coherence effects particularly in multi-level systems can be used to manipulate the optical properties.

1.2.1 Induced Coherences in Two level Atoms

Here we implement the general formalism developed in Sec. 1.1 to the simplest quantum mechanical system - a two-state system, to show how coherence evolves. In the process we will introduce the major approximations used repeatedly in this thesis. The energy levels of a real atomic system depend on the couplings between its various electrons and the nucleus. However in resonant optical processes, it is often sufficient to approximate the atom to be effectively a two-level (or a few-level) atom. This is so if the frequency of the laser field is resonant or near-resonant to the atomic transition frequency. This is known as *two-level approximation*.

Let us consider a two-level atom with $|e\rangle$ ($|g\rangle$) as excited (ground) state. It is excited by a laser field $\vec{E}_l = \vec{\epsilon}\mathcal{E}(z)e^{ikz-i\omega t} + c.c.$. The two-level approximation will be valid only if: (a) the laser is on resonance or near resonance with the atomic transition under consideration, i.e., $\omega \simeq \omega_0$ (ω_0 is the atomic frequency), and (b) the width of the external field is small compared to the energy separation between $|e\rangle$ and $|e'\rangle$; where $|e'\rangle$ could be a neighboring state of $|e\rangle$ to which atom can get excited. In the above approximation the unperturbed Hamiltonian $\mathcal{H}_0$ in terms of the atomic states is written as

$$\mathcal{H}_0 = \hbar\omega_0 A_{ee}; \tag{1.40}$$

and the interaction Hamiltonian $\mathcal{H}_I$ is

$$\mathcal{H}_I = -(\vec{d}_{eg}A_{eg} + \vec{d}_{ge}A_{ge}) \cdot \vec{E}_l(\vec{r}, t). \tag{1.41}$$

Here $\hbar\omega_0$ corresponds to the energy separation between $|e\rangle$ and $|g\rangle$, and $A_{ij} \equiv |i\rangle\langle j|$ represents the atomic transition operator for $i \neq j$, and atomic population for $i = j$. In writing (1.40), the ground state energy is scaled to zero energy. For the interaction Hamiltonian (1.41), we have replaced $\vec{d}$ in (1.35) by the corresponding operator

$$\vec{d} = \sum_{i,j} \vec{d}_{ij}A_{ij} \tag{1.42}$$

where $\vec{d}_{ij}$s' are the transition dipole matrix elements. The atomic wave function $|\psi\rangle$ will

satisfy the Schrödinger Eq. (1.19)

$$\frac{\partial|\psi\rangle}{\partial t} = -\frac{i}{\hbar}\mathcal{H}|\psi\rangle, \tag{1.43}$$

where $\mathcal{H} = \mathcal{H}_0 + \mathcal{H}_I$ is the total Hamiltonian of the system. We make a unitary transformation $U = \exp(i\omega_l A_{ee} t)$ on the wave function $|\psi'\rangle = U|\psi\rangle$; i.e., we make a transformation to a frame rotating at the frequency of the laser field ω_l. Substituting $|\psi'\rangle$ in (1.43) one gets

$$\frac{\partial|\psi'\rangle}{\partial t} = -\frac{i}{\hbar}\mathcal{H}_{\text{eff}}|\psi'\rangle, \tag{1.44}$$

where the effective Hamiltonian is

$$\mathcal{H}_{\text{eff}} = \hbar\delta_l A_{ee} - \hbar\left(g_l A_{eg} + g_l' A_{eg} e^{2i\omega_l t} + H.c.\right), \tag{1.45}$$

where $\delta_l = \omega_0 - \omega_l$ is frequency detuning of the laser field from the atomic frequency. The spatial dependent terms in the Hamiltonian can be dropped for the length of the medium much smaller compared to the wavelength of the laser field, e.g., $e^{\vec{k}_l\cdot\vec{r}} \simeq 1$ for an optical laser acting on an atomic beam or a single static atom. However for the laser field interacting with an atom moving at a velocity $\vec{v}$ [1], $(\vec{k}_l\cdot\vec{r})$ has to be replaced by $(\vec{k}_l\cdot\vec{v}t)$. The coupling coefficients in (1.45) are

$$g_l = \frac{\vec{d}\cdot\mathcal{E}_l}{\hbar}e^{i\vec{k}_l\cdot\vec{r}} \quad \text{and} \quad g_l' = \frac{\vec{d}\cdot\mathcal{E}_l^*}{\hbar}e^{-i\vec{k}_l\cdot\vec{r}}. \tag{1.46}$$

It may be noted that the interaction part $\mathcal{H}_{\text{eff}}$ in (1.45) contains two types of terms: the d.c. terms associated with g_l and rapidly oscillatory terms, oscillating at a frequency 2ω, associated with g_l'. For a continuous wave laser working at optical frequencies such that $g_l' \ll 2\omega$, these rapidly oscillatory terms are unimportant compared to the d.c. terms. This approximation is known as *rotating wave approximation (RWA)* [12]. Thus the effective Hamiltonian becomes

$$\mathcal{H}_{\text{eff}} = \hbar\delta_l A_{ee} - \hbar\left(g_l A_{eg} + H.c.\right). \tag{1.47}$$

This approximation breaks down when $g_l' \simeq \omega$, e.g., when the intensity of the incident laser field is very high. The coupling coefficient $2g_l$ is called *Rabi frequency* [13]. Using (1.47) in

[1] this case arises when an atomic cell at non-zero temperature is considered. This gives rise to Doppler broadening, we will consider the broadening effects in Chapter 4.

Eq. (1.25) the density matrix equations that describe the dynamics of the two-level atom are

$$\begin{aligned} \dot{\tilde{\rho}}_{ee} = -\dot{\tilde{\rho}}_{gg} &= i g_l \tilde{\rho}_{ge} - i g_l^* \tilde{\rho}_{eg}, \\ \dot{\tilde{\rho}}_{eg} &= -i\delta_l \tilde{\rho}_{eg} + i g_l (\tilde{\rho}_{gg} - \tilde{\rho}_{ee}), \end{aligned} \tag{1.48}$$

where $\tilde{\rho}$ represents the density matrix in the rotated frame. Note that instead of making the unitary transformation on the wave function, to obtain an effective Hamiltonian (1.47), one can also make RWA on density matrix elements. For example, one can use $\mathcal{H}_I$ (Eq. (1.41)) in Eq. (1.25) and then make a transformation $\rho \to \tilde{\rho}$ such that

$$\tilde{\rho}_{ee} \to \rho_{ee},\ \tilde{\rho}_{eg} \to \rho_{eg} e^{i\omega_l t}. \tag{1.49}$$

This would also give Eqs. (1.48). The over-dots in Eq. (1.48) represent the time derivatives. The solution for the atomic population inversion can be evaluated from Eq. (1.48) with the condition that initially the atom was in ground state

$$\tilde{\rho}_{gg} - \tilde{\rho}_{ee} = \frac{\delta_l^2}{\Omega_l^2} + \frac{4|g_l|^2}{\Omega_l^2} \cos(\Omega_l t); \tag{1.50}$$

where $\Omega_l = \sqrt{\delta_l^2 + 4|g_l|^2}$ is known as the generalized Rabi frequency. In deriving (1.50), we have used $\rho_{gg} = 1 - \rho ee$, which is due to the conservation of total population in the closed two-level system. It can be clearly seen from (1.50) that the atomic inversion will oscillate with a frequency Ω_l. When the control field is on resonance with the atomic transition, the atomic inversion oscillates between -1 and +1 with a frequency $2g_l$. A physical picture of this Rabi oscillation is provided by drawing an equivalence to Bloch vectors corresponding to spin-1/2 magnetic dipoles undergoing precession in a magnetic field [14, 15]. An excellent review of optical Rabi oscillation in two-level atoms is given in [16].

The above sets of Eqs. (1.48) are written when the system is not affected by any broadening mechanism. The natural line width due to spontaneous emission can be introduced phenomenologically in Eq. (1.48) to get

$$\begin{aligned} \dot{\tilde{\rho}_{ee}} = -\dot{\tilde{\rho}_{gg}} &= -2\gamma \tilde{\rho}_{ee} + i g_l \tilde{\rho}_{ge} - i g_l^* \tilde{\rho}_{eg}, \\ \dot{\tilde{\rho}_{eg}} &= -(\gamma + i\delta_l) \tilde{\rho}_{eg} + i g_l (\tilde{\rho}_{gg} - \tilde{\rho}_{ee}), \end{aligned} \tag{1.51}$$

where 2γ represents the spontaneous decay rate of the excited state. The spontaneous decay coefficients can be derived rigorously, which will be discussed in Chapter 5. Apart

from this there could be other broadening mechanisms involved in the system, e.g., collisional broadening, Doppler broadening etc. Due to spontaneous decays in (1.51), the Rabi oscillations will also decay to a constant value. Thus the system can achieve a steady state, i.e., $\dot{\rho} = 0$. Here we emphasize that from Eq. (1.51) the $\tilde{\rho}_{eg}$ value is non-zero. This means that coherence is attained in the medium [as explained in the discussion after (1.27)]. Note that the induced atomic polarization is related to the coherence by

$$\vec{\mathcal{P}} \equiv n\langle\vec{d}\rangle \equiv n\mathrm{Tr}(\vec{d}\rho) \equiv n(\vec{d}_{ge}\rho_{eg} + H.c.); \tag{1.52}$$

where n is the atomic number density. Comparing this equation with (1.11) and using the steady state values of ρ_{eg} one can get the linear susceptibility of the medium for a weak probe field

$$\chi = \frac{n|\vec{d}_{eg}|^2}{\hbar(\delta_l - i\gamma)}. \tag{1.53}$$

Clearly the medium properties are modified by the applied field. In the following, we briefly discuss some interesting manifestation of this coherence in two-level atoms that exist in the literature.

The first prediction on resonance fluorescence from a two-level atom shined by a monochromatic source was made by Mollow [17]. With his semi-classical calculation he showed a triplet structure (at ω_l and $\omega_l \pm \Omega$) in the power spectrum of light scattered by the two-level atom. Later they were named as *Mollow triplet*. This structure was experimentally confirmed by Hartig *et al* and Grove *et al* [18]. Further the coherence thus created by a intense laser can be probed by a weak probe laser, scanning over the probe frequency ω_p. It was first shown by Mollow [19] that the stimulated absorption and emission spectrums of the probe become asymmetric due to the coherence ρ_{eg}. He observed gain of the probe field at certain probe frequencies. An understanding of such behavior was given by Cohen-Tannoudji and Reynaud [20] by developing a dressed state [2] approach to describe the atom+field system. The sidebands observed in the Mollow triplet can be understood as due to the ac Stark splitting resulting in cascade of doublets in the quantum dressed state picture. Jaynes and Cummings gave the exact solution of the two-level atom interacting with a single mode quantized field [21]. Their model showed nonclassical effects

[2] the energy eigenstates of the total Hamiltonian of the atom+laser system are called *dressed states*; e.g., see Eq. (1.58).

like collapse and revival in a lossless medium [22]. Many other non-classical effects were reported; e.g. sub-Poissionian photon statistics was observed by Mandel [23], Kimble *et al* reported photon anti-bunching [24], atomic interaction with squeezed vacuum resulting phase sensitive Mollow triplet [25]. Resonance fluorescence from two-level atom was also observed to show squeezing [26]. A complete theory for quantum statistical treatment of the spontaneous emission in two-level atoms (as well as in multi-level systems) was developed by Agarwal [7, 27]. Many interesting non-linear effects due to the coherences in two-level atom exist in the literature - two-level atom interacting with strong bichromatic field showed new features in the spectrum [28], Rabi sideband generation by four wave parametric interaction in a two-level atom was reported in [29], Agarwal and Harshwardhan [30] have shown existence of population trapping states when a two level atom is driven by a frequency modulated field.

1.2.2 Coherent Control in Multilevel Systems

The idea of coherence introduced in Sec. 1.2.1 when used for multilevel systems interacting with monochromatic fields, the coherence effects are greatly enhanced both in terms of number of possible configurations and also in the number of new effects. In a typical three-level system, a strong field can be used in one transition that will modify the atomic behavior - the corresponding field will be called as *control field*. The changes thus created in the medium can be probed by a weak laser field which is called as a *probe field*. Depending on the level structure and the dipole transitions involved in the interaction, three level atoms can be of three types as shown in the Fig.(1.1). In absence of the decays, all the configurations are equivalent. The state $|i\rangle$ is coupled to $|1\rangle$ and $|2\rangle$ by two laser fields, a control field with frequency ω_c and a probe field with frequency ω_p. The fields are detuned from the respective transitions by Δ and δ. The Rabi frequencies corresponding to the control (probe) field is G (g). We write the effective Hamiltonian in appropriate rotating frame (three-level equivalent of (1.47)) for a Λ system as

$$\mathcal{H}_{\text{eff}} = \hbar(\delta - \Delta)A_{11} + \hbar\delta A_{ii} - \hbar(gA_{i2} + GA_{i1} + H.c.). \tag{1.54}$$

The corresponding density matrix equation (see Eq. (1.25)) is

$$\dot{\rho} = -\frac{i}{\hbar}[\mathcal{H}_{\text{eff}}, \rho] - (\Gamma_i\{A_{ii}, \rho\} + \gamma_i\{A_{ii}, \rho\} - 2\Gamma_i\rho_{ii}A_{11} - 2\gamma_i\rho_{ii}A_{22}) \\ -\Gamma_{12}^{\text{ph}}(A_{11}\rho A_{22} - A_{22}\rho A_{11}); \tag{1.55}$$

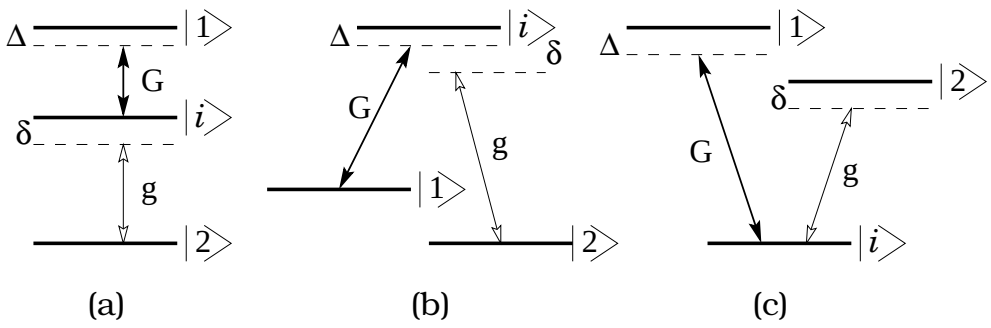

Figure 1.1: Schematic representation of the possible three-level configurations - (a) a ladder system (also known as Ξ system), (b) Λ system, and (c) V system.

where $2\Gamma_i$ and $2\gamma_i$ represent the rates of spontaneous emission from $|i\rangle$ to $|1\rangle$ and $|2\rangle$ respectively, and $\Gamma_{12}^{\rm ph}$ is the rate of dephasing of the ground state coherence ρ_{12} - this could be present due to the collision of the atoms with the wall of the atomic cell. The symbol $\{\ \}$ represents the anti-commutators. The steady state ($\dot{\rho} = 0$) solution of the coherence in the transition coupled by the probe can be calculated to lowest order in probe field g in the $|i\rangle \leftrightarrow |2\rangle$ transition

$$\rho_{i2} = \frac{ig(\Gamma_{12}^{\rm ph} - i(\Delta - \delta))}{|G|^2 + (\gamma_i + \Gamma_i + i\delta)(\Gamma_{12}^{\rm ph} - i(\Delta - \delta))}. \tag{1.56}$$

It may be noted that coherence created at the probe transition ρ_{i2} is a function of intensity ($|G|^2$) and frequency of the control laser. This demonstrates the possibility of coherent manipulation of atomic response to a probe field, what we call here as *coherent control*. A myriad of interesting phenomena has been observed using this concept of coherent manipulation of atomic states in last few decades. It is difficult, and of course out of scope of this thesis, to list all the discoveries. However we present below a brief survey of some of the interesting and important developments.

Coherent Population Trapping (CPT)

Alzetta *et al* [31] discovered that in the interaction of a multimode laser with sodium vapor, involving a Λ system, population gets trapped in certain atomic states. There was a sharp decrease in fluorescence of sodium when the frequency difference of two modes of the laser field matched the separation between the two ground states of Λ system. At the same time, CPT was independently investigated theoretically by Whitley and Stroud [32] and experimentally (in sodium atom) by Grey *et al* [33]. This decrease in fluorescence could be understood by writing the atom-field system in a new basis known as coupled/non-

coupled basis [34]. For a Λ system with a configuration shown in Fig. 1.1 (b), the system could be described by a new basis set $\{|i\rangle, |uc\rangle, |c\rangle\}$. If both the laser fields are in same phase, under Raman resonance condition ($\delta - \Delta = 0$) the state

$$|uc\rangle = \frac{g|1\rangle - G|2\rangle}{\xi} \quad (\xi = \sqrt{|g|^2 + |G|^2}), \tag{1.57}$$

is such that $\mathcal{H}_{\text{eff}}|uc\rangle = 0$, i.e., electrons in the state $|uc\rangle$ are uncoupled from the applied field and hence does not evolve further. Since this state is populated by spontaneous emission from $|i\rangle$, in the steady state the population is completely trapped in the coherent superposition state $|uc\rangle$. The CPT could also be interpreted as due to the destructive interference between two different excitation pathways [35, 33]. CPT has been investigated in different types of systems: e.g. in laser induced molecular excitation and dissociation [36], in atoms with upper state in continuum [37], in dense atomic system [38]. The role of m-degenerate levels on CPT is discussed [39]. Recently CPT with incoherent elliptically polarized light has been reported in [40]. CPT in open systems is discussed by Renzoni *et al* [41]. Harshawardhan and Agarwal [42] showed the possibility of using CPT for optical bistability. CPT also found applications in metrology [43], in laser cooling [44], in enhancement of non-linear optical signal generation [45].

Electromagnetically Induced Transparency (EIT)

It is well known in quantum mechanics that, if several transition amplitudes exist for a transition from a given initial state $|i\rangle$ to a given final state $|f\rangle$, then the transition amplitudes can interfere constructively or destructively. Such a phenomena is known as *quantum interference*; e.g. Fano interference [46]. However similar interference effect can be deliberately introduced in atomic systems by applying an external control laser field. The external field creates new absorption pathways for the electron to reach the same final state. For suitable field parameters, a destructive interference of these transition amplitudes renders transparency to a weak probe laser in the initially opaque medium. This phenomenon is known as Electromagnetically Induced Transparency (EIT).

EIT was first demonstrated by Harris and coworkers [47] in a Λ scheme of Sr using control field on the $4d5p^1D_2 \leftrightarrow 4d5d^1D_2$ transition at 570.3nm. A probe field acting on $4d5d^1D_2 \leftrightarrow 5s5p^1P_1$ transition at 337.1nm is rendered transparent. EIT can be understood as due to interference among the dressed states created by the control field. For example, consider a Λ scheme as shown in Fig. 1.1 (b). A control field acting on the transition $|1\rangle \leftrightarrow$

$|i\rangle$ can create dressed states $|\pm\rangle$ which, for a resonant control field, can be expressed in terms of the bare states as

$$|\pm\rangle \equiv \frac{1}{\sqrt{2}}\left(|1\rangle \pm |i\rangle\right). \tag{1.58}$$

In Raman resonance condition ($\Delta - \delta = 0$), the transition amplitudes for the absorption on $|\pm\rangle \leftrightarrow |2\rangle$ transition interfere destructively, causing an absorption minimum at this condition. The EIT spectra can be interpreted in terms of Lorentzian contributions from the new resonances and dispersive contributions from the interference terms [48]. Note that, for a strong control field ($G \gg \gamma$) the dressed states $|\pm\rangle$ will give rise to new resonances in probe absorption. These are well known to occur in the microwave range due to dynamic Stark effect, known as Autler-Townes (AT) splitting [49]. The first observation of this line splitting in optical region was reported by Hertz *et al* [50]. Though transparency also occurs between the AT resonances, the major different between AT splitting and EIT is - the AT splitting can occur for very strong control fields ($G \gg \gamma$), whereas EIT is observed for small control fields ($G \leq \gamma$) [51].

EIT has been studied in many different systems [52, 53, 54, 55, 56, 57, 58, 59] and a comparison of the effect in different configurations are reported in [58]. EIT has been observed in ideal plasma[55], laser cooled systems [56], in a limited number of solid samples [57] and also in samples kept in cavities [59]. For certain configuration EIT is shown to be phase dependent [60]. The polarization dependence of the laser fields on EIT has also been reported in [61]. EIT has found applications in laser pulse matching in pulse propagation [62], isotope separation [63], controlling optical bistability [42], electromagnetically induced grating [64]. Agarwal and Harshwardhan have generalized the idea to achieve two-photon EIT and its control [65], and using EIT Harris and Yamamoto [66] have proposed photon switching at a single photon level. Recently the two photon switching has been observed by Yan *et al* [67]. Many review articles on this subject now exist in literature [68].

Lasing Without Inversion

The manifestation of atomic coherence found applications to obtain lasing action without population inversion. The underlying principle of lasing without population inversion (LWI) is to create asymmetry between the absorption and emission process in an atomic system. Kocharovskaya and Khanin [69] were first to discover that ultra-short pulses

get amplified in a Λ system without population inversion. Harris [70] observed that decay from discrete state to identical continuum causes interference in absorption profile, whereas stimulated emission remains unchanged - hence could produce LWI. Imamoğlu and Harris [71] showed such possibility using control field. In another proposal, Scully and coworkers [72] showed that coherent superposition of ground levels in a Λ system can give rise to LWI. In early part of the last decade several theoretical proposals were made [73] and experiments were carried out [74]. In many of these [70, 72] it was found that, though there was no population inversion in the bare atomic basis, the inversion existed in the dressed basis. However in some other schemes [70, 73] population inversion does not occur in any basis. This was experimentally demonstrated in ^{87}Rb (V scheme) [75] and in Na beams (Λ scheme) [76]. Agarwal explained this phenomena is due to coherence among dressed states [77]. It is shown that Lasers operating with LWI can have ultra-narrow linewidths due to spontaneous emission noise quenching [78]. Menon and Agarwal [79] have shown that LWI can be observed in a Λ system due to cross coupling of control and probe fields on different transitions. Many reviews exist in the literature on LWI [80].

Giant Nonlinearities and Dispersion Control

Many nonlinear optical techniques and devices are available to generate higher harmonics or subharmonics of an incident laser. The prime requirement for this is large nonlinear susceptibility. In atomic vapors, the nonlinear susceptibilities are very high at the resonance but associated dispersion and absorption at resonant frequencies are also very high. Tewari and Agarwal [81] first proposed a method to circumvent this difficulty using a strong saturating laser field. They found that the field can change the phase matching conditions in the four wave mixing process and hence radiation in vacuum-ultraviolet (VUV) could be generated efficiently. Harris *et al* [82] demonstrated that EIT can be used to get destructive interference in linear susceptibility $\chi^{(1)}$ and constructive interference in the third order susceptibility $\chi^{(3)}$, enhancing the VUV generation. Further, Agarwal and Tewari [83] showed that using the amplification at the fundamental frequency and EIT together, much larger enhancement could be obtained in VUV generation. The first experimental demonstration of constructive interference in nonlinear susceptibility was done by Hakuta *et al* [84]. They demonstrated that Stark mixing of $2s$ and $2p$ states by a dc field in atomic hydrogen could lead to resonantly enhanced second harmonic generation with reduced absorption. Later Zhang *et al* [85] observed that a strong laser coupling, on

the $2s \leftrightarrow 2p$ transitions of hydrogen atom, could produce VUV radiation at $103nm$ without suffering resonant absorption and dispersion. Many other experiments followed the above in which atomic coherence is used to study the non-linear effects: e.g. phase matching condition was achieved in ^{208}Pb using a control laser [86], CPT was used to obtain very high efficient conversion of light at new frequencies [87] and also giant Kerr nonlinearity [88], efficient phase conjugation [89] are reported.

Using the idea of atomic coherence, Scully [90] has shown that a large index of refraction can be produced at vanishingly small absorption. This has been experimentally demonstrated by Zibrov *et al* [91] in Rb vapour. Such atomic mediums have shown potential applications in optical magnetometry and enhancement of magneto-optical rotation (details will be discussed in Chap. 2, 3 and 4). Yet another idea to create large index of refraction without absorption has been reported by Kocharovskaya, Scully and coworkers [93], where the dressed states created by a strong field are selectively populated.

Another application of coherent control of dispersion which brought many recent excitement is: control of the group velocity of light in a medium. The group velocity of a light pulse inside a dispersive medium is

$$v_g = \frac{c}{\eta + \omega_p \frac{\partial \eta}{\partial \omega_p}}; \tag{1.59}$$

where $\eta \simeq 1 + 2\pi \mathrm{Re}[\chi(\omega_p)]$ is the refractive index of the medium. Near the EIT peak the susceptibility $\chi \simeq 0$, and $\mathrm{Re}(\partial\eta/\partial\omega_p)$ depends on the width of the EIT window. A weak control field can produce very narrow windows. Hence the slope of η in the denominator of Eq. (1.59) can be made very large slowing down the group velocity in the medium. In a recent experiment Hau *et al* [94] demonstrated that using a weak control field ($1mW/cm^2$) in a Sodium Bose condensate, the group velocity of light can be slowed down to $17\ m/sec$. As a consequence a $750m$ long pulse (in free space) could be compressed to 42 μm inside the medium, and the effective nonlinear refractive index reported was as high as $0.18cm/W$. This is a *million* time larger compared to that in usual cold atoms. It followed by reports of slow light in hot gases by Scully's group [95] and Budker *et al* [96], in which they use special anti-relaxation coating on the vapour cell to reduce the inelastic collisions with the cell wall. Based on the same principle, Fleischhauer, Lukin and coworkers [97] have shown that light pulses can be decelerated and can be freezed to a full stop [98]. Using the combination of ultraslow light propagation and EIT technique

Harris and Hau [99] have shown possibility of carrying out non-linear processes at few photons per atomic cross section. More recently, in an exciting experiment, Phillips *et al* [100] have reported a proof-of-principle demonstration of trapping of light [97] and store the light pulse for a controlled period of time and then release on demand. They show that a spatially wide light pulse is compressed into a few centimeters and is converted into a collective spin excitations in ^{87}Rb vapour. After a controllable storage time, the process is reversed to get the light pulse back. In Another remarkable experiment, Liu *et al* [101] reported freezing of light in the cold cloud of sodium atom for up to $1\ mS$. They discuss its potential applications in quantum information processing.

Further it may be noted from Eq. (1.59) that for the spectral range, where $\partial\eta/\partial\omega_p < 0$, i.e. the dispersion is anomalous, the group velocity can be abnormal (e.g. $v_g > c, \infty$ or -ve) [102]. Many proposals exit in the literature on the superluminal group velocity of light. But in most of the cases there are large pulse distortion due to attenuation or amplification of the signal. Recently it is discovered [103] that a a large anomalous dispersion can occur in a region between two gain doublets. Wang *et al* [104] created two such Raman gain doublets in Cs vapour and demonstrated -ve group velocity without much distortion of the pulse. This phenomena is described by pulse reshaping, i.e., before the peak of the input pulse enters the medium a new pulse center is formed at the output. They have reported highest group index $\eta_g = c/v_g = -330$ in the optical region for a Gaussian pulse of width $\simeq 110Hz$. It may be noted that such velocities are not unphysical, and can be explained within the frame work of special relativity and principle of causality.

1.3 Brief Outline

The atomic coherence, introduced above, is the *key* to the novel phenomena reported in this thesis. Here atomic coherence is addressed in two different contexts; namely: (a) field induced anisotropy and their control via atomic coherence, and (b) coherences in spontaneous emission in free space, cavity or induced by a laser. In Chapter 2, we introduce the induced anisotropy in an initially isotropic medium either by a magnetic field or a laser field. A novel way to control this anisotropy in a homogeneously broadened medium and in an inhomogeneously broadened medium is presented in Chapter 3 and Chapter 4 respectively. In Chapter 5, the idea of *vacuum induced coherence (VIC)* is introduced, and a

detailed mathematical framework for the treatment of spontaneous emission is presented. Two radiatively coupled multilevel atoms in free space giving rise to VIC is discussed in Chapter 6. Cavity induced coherences in spontaneous emission by preselecting polarization modes of a cavity is demonstrated in Chapter 7. In Chapter 8, laser field induced coherences in spontaneous emission is investigated and resulting quantum beat in two-photon correlation in a cascade emission is presented.

Chapter 2

Field Induced Anisotropy

2.1 Introduction

In the previous chapter we described coherent control of atomic absorption and dispersion, where the polarization states of the laser fields were unimportant. Because, the atomic gas behaves as an isotropic medium in its response to different polarization components of a weak incident field. However this symmetry breaks for certain systems. In this chapter we will consider situations where the fields (magnetic field or a laser field) can induce anisotropy in the atomic response to different polarization components of a weak probe field. We discuss the resulting consequences. In the following section we show how polarization state of a probe modifies while passing through an anisotropic medium.

2.2 Response of an Anisotropic Medium to a Linearly Polarized Light

Let us consider an x-polarized incident probe field $\vec{E}_{in}$ with frequency ω_p propagating in an isotropic medium along z direction. The field amplitude can be written as

$$\vec{E}_{in}(z,t) = \vec{\mathcal{E}}_p(z)e^{-i\omega_p t + ik_p z} + c.c.\,. \tag{2.1}$$

We resolve the incident field amplitude $\vec{\mathcal{E}}_p$ into two circularly polarized (σ_+ and σ_-) components

$$\vec{\mathcal{E}}_p = \hat{\epsilon}_+\mathcal{E}_{p+} + \hat{\epsilon}_{p-}\mathcal{E}_{p-}, \tag{2.2}$$

where unit polarization vectors $\hat{\epsilon}_{\pm}$ corresponding to $\sigma_{\mp}$ polarization are defined in terms of unit vectors $\hat{x}$ and $\hat{y}$ as

$$\hat{\epsilon}_{\pm} = \frac{\hat{x} \pm i\hat{y}}{\sqrt{2}} \,. \tag{2.3}$$

The total polarization induced in the atomic medium due to a linearly polarized probe field can be expressed as [see Eq. (1.9)]

$$\vec{\mathcal{P}} = \{\hat{\epsilon}_{+}\chi_{+}(\omega_p)\mathcal{E}_{p+} + \hat{\epsilon}_{-}\chi_{-}(\omega_p)\mathcal{E}_{p-}\}\, e^{-i\omega_p t + ik_p z} + c.c.\,, \tag{2.4}$$

where $\chi_{\pm}(\omega_p)$ give response of the medium corresponding to $\sigma_{\mp}$ components of the electric field. When $\vec{E}_{in}$ passes through the anisotropic medium, the different polarization components $\mathcal{E}_{p\pm}(z)$ evolve. This dynamics is governed by Eq. (1.12). Our interest is the steady state situation, where $\mathcal{E}_{p\pm}$ and $\chi_{\pm}$ are independent of time. Further, substituting (2.4) in Eq. (1.12) and on using SVEA [see Eq. (1.14)] the equations for $\mathcal{E}_{p\pm}$ can be written as

$$\frac{\partial \mathcal{E}_{p+}}{\partial z} = 2\pi i k_p \chi_{+} \mathcal{E}_{p+}\,, \tag{2.5a}$$

$$\frac{\partial \mathcal{E}_{p-}}{\partial z} = 2\pi i k_p \chi_{-} \mathcal{E}_{p-}\,. \tag{2.5b}$$

In general, $\chi_{\pm}$ are functions of the fields $\mathcal{E}_{p\pm}$. However here we consider propagation of a weak probe, where $\chi_{\pm}$ are independent of $\mathcal{E}_{p\pm}$. Thus the solutions of the wave equation for $\mathcal{E}_{p\pm}$

$$\mathcal{E}_{p+}(z = l) = \mathcal{E}_{p+}(0)\exp(2\pi i k_p l \chi_{+}), \tag{2.6a}$$

$$\mathcal{E}_{p-}(z = l) = \mathcal{E}_{p-}(0)\exp(2\pi i k_p l \chi_{-}); \tag{2.6b}$$

that gives the output field amplitude

$$\vec{\mathcal{E}}_{out}(z = l) = \hat{\epsilon}_{+}\mathcal{E}_{p+}(0)e^{2\pi i k_p l \chi_{+}} + \hat{\epsilon}_{-}\mathcal{E}_{p-}(0)e^{2\pi i k_p l \chi_{-}}. \tag{2.7}$$

Here l is cell length of the medium along z. For an x-polarized incident field, say $\vec{\mathcal{E}}_{in} = \hat{x}\mathcal{E}_0$,

$$\mathcal{E}_{p+}(0) = \mathcal{E}_{p-}(0) = \frac{\mathcal{E}_0}{\sqrt{2}}, \tag{2.8}$$

and the output field in Eq. (2.7) takes the form

$$\vec{\mathcal{E}}_{out} = \frac{\mathcal{E}_0}{\sqrt{2}}\left(\hat{\epsilon}_{+}e^{2\pi i k_p l \chi_{+}} + \hat{\epsilon}_{-}e^{2\pi i k_p l \chi_{-}}\right). \tag{2.9}$$

Thus the output field $\vec{\mathcal{E}}_{out}$ consists of both x and y-polarization components. The direction of light polarization *rotates* with respect to the polarization of the incident light. Experimentally the intensity of transmission through a crossed polarizer at the output gives the measure of the rotation. In the above case the intensity of transmission through a y-polarized analyzer is given by

$$T_y = \frac{|(\vec{\mathcal{E}}_{out})_y|^2}{|\vec{\mathcal{E}}_{in}|^2} = \frac{1}{4}\left| e^{2\pi i k_p l \chi_+} - e^{2\pi i k_p l \chi_-} \right|^2, \tag{2.10}$$

where the output intensity is normalized with respect to the input. It may be noted that for a resonant or near-resonant probe field, $\chi_\pm$ will be complex and therefore due to large absorption by the medium, there will be large attenuation of output signal. However assuming that $\chi_\pm$ is real, from Eq. (2.9) we get

$$\frac{\mathcal{E}_y}{\mathcal{E}_x} = \tan\theta = \tan[\pi k_p l \mathrm{Re}(\chi_- - \chi_+)]. \tag{2.11}$$

On using the Eq. (1.17a), the rotation θ can be written as

$$\theta = \pi k_p l \mathrm{Re}(\chi_- - \chi_+) \tag{2.12}$$

$$= \frac{k_p l}{2}(\eta_- - \eta_+); \tag{2.13}$$

where $\eta_\pm = 1 + 2\pi \mathrm{Re}\chi_\pm$ is the refractive index of the medium corresponding to the $\sigma_\mp$ polarization components of the input field. This corresponds to the polarization rotation in the systems where absorption is small. In the rest of this section, we will discuss how anisotropy can be created in an isotropic medium.

2.3 Magneto-optical Rotation

An isotropic medium consisting of atoms having m-degenerate sublevels when subjected to a magnetic field exhibits birefringence[1] in its response to a polarized optical field. This is due to the fact that Zeeman splitting of the magnetic sublevels causes asymmetry in the refractive indices for left and right circular polarization components of the optical field.

[1] A medium is called as a birefringent medium if the refractive indices corresponding to different polarization components of an incident EM field are different; and the associated phenomena is known as birefringence. Similarly the phenomenon due to which the different polarization components of the EM field experience different absorption is known as *dichroism*.

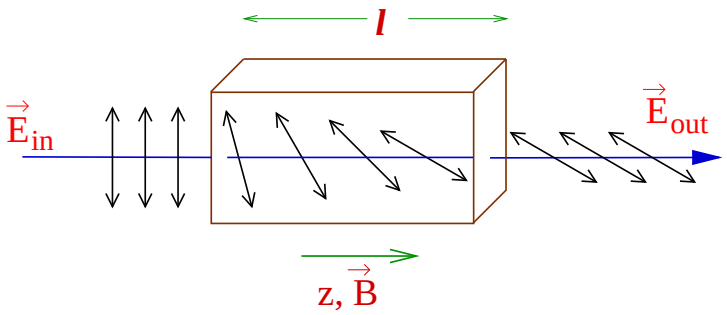

Figure 2.1: Magneto-optical rotation of a linearly polarized probe field in Faraday configuration. Here the propagation direction of the incident probe field is parallel to the direction of magnetic field applied.

Therefore the two circular polarization components of the field travel in two different velocities causing a phase shift at the output. The result is *magneto-optical rotation (MOR)*; i.e., the plane of polarization of the light emerging out of the medium is rotated with respect to that of the incident as shown in Fig. 2.1.

The history of MOR can be traced back to the discovery of Faraday rotation [105], which was the first evidence of connection between light and magnetic field. However our usage of MOR should be understood as a generalization of the Faraday rotation; e.g., unlike in Faraday configuration where the magnetic field is parallel to the propagation direction of the light field, the field configurations in MOR, in principle, can be arbitrary. Moreover the light source used in MOR, in general, is a coherent field. The amount of rotation observed in conventional Faraday rotation, is extremely small even in bulk samples. Thus the effect would seem to be almost impossible to detect in dilute gas samples. But in contrast, large dispersion that occurs at atomic resonances could cause a large rotation even in dilute samples, when the MOR is probed with a resonant or near-resonant EM field [106].

The polarization rotation in a magneto-optical system can be clearly understood from the quantum mechanical response of an atom to a laser field in presence of a magnetic field. For example consider a V-scheme (say ^{40}Ca system), with $4\ ^1S_0$ as ground state and $4\ ^1P_1$ as its excited states, is subjected to a magnetic field $\vec{B}$. See Fig. 2.1. We probe it by a laser which is linearly polarized and propagating along $\vec{B}$. Then the susceptibilities χ_+ and χ_- corresponding to the right and left circular polarizations would be (a detailed

calculation is given in Chap. 3)

$$\chi_{\pm} = \left(\frac{\alpha}{4\pi k_p}\right) \frac{\gamma}{(\delta \pm \zeta - i\gamma)}, \tag{2.14}$$

where $2\hbar\zeta$ is the Zeeman splitting between the levels $|1\rangle \equiv |j = 1, m = 1\rangle$ and $|2\rangle \equiv |j = 1, m = -1\rangle$; δ is detuning between the the probe frequency and the frequency ω_{10} of the $j = 1 \leftrightarrow j = 0$ transition (with zero magnetic field) and is given by

$$\delta = \omega_{10} - \omega_p. \tag{2.15}$$

In Eq. (2.14), 2γ is the decay rate of the level $|j = 1, m = \pm 1\rangle$ to the level $|j = 0, m = 0\rangle$. The quantity αl gives the probe absorption at the line center and is given by

$$\alpha l = \frac{4\pi k_p l |d|^2 n}{\hbar\gamma}, \tag{2.16}$$

where n is the density of atoms and d is dipole matrix element for the transition. It is to be noticed that $\chi_+ = \chi_-$ for zero magnetic field. For small absorptions, the polarization rotation is given by [see Eq. (2.12)]

$$\theta = \left(\frac{\alpha l}{2}\right) \frac{\gamma\zeta(\delta^2 - \gamma^2 - \zeta^2)}{(\delta^2 - \gamma^2 - \zeta^2)^2 + 4\gamma^2\delta^2}. \tag{2.17}$$

Note that $\chi_{\pm}$ depend on the number density of atoms and the oscillator strength of the transition. Therefore larger is the asymmetry between χ_+ and χ_-, larger is the rotation. Clearly, from (2.17), θ will be large if magnetic field (and hence 2ζ) is large.

Traditionally MOR was used as a tool in polarization spectroscopy using continuum sources [107]. The interest in MOR was intensified in the atomic and molecular physics with the availability of intense light sources of definite polarization [108] and frequency [109]. Several reviews exist in the literature on this subject including several interesting applications (e.g., see [110]). Using saturating fields the non-linear MOR has also been studied at length [111, 112, 113, 114]. Recently, combining the ideas of enhancement of refractive index using atomic coherence [90] and the non-linear MOR, Scully and his coworkers have investigated a possible application to high-precision optical magnetometry [115, 116]. They have demonstrated this possibility both theoretically [115] and experimentally [116], considering the rotation of polarization of a strong linearly polarized probe caused by an optically thick cell containing ^{87}Rb vapor. They consider a Λ configuration with the laser field tuned to $F = 2 \leftrightarrow F = 1$ transition absorption line of ^{87}Rb D_1. The maximum

sensitivity reported in their experiment is $\sim 6 \times 10^{-12}\mathrm{G}/\sqrt{\mathrm{Hz}}$, which is superior to other existing high precision magnetometer, e.g., SQID (superconducting quantum interference device) magnetometer. Budker *et al* at Berkeley have also reported high sensitive optical magnetometry in a series of papers [117], based on the non-linear MOR involving ultra-narrow resonances ($\simeq 2\pi \times 1.3$Hz). They use special ^{85}Rb vapor cell with high quality anti-relaxation paraffin coating that enables the atomic coherence to survive even after a large number of collisions with the wall. Using a similar configuration, Budker *et al* have shown reduction of the group velocity of light to $\simeq 8\ m/sec$ in a non-linear magneto-optical system [96]. MOR with a transverse magnetic fields [118] (known as Voigt effect) and with inclined magnetic fields [119] have also been studied.

2.4 Laser Induced Polarization Rotation

Laser field alone can also break the symmetry in the response of an atomic gas to different polarization components of a probe field. For example, let us consider $j = 0 \leftrightarrow j = 1$ transitions of an atomic gas containing V systems. When a linearly polarized weak probe field passes through the medium, the $\sigma_{\mp}$ components of the probe field couple the $|j = 0, m = 0\rangle$ with the degenerate states $|j = 1, m = \pm 1\rangle$. The susceptibilities $\chi_{\pm}$ of the medium to these two components $\sigma_{\mp}$ are same; i.e., response of the medium is symmetric to both the components. This is clear from the discussion in our previous section, particularly when we put $\zeta = 0$ in Eq. (2.14). However when a σ_- polarized strong (control) field is applied on the $|j = 0, m = 0\rangle \leftrightarrow |j = 1, m = 1\rangle$ transition, the susceptibility χ_+ is modified by the control field parameters creating asymmetry between χ_+ and χ_-. Thus the plane of polarization of the probe field rotates (as observed in magneto-optical systems). Note that, this rotation is solely due to the laser field and is a function of control field parameters.

The light-induced polarization rotations were extensively studied in optical pumping experiments with incoherent light [120]. Resonant birefringence was observed due to optically induced level shift [121]. Liao and Bjorklund [122] were the first to observe polarization rotation in a three level system by resonant enhancement of two-photon dispersion in the $3s^2S_{1/2} \leftrightarrow 5s^2S_{1/2}$ of sodium vapor. They showed that a linearly polarized probe laser of frequency ω_1 experiences a polarization rotation by a circularly polarized control laser of frequency ω_2, when $\omega_1 + \omega_2$ was tuned to the two-photon transition. The rotation is

result of the selection rule for the two-photon transition, e.g., for the two-photon transition $S \leftrightarrow S$, the photons must have opposite sense of polarization. Hence a σ_+ polarized pump will affect only σ_- component of the linearly polarized probe. Thus the dispersive and absorptive parts of the two-photon susceptibility will cause light-induced birefringence and dichroism. Hänch and coworkers [123] have used this polarization rotation as a high resolution spectroscopic technique. Heller *et al* [124] extended this idea to atomic systems involving the ionization continuum. Experimental and theoretical work has been reported by Ståhlberg *et al* [125] on laser induced dispersion in a three level cascade system of Ne discharge. Pavon *et al* [126] introduced the idea of quantum coherence to obtain significant atomic birefringence in presence of EIT. Winelandy and Gaeta [127] used quantum coherence to control the polarization state of a probe field. They reported a large birefringence and hence a large polarization rotation in a three-level cascade ($7^2S_{1/2} \leftrightarrow 5^2P_{3/2} \leftrightarrow 5^2S_{1/2}$) of ^{85}Rb. Using a similar configuration, Fortson and coworkers [128] have showed a possible utility of the polarization rotation at EIT to measure the atomic parity non-conservation signal with a better efficiency.

2.5 Summary and Perspectives

In summary, we have shown that a magnetic field or a laser field can create anisotropy in an isotropic medium. As a result the polarization of a linearly polarized weak probe passing through the medium rotates. The combined effects of the laser field and the magnetic field will be interesting to investigate in the context of *coherent control* of the rotation of polarization. We consider this coherent control both for the stationary atom and Doppler broadened medium. in Chapters 3 [129] and in Chapter 4 [130, 131] respectively.

Chapter 3

Laser Field Induced Birefringence and Enhancement of Magneto-optical Rotation

3.1 Introduction

An initially isotropic medium, when subjected to either a magnetic field or a coherent field, can induce anisotropy in the medium and can cause the polarization of a probe field passing through the medium to rotate. Therefore the rotation of probe polarization, due to magnetic field alone, can be controlled efficiently with the use of a coherent control field. In this Chapter we investigate the possibility of the enhancement of magneto-optical rotation (MOR) produced by the control laser. The rotation angle is $\theta = \pi k_p l \mathrm{Re}(\chi_- - \chi_+)$ for small absorption [see Eq. (2.12)]. Therefore larger the asymmetry between χ_+ and χ_-, larger will be the enhancement of MOR. The present study is motivated by the possibility that susceptibilities $\chi_\pm$ can be manipulated by application of a control laser [81, 82, 83, 90, 91, 92, 93, 52]. In a recent experiment, Wielandy and Gaeta [127] demonstrated control of polarization state of the probe field in an initially isotropic medium. In this Chapter we demonstrate the laser induced birefringence. And we show that an interplay between the control laser and magnetic field can produce large enhancement in MOR in the regions - identified by our analytical results [129].

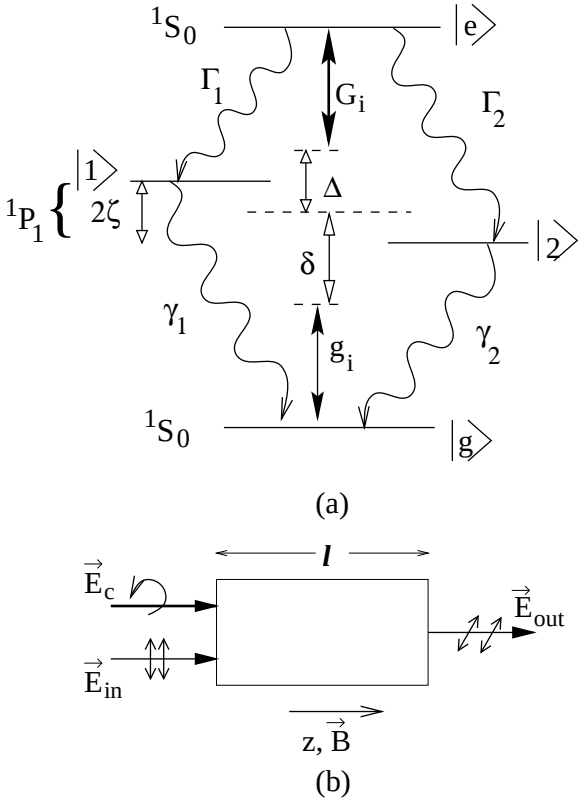

Figure 3.1: (a) The four-level model scheme (say of ^{40}Ca) having m-degenerate sub-levels as its intermediate states. The symbols in left hand side denote the energy levels of ^{40}Ca atom. $2\Gamma_j$ and $2\gamma_i$ are the spontaneous decays, $2g_j$ ($2G_j$) is Rabi frequency of the probe (control) field due to coupling of the intermediate states $|i\rangle$ with $|g\rangle$ ($|e\rangle$). The detuning of probe (control) field from the center of $|1\rangle$ and $|2\rangle$ are represented by δ (Δ). 2ζ is the Zeeman splitting between the intermediate states. (b) A block diagram that shows the configuration under consideration. $\vec{B}$ defines the quantization axis z. The input probe $\vec{E}_{in}$ is x-polarized and the control field is left circularly polarized. Both the fields propagate along z. After passing through the cell, output is observed through a y-polarized analyzer.

3.2 The Model System and The Dynamical Equations

We consider a model system [see Fig. 3.1] involving, say, cascade of transitions $|j = 0, m = 0\rangle$ (level $|g\rangle$) $\leftrightarrow$ $|j = 1, m = \pm 1\rangle$ (level $|1\rangle$ and $|2\rangle$) $\leftrightarrow$ $|j = 0, m = 0\rangle$ (level $|e\rangle$). This scheme for example will be relevant for expressing ^{40}Ca. A weak probe $\vec{E}_p$ will act between the levels $|g\rangle$ and $|1\rangle, |2\rangle$. We assume in addition the interaction of a control laser $\vec{E}_c$ to be nearly resonant with the transition $|e\rangle \leftrightarrow |1\rangle, |2\rangle$. For simplicity we drop the transition $m = 0 \leftrightarrow m = 0$. We thus assume the loss to $m = 0$ state by spontaneous emission could be pumped back by an incoherent pump. Let $\omega_{\alpha\beta}$ be the transition frequency between the

levels $|\alpha\rangle$ and $|\beta\rangle$. The total Hamiltonian of the atom interacting with the control and probe fields is

$$\begin{aligned}\mathcal{H} &= \hbar\omega_{eg}|e\rangle\langle e| + \hbar\omega_{1g}|1\rangle\langle 1| + \hbar\omega_{2g}|2\rangle\langle 2| \\ &\quad -\vec{d}\cdot(\vec{E}_c + \vec{E}_p),\end{aligned} \tag{3.1}$$

where both $\vec{E}_c$ and $\vec{E}_p$ are given by Eqs. (2.1) and (2.2). We make rotating wave approximation (see discussion after Eq. (1.46)) and thus we approximate the interaction part of the Hamiltonian by

$$\begin{aligned}-\frac{\vec{d}\cdot(\vec{E}_c + \vec{E}_p)}{\hbar} \approx &- G_1|e\rangle\langle 1|e^{-i\omega_c t + ik_c z} - G_2|e\rangle\langle 2|e^{-i\omega_c t + ik_c z} \\ &- g_1|1\rangle\langle g|e^{-i\omega_p t + ik_p z} - g_2|2\rangle\langle g|e^{-i\omega_p t + ik_p z} + H.c.,\end{aligned} \tag{3.2}$$

where $2G_j$s and $2g_j$s represent Rabi frequencies of the control and the probe laser -

$$G_j = \frac{\vec{D}_{ej}\cdot\vec{\mathcal{E}}_c}{\hbar},\ g_j = \frac{\vec{d}_{jg}\cdot\vec{\mathcal{E}}_p}{\hbar};\quad [j = 1, 2]. \tag{3.3}$$

In order to proceed further we make the following transformations on the off-diagonal elements of the density matrix which removes all explicit dependence on the optical temporal and spatial frequencies

$$\begin{aligned}\rho_{ej} = \tilde{\rho}_{ej}e^{-i\omega_c t + ik_c z}, \rho_{jg} = \tilde{\rho}_{jg}e^{-i\omega_p t + ik_p z}, \\ \rho_{eg} = \tilde{\rho}_{eg}e^{-i(\omega_c+\omega_p)t + i(k_c+k_p)z}.\end{aligned} \tag{3.4}$$

In the following we drop tildes from the density matrix equation. However the full density matrix in Schrödinger picture is to be obtained by using Eq. (3.4). On introducing the various rates of spontaneous emission, we can write the equations for density matrix elements

as

$$\begin{aligned}
\dot{\rho}_{ee} &= -2(\Gamma_1+\Gamma_2)\rho_{ee} + iG_1\rho_{1e} - iG_1^*\rho_{e1} + iG_2\rho_{2e} - iG_2^*\rho_{e2},\\
\dot{\rho}_{e1} &= -(\Gamma_1+\Gamma_2+\gamma_1+i(\Delta-\zeta))\rho_{e1} + iG_1(\rho_{11}-\rho_{ee}) + iG_2\rho_{21} - ig_1^*\rho_{eg},\\
\dot{\rho}_{e2} &= -(\Gamma_1+\Gamma_2+\gamma_2+i(\Delta+\zeta))\rho_{e2} + iG_2(\rho_{22}-\rho_{ee}) + iG_1\rho_{12} - ig_2^*\rho_{eg},\\
\dot{\rho}_{eg} &= -(\Gamma_1+\Gamma_2+i(\Delta+\delta))\rho_{eg} + iG_1\rho_{1g} + iG_2\rho_{2g} - ig_1\rho_{e1} - ig_2\rho_{e2},\\
\dot{\rho}_{11} &= 2\Gamma_1\rho_{ee} - 2\gamma_1\rho_{11} + iG_1^*\rho_{e1} - iG_1\rho_{1e} + ig_1\rho_{g1} - ig_1^*\rho_{1g},\\
\dot{\rho}_{12} &= -(\gamma_1+\gamma_2+2i\zeta)\rho_{12} + iG_1^*\rho_{e2} + ig_1\rho_{g2} - iG_2\rho_{1e} - ig_2^*\rho_{1g},\\
\dot{\rho}_{1g} &= -(\gamma_1+i(\delta+\zeta))\rho_{1g} + ig_1(\rho_{gg}-\rho_{11}) + iG_1^*\rho_{eg} - ig_2\rho_{12},\\
\dot{\rho}_{22} &= 2\Gamma_2\rho_{ee} - 2\gamma_2\rho_{22} + iG_2^*\rho_{e2} - iG_2\rho_{2e} + ig_2\rho_{g2} - ig_2^*\rho_{2g},\\
\dot{\rho}_{2g} &= -(\gamma_2+i(\delta-\zeta))\rho_{2g} + ig_2(\rho_{gg}-\rho_{22}) + iG_2^*\rho_{eg} - ig_1\rho_{21},\\
\dot{\rho}_{gg} &= 2\gamma_1\rho_{11} + 2\gamma_2\rho_{22} + ig_1^*\rho_{1g} - ig_1\rho_{g1} + ig_2^*\rho_{2g} - ig_2\rho_{g2},
\end{aligned} \tag{3.5}$$

where the detunings are defined by

$$\begin{aligned}
\Delta = (\omega_{e1}-\omega_c+\zeta) = (\omega_{e2}-\omega_c-\zeta),\ \omega_{12} = 2\zeta,\\
\delta = (\omega_{1g}-\omega_p-\zeta) = (\omega_{2g}-\omega_p+\zeta).
\end{aligned} \tag{3.6}$$

In Eq. (3.5) $2\Gamma_j$ ($2\gamma_j$) represents rate of spontaneous emission from $|e\rangle$ to $|j\rangle$ ($|j\rangle$ to $|g\rangle$). However in further calculations we assume $\gamma_1 = \gamma_2 = \gamma$ for simplicity. The dipole matrix elements in (3.3) are given in terms of vectors (2.3) as

$$\begin{aligned}
\vec{D}_{e1} &= -D\hat{\epsilon}_+,\ \vec{D}_{e2} = D\hat{\epsilon}_-,\\
\vec{d}_{1g} &= -d\hat{\epsilon}_-,\ \vec{d}_{2g} = d\hat{\epsilon}_+.
\end{aligned} \tag{3.7}$$

Here D (d) denotes the reduced dipole matrix element corresponding to $|e\rangle \leftrightarrow |j\rangle$ ($|j\rangle \leftrightarrow |g\rangle$) transitions. Clearly we also have

$$\begin{aligned}
G_1 = -\frac{D\mathcal{E}_{c-}}{\hbar} \quad , \quad G_2 = \frac{D\mathcal{E}_{c+}}{\hbar},\\
g_1 = -\frac{d\mathcal{E}_{p+}}{\hbar} \quad , \quad g_2 = \frac{d\mathcal{E}_{p-}}{\hbar}.
\end{aligned} \tag{3.8}$$

This should be kept in view to determine the component of circular polarization that connects various transitions.

3.3 Calculation of $\chi_\pm$ and polarization rotation in presence of a control laser

In Sec. 1.3 we have discussed the polarization rotation of a linearly polarized light - that could occur while passing through an anisotropic medium. We have also given an example in Sec. 1.3.2, where we show the anisotropy created by a magnetic field. In what follows below, we calculate the susceptibilities of our model system to the linearly polarized probe field (2.1) using the solutions of Eq. (3.5), in presence of the control field.

The induced polarization (i.e. induced dipole moments per unit volume) at frequency ω_p will be obtained from off-diagonal elements ρ_{1g}, ρ_{2g}:

$$\begin{aligned} \vec{\mathcal{P}} &= n\mathrm{Tr}(\vec{d}\rho) = n(\vec{d}_{g1}\rho_{1g} + \vec{d}_{g2}\rho_{2g} + c.c.) \\ &= n(\vec{d}_{g1}\rho_{1g} + \vec{d}_{g2}\rho_{2g})e^{-i\omega_p t + ik_p z} + c.c.\,. \end{aligned} \tag{3.9}$$

The exponential factors in (3.9) come from the transformation in (3.4). As indicated earlier, ρ_{1g} and ρ_{2g} will be computed to the lowest order in the probe field. We choose the probe field polarization such that $g_j \neq 0$. Let us define

$$\rho_{1g} = \left(\frac{g_1}{\gamma}\right) s^+, \rho_{2g} = \left(\frac{g_2}{\gamma}\right) s^-. \tag{3.10}$$

Comparing the induced polarization in an anisotropic medium given in Eq. (2.4) and (3.9), and on using (3.7) and (3.10) we get

$$\chi_\pm = \left(\frac{\alpha}{4\pi k_p}\right) s^\pm; \tag{3.11}$$

where the quantity αl represents the probe absorption at the line center [defined in Eq. (2.16)] and $s^\pm$ represent the normalized susceptibilities corresponding to $\sigma_\mp$ components of the probe field.

We have been able to obtain analytical solutions for $s^\pm$ which we give below -

$$s^+ = \frac{i\gamma\left[|G_2|^2 + (\gamma + i(\delta-\zeta))(\Gamma_1+\Gamma_2+i(\Delta+\delta))\right]}{|G_2|^2(\gamma+i(\delta+\zeta)) + (\gamma+i(\delta-\zeta))\left[|G_1|^2 + (\gamma+i(\delta+\zeta))(\Gamma_1+\Gamma_2+i(\Delta+\delta))\right]}, \tag{3.12}$$

$$s^- = \frac{i\gamma\left[|G_1|^2 + (\gamma + i(\delta+\zeta))(\Gamma_1+\Gamma_2+i(\Delta+\delta))\right]}{|G_1|^2(\gamma+i(\delta-\zeta)) + (\gamma+i(\delta+\zeta))\left[|G_2|^2 + (\gamma+i(\delta-\zeta))(\Gamma_1+\Gamma_2+i(\Delta+\delta))\right]}. \tag{3.13}$$

Note that the analytical results (3.12) and (3.12) have been derived for arbitrary complex control fields which enter through the Rabi frequencies G_1 and G_2. However, the final results do *not* depend on the phases of G_1 and G_2. Thus the ellipticity of the control field plays no role in determining the amount of magneto-optical rotation. Note further that the results (3.12) and (3.13) reduce to well known results (2.14) in the absence of the control field [i.e., $G_1 = G_2 = 0$]. The polarization rotation is obtained by substituting (3.12) and (3.13) in (2.10)

$$T_y = \frac{1}{4}\left|\exp\left(i\frac{\alpha l}{2}s^+\right) - \exp\left(i\frac{\alpha l}{2}s^-\right)\right|^2. \tag{3.14}$$

As mentioned earlier, we choose the parameters in such a way that there is maximum asymmetry between χ_+ and χ_-. An important case occurs when, say, $G_2 = 0$, i.e., the control field is σ_+ polarized ($\mathcal{E}_{c+} = 0$, $\mathcal{E}_{c-} \neq 0$). Clearly s^- in absence of the control field becomes

$$s^- = \frac{i\gamma}{(\gamma + i(\delta - \zeta))}; \tag{3.15}$$

whereas s^+ is strongly dependent on the strength and frequency of the control field given by the relation

$$s^+ = \frac{i\gamma(\Gamma_1 + \Gamma_2 + i(\Delta + \delta))}{|G_1|^2 + (\gamma + i(\delta + \zeta))(\Gamma_1 + \Gamma_2 + i(\Delta + \delta))}. \tag{3.16}$$

In absence of the control field, the susceptibilities reduce to

$$s^\pm = \frac{\gamma}{((\delta \pm \zeta) - i\gamma)}; \tag{3.17}$$

which clearly indicates that $s^\pm$ are completely symmetric in absence of magnetic field (i.e. $\Omega = 0$). Most of the MOR studies with a weak coherent field use the susceptibility in (3.17). However in presence of large control field (large $|G_1|$), both real and imaginary parts of s^+ in Eq. (3.16 will show Autler-Townes splitting. Note further that even when no magnetic field is applied (i.e., $\zeta = 0$),

$$s^-(\zeta = 0) \neq s^+(\zeta = 0), \text{ for } |G_1| \neq 0. \tag{3.18}$$

In this case we have *control laser induced birefringence*. A particularly attractive possibility is to consider the case when $|G_1|$ is large, and we work in the regime of other parameters so that $|s^+| \ll |s^-|$. Under such conditions we will have large MOR or large signal T_y. The experiments of Wielandy and Gaeta [127] focus on the laser induced birefringence.

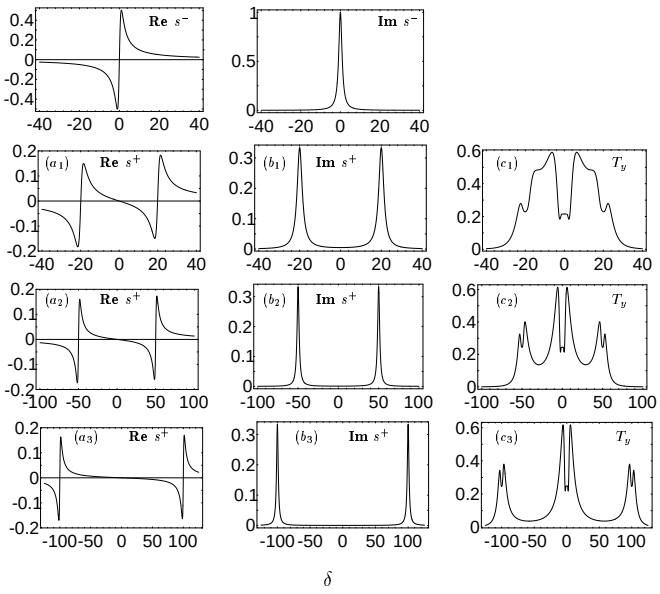

Figure 3.2: Plots to show the control field induced birefringence in absence of magnetic field ($\zeta = 0$). Control field is left circularly polarized and is in resonance with $|i\rangle \rightarrow |e\rangle$ transition ($\Delta = 0$). In the above figure, first row refers to real and imaginary part s^- (Eq. (29)) which is independent of the σ_- control field. The frames (a_j), (b_j) and (c_j) represent Re s^+, Im s^+ and T_y respectively. Three rows for $j = 1,\ 2,\ 3$ correspond to control field strengths $G_1 = 20,\ 50,\ 100$ respectively. The x-axis represents the detuning of probe laser with respect to the position of the $j = 1$ level with zero magnetic field.

3.4 Numerical Results on Laser Induced Birefringence

In this section section we present numerical results to demonstrate the coherent control of $\chi_\pm$ and hence the control of polarization rotation of a linearly polarized probe field using the analytical results obtained earlier. Note that the parameter space is rather large in (3.12, 3.13) and the results will depend on the choice of $|G_1|$, $|G_2|$, magnetic field, control laser detuning, and of course the probe laser detuning. We have carried out the numerical results for a large range of parameters and present some interesting results below. In all the numerical results we scale all the frequencies with respect to $\Gamma_j (= \gamma)$ and we take the absorption co-efficient αl as 30. This value would correspond to $\sim 10^{10}\ atoms/cm^3$, for a typical sample length (l) of $5cm$ containing ^{40}Ca atoms.

In Fig. 3.2 we consider the rotation of plane of polarization in the absence of the magnetic field. For no control laser, the rotation vanishes. For non-zero G_1, the medium becomes anisotropic **(**Eq. (3.18)**)**, we obtain substantial rotation of the plane of polarization.

The Fig. 3.2 also shows the real and imaginary part of $s^{\pm}$.

3.5 Laser Induced Enhancement of Magneto-optical Rotation

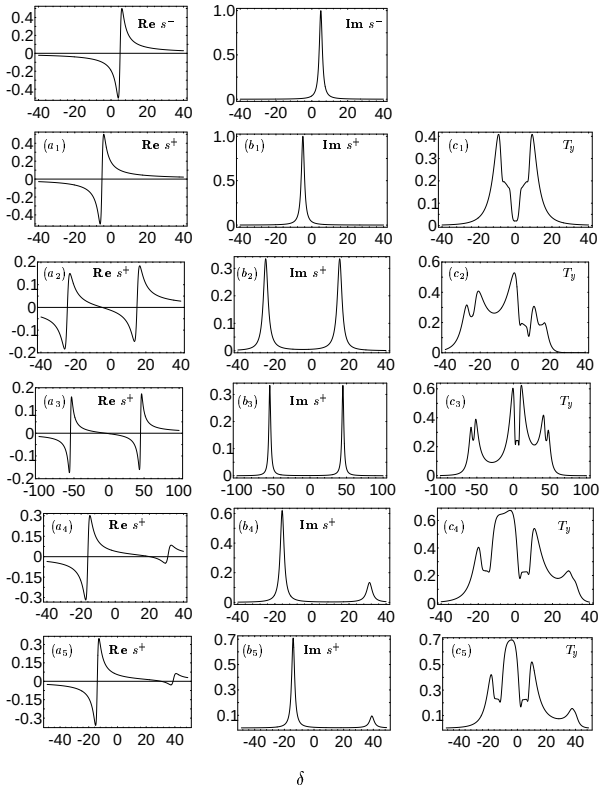

Figure 3.3: Enhancement of MOR by use of a σ_- control laser with the intermediate levels being split by a magnetic field with Zeeman splitting $2\zeta = 10$. The graphs (a_j) and (b_j) represent the control field induced changes in Re s^+ and Im s^+ respectively and (c_j) represents the corresponding T_y, and $j = 1,\ 2,\ 3$ refer to the case of resonant control field (i.e. $\Delta = \zeta$) with strengths $G_1 = 0,\ 20,\ 50$ respectively. Clearly large fields result in significant enhancement and in addition new regions appear with large MOR. Further enhancement is observed by use of a detuned laser as seen in frames (c_4) and (c_5) which are for $G_1 = 20$ and control laser detuning $\Delta = -20,\ -30$ respectively.

In this section we present numerical results to demonstrate how the MOR can be enhanced. In Fig. 3.3, we show the results for non-zero value of magnetic field. We find definite enhancement in the magneto-optical rotation. The reason for this enhancement can be traced back to the *flipping of the sign of Re χ_+ which is caused by the control field*. In addition we can produce large rotation for probe frequencies in the neighborhood of the frequencies of the

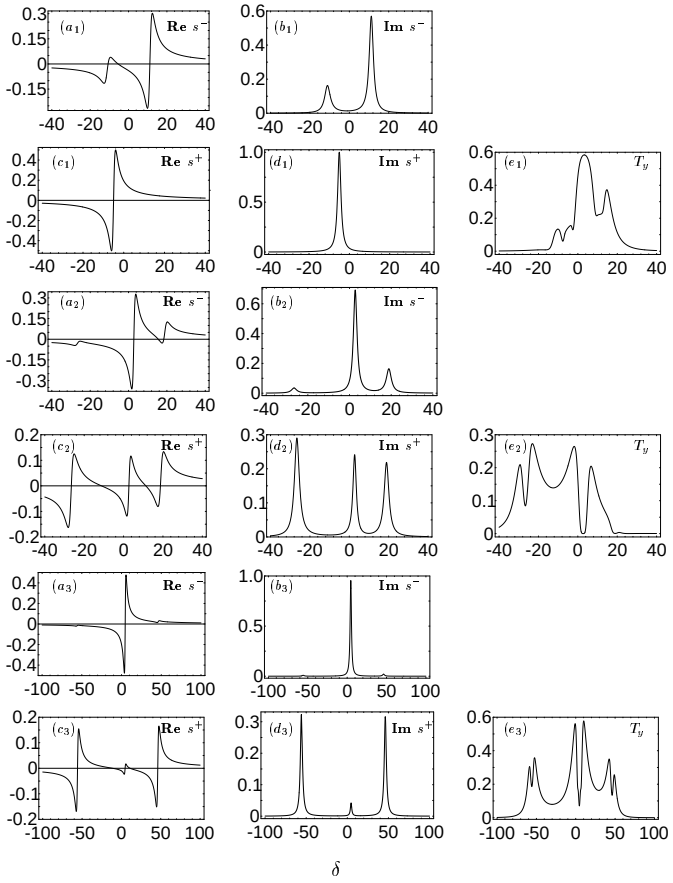

Figure 3.4: Plots represent MOR enhancement with an elliptically polarized control (i.e. $G_2 \neq 0$) and $\Delta = \zeta = 5$. Here we have considered the case of $G_2 = 10$. The frames (a_j), (b_j), (c_j), (d_j) and (e_j) represent Re s^-, Im s^-, Re s^+, Im s^+ and T_y respectively, and $j = 1,\ 2,\ 3$ correspond to $G_1 = 0,\ 20,\ 50$ respectively. The off-resonant control field can also be advantageous (results not shown) as in Fig. 3.3.

Autler-Townes components. In Fig. 3.3 we also show how the non-resonant control field can produce further enhancement. Our calculations also suggest some interesting domain in which the probe should be tuned to obtain large MOR. Application of the control laser permits us to obtain large MOR in totally different frequency regime.

In Fig. 3.4 we show the changes in the transmitted signal if $G_2 \neq 0$. The absorption and dispersion profiles now exhibit a triplet structure. As noted earlier, intensity of the transmitted y-component of the signal depends on the asymmetry between χ_+ and χ_-. When asymmetry becomes less, as for example, in the third and fourth row [from (a_2) to (e_2)] of Fig. 3.4, then T_y can decrease. In our model the control of $\chi_\pm$ is *not* independent

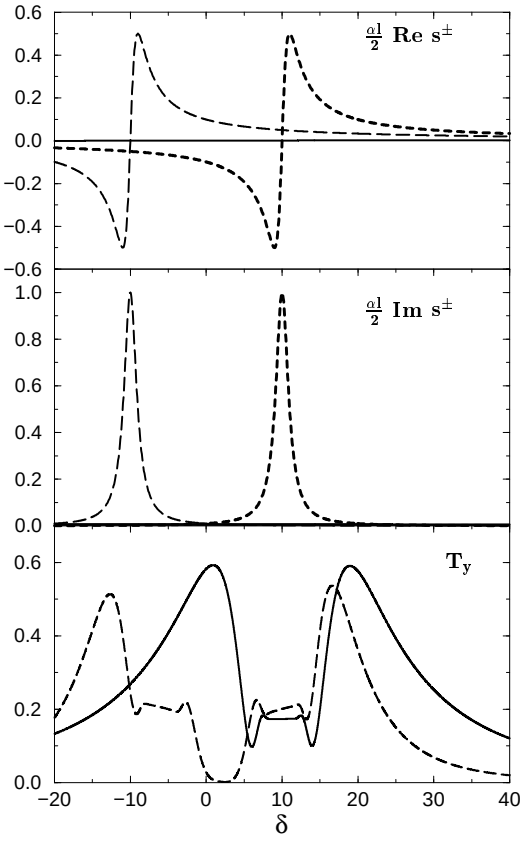

Figure 3.5: The enhancement of MOR when the control field and probe field are on two-photon resonance with $|e\rangle \leftrightarrow |g\rangle$ transition. The solid lines correspond to $G_1 = 20$. All other lines correspond to the case of no control field. The thick dashed line corresponds to s^- and the long dashes lines correspond to s^+. The other parameters used in the plot are $\zeta = 10$ and $\alpha l = 50$.

of each other as we connect to a common final level. Clearly a large enhancement would be possible if $\chi_\pm$ could be independently manipulated. The values of different physical parameters used are the following: the Rabi frequency $G = 20$ would correspond to a laser intensity of $\sim 0.107 W/cm^2$, $\zeta = 5$ corresponds to a magnetic field of $100\ Gauss$.

3.6 MOR in Two-photon Resonance Condition

In this section we consider the enhancement of MOR when the σ_+ polarized control filed and the probe field are on two-photon resonance with $|e\rangle \leftrightarrow |g\rangle$ transition ($\Delta + \delta = 0$).

Under this condition, the susceptibility s^+ reduces to

$$s_c^+ = \frac{i\gamma}{\left(\frac{|G_1|^2}{\Gamma_1+\Gamma_2}+\gamma\right)+i(\delta+\zeta)}; \tag{3.19}$$

which is a Lorentzian profile with a width given by $\left(\frac{|G_1|^2}{\Gamma_1+\Gamma_2}+\gamma\right)$. The width is too large for a control field $G_1 \gg \gamma$, causing large power broadening. Thus for small values of $\delta+\zeta$, s^+ is negligibly small (see Fig. 3.5). However, s^- remains unchanged. Therefore T_y (in Eq. (3.14)) reduces to

$$T_y = \frac{1}{4}\left|1-e^{i\frac{\alpha l}{2}s^-}\right|^2; \tag{3.20}$$

and hence T_y becomes independent of the control field for $|G_1|^2 \gg \zeta$. The $(T_y)_{max}$ value thus remains the same for any arbitrary value of ζ; e.g. for $G_1 = 20$, $(T_y)_{max} \sim 60\%$ for very large values of ζ. However changing the magnetic field, the T_y structure shifts along δ. Thus $(T_y)_{\max}$ can be shifted to the regions where MOR is small and hence get large enhancement of MOR. For example, at $\delta = 0.45$ MOR is enhanced by a factor of ~ 29.2 by the control field.

3.7 Summary

In summary, we have shown how a control laser can produce birefringence in an isotropic medium to obtain large polarization rotation of a linearly polarized weak probe field. We have also demonstrated that large enhancement of magneto-optical rotation effect can be produced by suitably choosing the control field parameters. Further we show that the control field can also produce *new frequency regions* which show very significant magneto-optical rotation. We also show that a large enhancement of MOR can be achieved when the probe and control field are in two-photon resonance.

Chapter 4

Coherent Control of MOR in Doppler Broadened Medium

4.1 Introduction

In the previous Chapter we have discussed laser field induced birefringence and control of MOR in homogeneously broadened medium in the limit of stationary atoms. However most experiments are carried out at finite temperature where the atoms move inside the cell randomly. This introduces an additional broadening in the system which is inhomogeneous in nature - known as *Doppler broadening*. Coherent control of atomic dispersion and absorption in Doppler broadened medium has been studied extensively [52]. Sub-Doppler resolution has been reported using intense control fields [132].

In this Chapter we generalize our previous study of manipulation of MOR (Chapter 2) in a Doppler broadened medium [129]. In this case, a large broadening is introduced in both the susceptibilities $\chi_{\pm}$. This is desirable to get large MOR for a broad range of probe frequencies. But on the other hand, broadening reduces the magnitude of rotation considerably. However, one can work with a denser medium to enhance the magneto-optical effect when the Doppler effect is included in the calculation. With a detailed calculation and analysis, we *identify* probe frequency regions to obtain large MOR. We present numerical results to demonstrate how the birefringence can be controlled efficiently, leading to large enhancement in MOR. We also show that with suitable selection of control field parameters, one can even realize a *magneto-optical switch* - that switches the polarization state of the incident probe field to its orthogonal component [130].

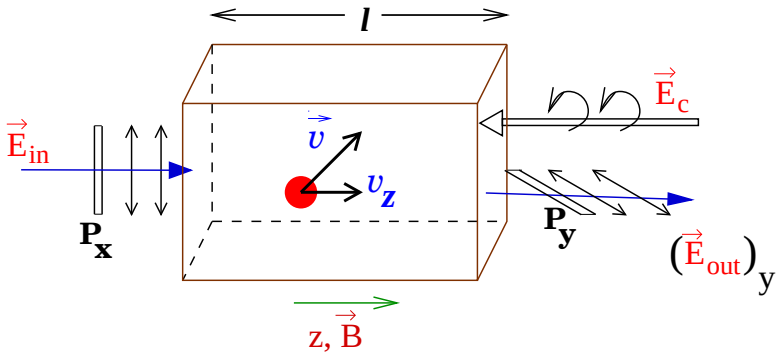

Figure 4.1: The configuration under consideration that gives rise to significantly large MOR and large enhancements. The direction of magnetic field $\vec{B}$ fixes quantization axis (z-axis). The control field ($\vec{E}_c$) and the input probe field ($\vec{E}_{in}$) are counter propagating along the z-axis. The atom in the cell moves with velocity $\vec{v}$ in arbitrary directions. P_x and P_y are x-polarizer at input and y-polarized analyzer at the output respectively. $(\vec{E}_{out})_y$ is the output probe after passing through P_y.

4.2 The Model and The Susceptibilities

We consider coherent control of MOR in a configuration as depicted in Fig. 4.1. The atoms move randomly inside the cell with velocity $\vec{v}$. The probe field and control field are taken to be counter propagating. The model scheme we consider (Fig. (4.2)) is similar to the scheme in previous Chapter. Here we have included the spontaneous decays between $m = 0 \leftrightarrow m = 0$ states in the calculation, which was neglected in Chapter 2. The decay coefficient corresponding to $|e\rangle \rightarrow |o\rangle$ ($|o\rangle \rightarrow |g\rangle$) transition is denoted by $2\Gamma_o$ ($2\gamma_o$). In what follows below, we outline the calculation of susceptibilities of the atoms, moving at $\vec{v}$, to the $\sigma_\pm$ components of the probe field.

In the rotating wave approximation, the interaction Hamiltonian $\mathcal{H}_1$ corresponding to the scheme in Fig. 4.2 is

$$\mathcal{H}_I(t) = -\hbar \sum_{i=1,2} \left[|i\rangle\langle g| g_i e^{-i\omega_p t + i\vec{k}_p\cdot\vec{v}t} + |e\rangle\langle i| G_i e^{-i\omega_c t + i\vec{k}_c\cdot\vec{v}t} + H.c. \right]; \tag{4.1}$$

where Rabi frequencies $2G_i$ and $2g_i$ of the control and probe lasers are given by Eq. (3.8). In terms of Fig. 4.2, the unperturbed Hamiltonian $\mathcal{H}_0$ is

$$\mathcal{H}_0 = \hbar(\omega_{eo} + \omega_{og})|e\rangle\langle e| + \hbar(\omega_{og} + \zeta)|1\rangle\langle 1| + \hbar\omega_{og}|o\rangle\langle o| + \hbar(\omega_{og} - \zeta)|2\rangle\langle 2|. \tag{4.2}$$

Here $\hbar\omega_{eo}$ ($\hbar\omega_{og}$) is the energy separation between $|e\rangle$ ($|g\rangle$) and $|o\rangle$, and $2\zeta = \mu_B B/\hbar$ is the Zeeman splitting of the degenerate levels, caused by the magnetic field B. The atomic

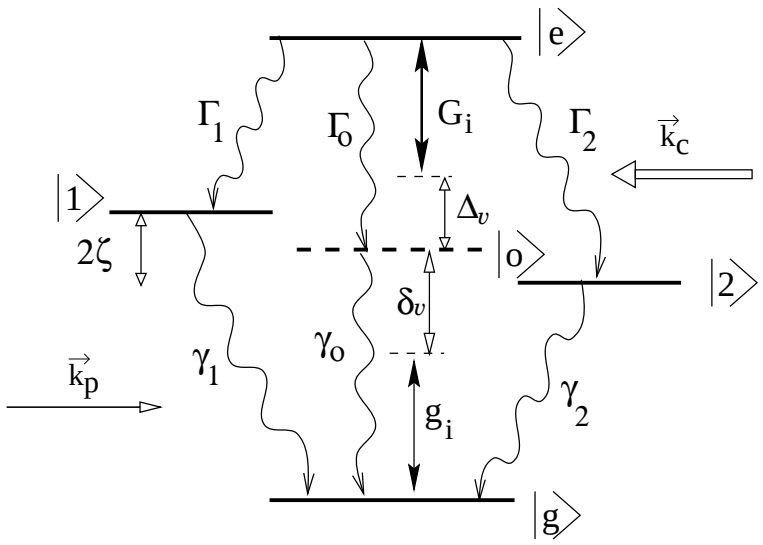

Figure 4.2: The four-level model scheme having m-degenerate sub-levels $|1\rangle$ and $|2\rangle$ as its intermediate states. The magnetic field $\vec{B}$ gives rise to Zeeman splitting 2ζ. The spontaneous decay rates are denoted by $2\Gamma_i$ and $2\gamma_i$. The probe field ($\vec{k}_p$) and the control field ($\vec{k}_c$) are counter propagating. The Rabi frequencies of the probe field and the control field are given by $2g_i$ and $2G_i$, corresponding to the $|i\rangle \leftrightarrow |g\rangle$ and $|e\rangle \leftrightarrow |i\rangle$ couplings respectively ($i = 1, 2$). The detunings of the probe and the control fields from the degenerate $j = 1$ state, in the moving atomic frame of reference, are δ_v and Δ_v respectively.

dynamics is described by the master equation

$$\dot{\rho} = \frac{-i}{\hbar}[\mathcal{H}_0 + \mathcal{H}_I(t), \rho] - \sum_{i=o,1,2} (\Gamma_i\{|e\rangle\langle e|, \rho\} + \gamma_i\{|i\rangle\langle i|, \rho\} - 2\Gamma_i\rho_{ee}|i\rangle\langle i| - 2\gamma_i\rho_{ii}|g\rangle\langle g|)\,. \tag{4.3}$$

The second term under the summation sign represents the natural decays of the system. The curly bracket represents the anti-commutator. The explicit time dependence can be eliminated by making a transformation $\rho \to \tilde{\rho}$ such that

$$\begin{aligned} \tilde{\rho}_{ii} &= \rho_{ii},\ \tilde{\rho}_{ig} = \rho_{ig}e^{i\omega_p t - i\vec{k}_p\cdot\vec{v}t}, \\ \tilde{\rho}_{ei} &= \rho_{ei}e^{i\omega_c t - i\vec{k}_c\cdot\vec{v}t},\ \tilde{\rho}_{eg} = \rho_{eg}e^{i(\omega_p+\omega_c)t - i(\vec{k}_p+\vec{k}_c)\cdot\vec{v}t}. \end{aligned} \tag{4.4}$$

The matrix equation for $\tilde{\rho}$ is found to be

$$\dot{\tilde{\rho}} = \frac{-i}{\hbar}[\mathcal{H}_{\text{eff}}, \tilde{\rho}] - \sum_{i=o,1,2} (\Gamma_i\{|e\rangle\langle e|, \tilde{\rho}\} + \gamma_i\{|i\rangle\langle i|, \tilde{\rho}\} - 2\Gamma_i\tilde{\rho}_{ee}|i\rangle\langle i| - 2\gamma_i\tilde{\rho}_{ii}|g\rangle\langle g|)\,, \tag{4.5}$$

with the effective Hamiltonian in the transformed frame

$$\begin{aligned}\mathcal{H}_{eff} &= \hbar(\delta_v+\Delta_v)|e\rangle\langle e| + \hbar(\delta_v+\zeta)|1\rangle\langle 1| + \hbar(\delta_v-\zeta)|2\rangle\langle 2| \\ &- \hbar\sum_{i=1,2}(g_i|i\rangle\langle g| + G_i|e\rangle\langle i| + H.c.)\,; \end{aligned} \tag{4.6}$$

where

$$\delta_v = \delta + k_p v_z,\ \Delta_v = \Delta - k_c v_z. \tag{4.7}$$

Here $\delta = \omega_{og} - \omega_p,\ \Delta = \omega_{eo} - \omega_c$ correspond to the detunings of the probe and control field when the atom is stationary. Further we assume $k_p \approx k_c$ for simplicity. Thus one can write

$$\Delta_v + \delta_v \approx \Delta + \delta. \tag{4.8}$$

Here it may be noted that due to our particular choice of counter propagating probe and control fields, the two-photon resonant terms can be made independent of atomic velocity [See e.g. in Eq. (4.12)]. The configuration consisting of counter propagating probe and control field in ladder system has been shown to be useful in Doppler free polarization spectroscopy [123], EIT [52] and LWI [132].

The susceptibilities of the medium corresponding to the different polarization components of the probe field, can be expressed in terms of the off-diagonal density matrix elements Eqs. (3.10) and (3.11). Therefore $\chi_\pm$ is obtained by solving Eq. (4.5) following the similar procedure as in Chapter 2. For simplicity, we assume $\gamma_1 = \gamma_2 = \gamma$. Under steady state conditions, we solve Eq. (4.5) to obtain complete analytical solutions for the susceptibilities $\chi_\pm$ or the normalized susceptibilities $s^\pm$

$$s^+ = \frac{i\gamma\left[|G_2|^2 + (\gamma+i(\delta_v-\zeta))(\Gamma_o+\Gamma_1+\Gamma_2+i(\Delta_v+\delta_v))\right]}{|G_2|^2(\gamma+i(\delta_v+\zeta)) + (\gamma+i(\delta_v-\zeta))\left[|G_1|^2+(\gamma+i(\delta_v+\zeta))(\Gamma_o+\Gamma_1+\Gamma_2+i(\Delta_v+\delta_v))\right]}, \tag{4.9}$$

$$s^- = \frac{i\gamma\left[|G_1|^2 + (\gamma+i(\delta_v+\zeta))(\Gamma_o+\Gamma_1+\Gamma_2+i(\Delta_v+\delta_v))\right]}{|G_1|^2(\gamma+i(\delta_v-\zeta)) + (\gamma+i(\delta_v+\zeta))\left[|G_2|^2+(\gamma+i(\delta_v-\zeta))(\Gamma_o+\Gamma_1+\Gamma_2+i(\Delta_v+\delta_v))\right]}. \tag{4.10}$$

In writing (4.9) and (4.10), we have used the condition (4.8). We note that the atomic velocity dependence of $s^\pm$ comes via δ_v. The results presented above are susceptibilities of the atoms moving at $\vec{v}$, to the lowest order in the probe field. The response of the medium

to the input probe field can be obtained by averaging $s^{\pm}$ over the distribution of velocities. In the limit $\vec{v} \to 0$, Eqs. (4.9) and (4.10) reduce to Eqs. (3.12) and (3.13) respectively.

It may be noted that the parameter space in Eqs. (4.9) and (4.10) is very large. Therefore we identify a particular configuration of our interest and work only in the region which gives large asymmetry between $\langle s^{+} \rangle$ and $\langle s^{-} \rangle$ ($\langle\ \rangle$ represents average over the velocity distribution of atoms inside the cell), and can lead to large MOR. We focus on a particularly interesting case when $G_2 = 0$; i.e., the control field is σ_{+}-polarized ($\mathcal{E}_c \equiv \mathcal{E}_{c-} \neq 0$ and $\mathcal{E}_{c+} = 0$) and it couples to the $|1\rangle \leftrightarrow |e\rangle$ transition only. Clearly s^{-} becomes

$$s^{-} = \frac{i\gamma}{(\gamma + i(\delta_v - \zeta))}; \tag{4.11}$$

which is independent of the control field parameters. Whereas s^{+} is strongly dependent on the strength and frequency of the control field and is given by

$$s^{+} = \frac{i\gamma(\Gamma_o + \Gamma_1 + \Gamma_2 + i(\Delta + \delta))}{|G_1|^2 + (\gamma + i(\delta_v + \zeta))(\Gamma_o + \Gamma_1 + \Gamma_2 + i(\Delta + \delta))}. \tag{4.12}$$

In absence of the control field, the susceptibilities reduce to

$$s^{\pm} = \frac{\gamma}{((\delta_v \pm \zeta) - i\gamma)}; \tag{4.13}$$

which clearly indicates that $s^{\pm}$ are completely symmetric in absence of magnetic field (i.e. $\zeta = 0$). Most of the MOR studies with a weak coherent field use the susceptibility in (4.13).

4.3 Susceptibilities $\chi_{\pm}$ of the Doppler Broadened Medium

Next we calculate the $\chi_{\pm}$ of a Doppler broadened medium. Here, as mentioned in Sec. 3.2, one needs to average $s^{\pm}$ over the atomic velocity distribution $\sigma(v_z)$ inside the cell to obtain the response of the medium

$$\langle s^{\pm} \rangle = \int_{-\infty}^{\infty} s^{\pm}(v_z)\sigma(v_z)dv_z. \tag{4.14}$$

It is assumed that at thermal equilibrium, the atoms in the cell follow Maxwell-Boltzmann velocity distribution

$$\sigma(v_z) = (2\pi K_B T/M)^{-1/2} \exp(-Mv_z^2/2K_B T), \tag{4.15}$$

where mass of the moving atom is M, temperature of the cell T and K_B is Boltzmann constant. For convenience, transforming the integral in Eq. (4.14) from velocity space to frequency space [133], we get

$$\langle s^{\pm} \rangle = \int_{-\infty}^{\infty} s^{\pm}(\delta_v)\sigma(\delta_v)d\delta_v \ , \tag{4.16}$$

where the σ distribution in frequency space is

$$\sigma(\delta_v) \equiv \frac{1}{\sqrt{2\pi\omega_D^2}} \exp\left[-(\delta_v - \delta)^2/2\omega_D^2\right] \ ; \ \omega_D \simeq \omega_{og}(K_B T/Mc^2)^{\frac{1}{2}}. \tag{4.17}$$

Here ω_D represents the Doppler width in frequency space. For our case of σ_+ polarized control field, we substitute $s^{\pm}$ from Eqs. (4.11) and (4.12) in Eq. (4.16) and evaluate the integral. We could obtain the complete analytical results for the Doppler averaged susceptibilities, in terms of complex error functions [134] as

$$\langle s^{-} \rangle \equiv \frac{i\pi\gamma}{\sqrt{2\pi\omega_D^2}} \mathcal{W}\left(\frac{\zeta - \delta + i\gamma}{\sqrt{2}\omega_D}\right); \tag{4.18}$$

$$\langle s^{+} \rangle \equiv \frac{i\pi\gamma}{\sqrt{2\pi\omega_D^2}} \mathcal{W}(\xi); \tag{4.19}$$

$$\xi = \frac{1}{\sqrt{2}\omega_D}\left[i\gamma - \zeta - \delta + \frac{|G_1|^2}{\Delta + \delta - i(\Gamma_o + \Gamma_1 + \Gamma_2)}\right]. \tag{4.20}$$

The $\mathcal{W}$ function is defined as

$$\mathcal{W}(z) = \frac{i}{\pi}\int_{-\infty}^{\infty} \frac{e^{-t^2}dt}{z - t}. \tag{4.21}$$

It can be written in terms of the error function $\mathrm{Erf}(z)$ as

$$\mathcal{W}(\alpha) = e^{-\alpha^2}(1 - \mathrm{Erf}(-i\alpha)); \ \mathrm{Erf}(z) = \frac{2}{\sqrt{\pi}}\int_0^z e^{-t^2}dt. \tag{4.22}$$

It may be noted that the argument of $\mathcal{W}$ function in $\langle s^{-} \rangle$ will show usual Doppler profile since it is independent of the control field but the argument of $\mathcal{W}$ function in $\langle s^{+} \rangle$ is strongly dependent on the strength and frequency of the control field and therefore, the Doppler profile can be modified with these control field parameters.

4.4 Condition for Enhancement of MOR

In this section we *identify* the regions of our interest and discuss how the control field can be used efficiently to control and hence enhance the MOR. For the Doppler broadened medium $s^{\pm}$ will be replaced by their averaged values ($\langle s^{\pm}\rangle$) in Eq. (3.14) to obtain the polarization rotation

$$T_y = \frac{1}{4}\left|\exp\left(i\frac{\alpha l}{2}\langle s^{+}\rangle\right) - \exp\left(i\frac{\alpha l}{2}\langle s^{-}\rangle\right)\right|^2 . \tag{4.23}$$

From Eq. (2.10), one observes the following:

(i) When $\langle s^{+}\rangle \approx \langle s^{-}\rangle$, $T_y \to 0$.

(ii) When Re $\langle s^{+}\rangle \simeq$ Re $\langle s^{-}\rangle$ but Im $\langle s^{+}\rangle \neq$ Im $\langle s^{-}\rangle$, T_y reduces to

$$T_y \simeq \frac{1}{4}\left|e^{\left(-\frac{\alpha l}{2}\mathrm{Im}\langle s^{+}\rangle\right)} - e^{\left(-\frac{\alpha l}{2}\mathrm{Im}\langle s^{-}\rangle\right)}\right|^2 . \tag{4.24}$$

If both $\frac{\alpha l}{2}\mathrm{Im}\langle s^{\pm}\rangle$ are large, $T_y \to 0$. However if $\frac{\alpha l}{2}\mathrm{Im}\langle s^{+}\rangle$ is large but $\frac{\alpha l}{2}\mathrm{Im}\langle s^{-}\rangle$ is small (or vice versa), we obtain

$$T_y \simeq \frac{e^{\alpha l\ \mathrm{Im}\langle s^{-}\rangle}}{4} \to \frac{1}{4}; \tag{4.25}$$

which is the rotation due to *dichroism only*.

(iii) Further when Im $\langle s^{+}\rangle \approx$ Im $\langle s^{-}\rangle = \beta$ (say) but Re $\langle s^{+}\rangle \neq$ Re $\langle s^{-}\rangle$, we get

$$T_y \simeq \frac{e^{(-\alpha l\beta)}}{4}\left|1 - e^{i\frac{\alpha l}{2}\mathrm{Re}(\langle s^{-}\rangle - \langle s^{+}\rangle)}\right|^2 . \tag{4.26}$$

If $\alpha l\beta$ is small,

$$T_y \simeq \frac{1}{4}\left|1 - e^{i\frac{\alpha l}{2}\mathrm{Re}(\langle s^{-}\rangle - \langle s^{+}\rangle)}\right|^2 , \tag{4.27}$$

thus when

$$\frac{\alpha l}{2}\mathrm{Re}(\langle s^{-}\rangle - \langle s^{+}\rangle) = (2n+1)\pi \ \ (n = 0, 1, 2, ...),\ T_y = 1. \tag{4.28}$$

This is the most *useful region* for our system. This rotation is solely due to birefringence. However if $\alpha l\beta$ is large then $T_y \to 0$. This is because a large attenuation of the MOR signal occurs. Thus we have identified that *the most interesting frequency region corresponds to very small value of* $\mathrm{Im}\langle s^{\pm}\rangle$ *and when the asymmetry between* $\mathrm{Re}\langle s^{\pm}\rangle$ *satisfies the condition (4.28)*. Therefore our objective is to select proper control field parameters so that above condition can be achieved.

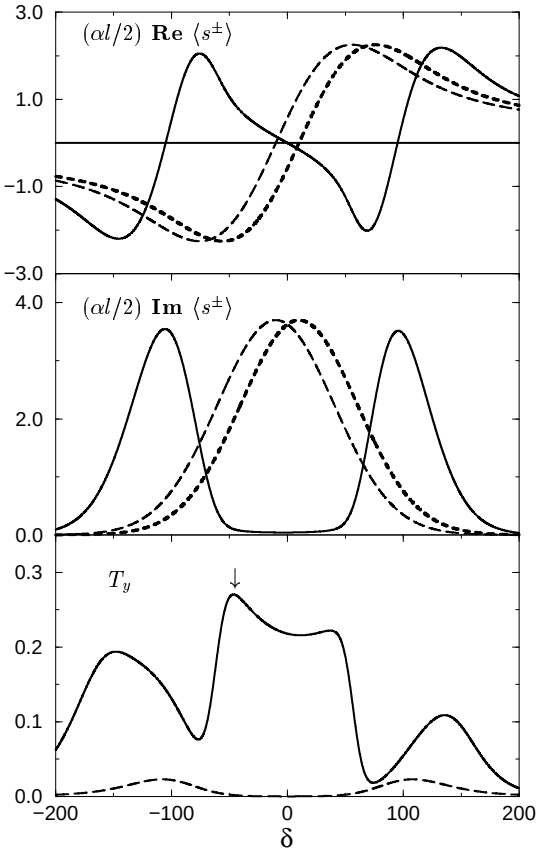

Figure 4.3: The enhancements of MOR for a control field tuned to $|e\rangle \leftrightarrow |o\rangle$ transition ($\Delta = 0$) with Rabi frequency $G_1 = 100$. In the plots for $\frac{\alpha l}{2}\langle s^{\pm}\rangle$, the thick-dashed (long-dashed) lines represent $\frac{\alpha l}{2}\langle s_0^-\rangle$ ($\frac{\alpha l}{2}\langle s_0^+\rangle$) and solid lines represent $\frac{\alpha l}{2}\langle s_c^+\rangle$. In the plot for T_y, dashed (solid) curve represents the rotation without (with) control field. The other parameters used are $\omega_D = 50$, $\zeta = 10$ and $\alpha l = 300$. All frequencies are scaled with $\Gamma_o = \Gamma_1 = \Gamma_2 = \gamma$.

4.5 Numerical Results on Coherent Control of MOR

Based on the above observations, we present some interesting numerical results for different parameters to demonstrate the large enhancement of MOR. We define the MOR signal enhancement factor

$$\eta = \frac{(T_y)_{G_1 \neq 0}}{(T_y)_{G_1 = 0}}. \tag{4.29}$$

For a given δ, η represents the enhancement (if $\eta > 1$) or suppression (if $\eta < 1$) of MOR signal by a control field, when compared to the MOR without control field. We use the notation $\langle s_0^{\pm}\rangle$ to represent susceptibilities corresponding to $\sigma_{\mp}$ components of the probe

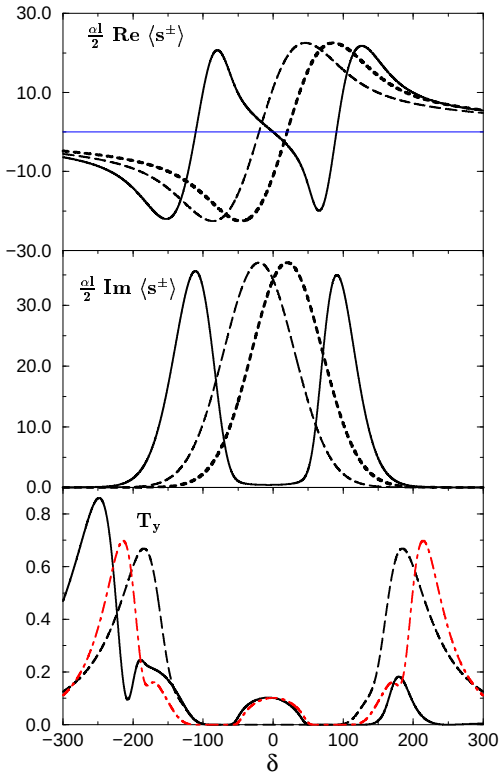

Figure 4.4: Enhancement and suppression of MOR in a denser medium with $\alpha l = 3000$. The legends of the curves used are same as in Fig. 4.3. The magnetic field used in this plot is $\zeta = 20$, the control field Rabi frequency is taken to be $G_1 = 100$ and the Doppler width is $\omega_D = 50$. A plot of T_y with $\zeta = 0$ but with $\mathcal{E}_c \neq 0$ (dot-dashed line in the plot for T_y) is also presented to isolate the roles of $\mathcal{E}_c$ and B in controlling the MOR. All frequencies are scaled with $\Gamma_o = \Gamma_1 = \Gamma_2 = \gamma$.

when control field is absent and $\langle s_c^+ \rangle$ to represent the susceptibility modified by the control field. In the following we give some typical values of diffrent various physical parameters used here: the Doppler width $\omega_D = 50\gamma$ corresponds to ^{40}Ca cell at a temprature of $\sim 500K$. For length of the cell $l = 5cm$, $\alpha l = 300$ corresponds to an atomic density of $\sim 10^{12}\ atoms/cm^3$, a Zeeman splitting of $2\zeta = 20\gamma$ corresponds to a magnetic field of strength $\sim 200\ Gauss$, and $G_1 = 100\gamma$ would correspond to a laser field of strength $\sim 5\ W/cm^2$.

In Fig. 4.3, we consider the effect of the control field which is on resonance with the transition $|e\rangle \leftrightarrow |o\rangle$ (i.e. $\Delta = 0$). We consider density of atoms in the cell such that $\alpha l = 300$. We observe significant enhancement of MOR for a large range of probe frequencies. (i) We

get the enhancement factor $\eta = 1.04 \times 10^3$ for $\delta = 0$. This can be understood as follows: in the absence of the control field and for $\delta = 0$, $\mathrm{Im}\langle s_0^+\rangle = \mathrm{Im}\langle s_0^-\rangle = \beta$ (say) and $\alpha l \beta$ is large, leading to $T_y \approx 0$ due to large signal attenuation by absorption [see Eq. (4.27)]. By application of a control field, the absorption peak (Im $\langle s_0^+\rangle$) splits giving rise to Autler-Townes doublet. The minimum of $\mathrm{Im}\langle s_c^+\rangle$ appears at $\delta \sim 0$. Thus MOR signal at this frequency is enhanced by suppressing the σ_- component of the probe field as a result of its large absorption. (ii) Further large MOR signal $T_y \approx 27\%$ is observed at $\delta \approx -46.4$ which is attributed to the flipping of the sign of $\mathrm{Re}\langle s^+\rangle$ causing a larger asymmetry between $\mathrm{Re}\langle s_c^+\rangle$ and $\mathrm{Re}\langle s_0^-\rangle$.

In Fig. 4.4, we consider the control of MOR in a denser medium. Here $\alpha l = 3000$ and the magnetic field is such that $\zeta = 20$. In order to demonstrate the combined effect of $\mathcal{E}_c$ and B, and then to isolate the contribution of magnetic field in obtaining large T_y, we have also plotted T_y for $B = 0$ but $\mathcal{E}_c \neq 0$. In the following we discuss the contribution of $\mathcal{E}_c$ and B in different probe frequency regions. To understand the enhancements and suppressions of the MOR signal at different probe frequencies, we divide the whole range of δ into following four regions:

Region I: For $-50 < \delta < 50$, Im $\langle s_0^\pm\rangle$ are large. Thus in the absence of control field, T_y in this region is almost zero. However by application of control field, an absorption minimum for σ_- polarization component ($\mathrm{Im}\langle s_c^+\rangle$) occurs due to EIT at $\delta = 0$. Thus a large enhancement of MOR is obtained when $\mathcal{E}_c \neq 0$ compared to the case of $\mathcal{E}_c = 0$. However T_y value is only 10.2% of the input probe intensity at $\delta = 0$, because $\frac{\alpha l}{2}\mathrm{Im}\langle s_0^-\rangle$ has a large value and therefore

$$T_y \approx \frac{1}{4}\left|e^{i\frac{\alpha l}{2}\langle s_c^+\rangle}\right|^2 \approx \frac{1}{4}e^{-\alpha l \mathrm{Im}\langle s_c^+\rangle} \tag{4.30}$$

which is a small value and this rotation is solely due to *dichroism* created by the control laser. Comparing the T_y values with $B = 0, \mathcal{E}_c \neq 0$ (dot-dashed line) and $B \neq 0, \mathcal{E}_c \neq 0$ (dashed line), it is clear from the Fig. 4.4 that the magnetic field contribution is very small in this region.

Region II: In the region $-150 < \delta < -50$ and $50 < \delta < 150$, there are residual absorptions at the tail of the Lorentzian Im $\langle s_0^\pm\rangle$. Further Im $\langle s_c^+\rangle$ is also large in this region. Therefore though there is a large asymmetry between Re $\langle s_0^-\rangle$ and Re $\langle s_c^+\rangle$, very large attenuation makes the value of T_y extremely small.

Region III: In the probe frequency region $-200 < \delta < -150$ and $150 < \delta < 200$, minimum of Im $\langle s_0^{\pm} \rangle$ occurs but Im $\langle s_c^{+} \rangle$ still has large value in this region. Thus the rotation is large in absence of $\mathcal{E}_c$ but with the control field, there occurs a large suppression of the MOR signal.

Region IV: For $-300 < \delta < -200$ and $200 < \delta < 300$, we get the most interesting region because the Im $\langle s_0^{\pm} \rangle$ and Im $\langle s_c^{+} \rangle$ are very small. Thus even though the asymmetry between Re $\langle s^{\pm} \rangle$ is small, the birefringence contribution shows up in the form of very large rotation in the -ve δ region. For example, the MOR signal at $\delta = -248.3$ is 86.1% of the input intensity. However in the +ve δ region, the asymmetry between $\langle s_0^{-} \rangle$ and $\langle s_c^{+} \rangle$ is decreased, and hence MOR is suppressed. The comparison of control field induced T_y in presence and absence of magnetic field clearly demonstrates that presence of magnetic field causes larger asymmetry between $\langle s_c^{+} \rangle$ and $\langle s_0^{-} \rangle$ in -ve δ region but reduces the amount of asymmetry in the +ve δ region. Hence at $\delta \approx -300$, T_y in presence of magnetic field is about 5 times larger compared to T_y without magnetic field.

In order to bring out the role of magnetic field in the enhancement of T_y observed in this region, we present Fig. 4.5(a) - where T_y vs magnetic field is plotted with a probe frequency fixed ($\delta = -250$) in the region *IV*. The figure clearly demonstrates the contribution of magnetic field and laser field separately in the enhancement of T_y. For clarity of the explanation, we have marked some points in the graph. The point A_1 (B_1) represents the rotation due to control field alone with $G_1 = 100$ ($G_1 = 50$). The points A_2 (A_3) gives the amount of T_y without (with) the control field for a given value of $\zeta = 22.4$ ($\zeta = 44.45$). Thus clearly, A_3 represents enhancement of rotation by a factor of 2.37 due to the magnetic field with respect to A_1, and when compared with A_2, the point A_3 represents enhancement due to the control field by a factor of 2.66. Very large $T_y (\approx 86.8\%$ of input intensity) is obtained for $\zeta = 22.4$. The plot with $G_1 = 50$ shows a large T_y ($\approx 90.9\%$ of input intensity) value at $\zeta = 44.54$ which corresponds to an enhancement of 4.5×10^3 times the value compared to the point B_1. Similarly large suppression of MOR can be observed when the magnetic field is flipped (i.e. ζ is negative); e.g., the point A_4. The large MOR signals and enhancements described above are interpreted by the condition (4.28). *The points where the condition (4.28) is satisfied are marked by arrows in Fig. 4.5(b).* The Fig. 4.5(b) also depicts the parameters for which the rotations are optimal. Note that larger magnetic fields can produce large T_y. Here in Fig. 4.5 we show that using a small magnetic field and applying

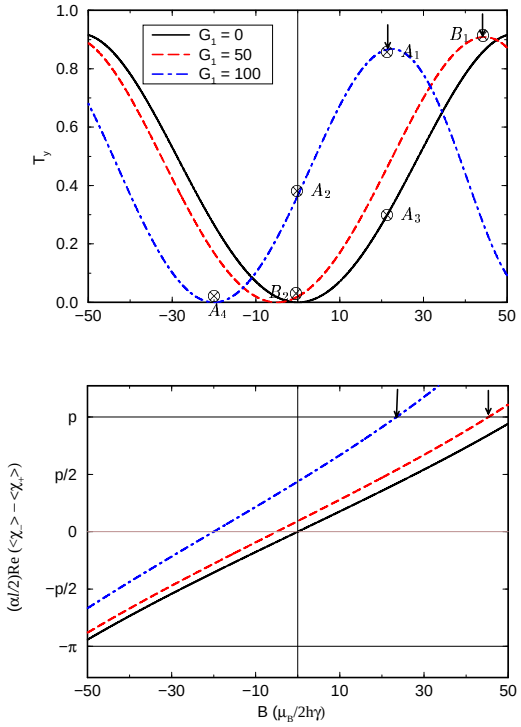

Figure 4.5: (a) The plot of T_y as a function of B to investigate the role of magnetic field. This plot corresponds to $\delta = -250$ (in the region IV of Fig. 4.4). All other parameters are same as in Fig. 4.4. (b) The asymmetry between $\langle s^+ \rangle$ and $\langle s^- \rangle$ is plotted as a function of B corresponding to the plots of T_y in (a). The points marked by the arrows satisfy the condition for maximal rotation (4.28).

the control field one can produce same T_y. This could be advantageous as it is difficult to get large magnetic fields in laboratory. Further using the large enhancements (η) of MOR it is possible to realize a *magneto-optical switch,* that can switch the incident polarization of the probe to its orthogonal polarization [130].

4.6 MOR in Two-photon Resonance Condition

In this section we consider the enhancement of MOR when the σ_+ polarized control filed and the probe field are on two-photon resonance with $|e\rangle \leftrightarrow |g\rangle$ transition ($\Delta + \delta = 0$). Under this condition $\langle s^+ \rangle$ in Eq. (4.19) is modified which contains the control field parameters but the $\langle s^- \rangle$ remains unchanged. The argument of $\mathcal{W}$ function in Eq. (4.19) would reduce

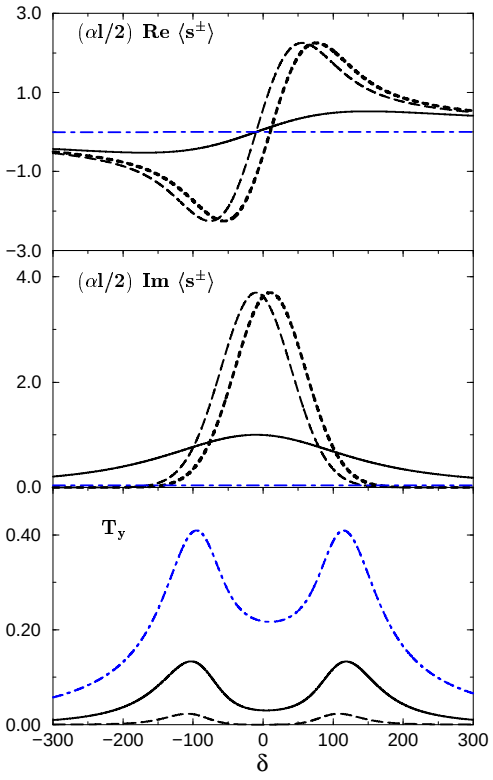

Figure 4.6: Enhancement of MOR in a Doppler broadened medium when the control field and the probe field are on two-photon resonance with $|e\rangle \leftrightarrow |g\rangle$ transition. The legends used are same as in Fig. 4.3, the solid line corresponds to $G_1 = 20$ and the dot dashed line corresponds to $G_1 = 100$. Here $G_1 = 100$ corresponds to the expansion in (4.33). The other parameters used in the plot are $\zeta = 10$ and $\alpha l = 300$.

to

$$\xi = \frac{1}{\sqrt{2}\omega_D}\left[-(\delta+\zeta) + i\left(\gamma + \frac{|G_1|^2}{\Gamma_o+\Gamma_1+\Gamma_2}\right)\right]. \tag{4.31}$$

In the limit $|G_1| \gg \omega_D,\ \xi \to \infty$. The asymptotic expansion of $\mathcal{W}$ function in terms of Γ function for $|\arg\xi| < 3\pi/4$ is given by [134]

$$\mathcal{W}(\xi) = \frac{i}{\pi}\left[\frac{\Gamma(1/2)}{\xi} + \frac{\Gamma(3/2)}{\xi^3} + ...\right];\ \ \Gamma(z) \equiv \int_0^\infty e^{-z}t^{z-1}\,dt. \tag{4.32}$$

Using the expansion (4.32) and retaining only the first order term, we get

$$\mathcal{W} \approx i\sqrt{\frac{2}{\pi}}\left(\frac{\omega_D}{-(\delta+\zeta) + i\frac{|G_1|^2}{\Gamma_o+\Gamma_1+\Gamma_2}}\right). \tag{4.33}$$

Therefore $\langle s^+ \rangle$ in Eq. (4.19) reduces to

$$\langle s^+ \rangle \equiv \langle s_c^+ \rangle = \frac{i\gamma}{\frac{|G_1|^2}{\Gamma_o+\Gamma_1+\Gamma_2} + i(\delta+\zeta)}. \tag{4.34}$$

This value of $\langle s^+ \rangle$ is equal to the corresponding stationary atom value in s^+ in Eq. (3.19). However, note that $\langle s^- \rangle$ [in Eq. (4.18)] is still velocity dependent. In the above limit, large power broadening is introduced in $\langle s^+ \rangle$ and amplitude of $\langle s_c^+ \rangle$ is reduced. However, this turns out to be advantageous, particularly because large asymmetry is created between $\langle s_c^+ \rangle$ and $\langle s^- \rangle$ around $\delta = \zeta$. And since $\langle s^- \rangle$ is Doppler broadened and $\langle s_c^+ \rangle$ is reasonably small and flat for a broad range of δ, one gets large enhancement in of T_y for a broad range of probe frequencies compared to the homogeneously broadened case. Further, MOR in two-photon resonance condition turns out to be advantageous for smaller magnetic fields where very large enhancement of MOR is obtained.

4.7 Summary

We have shown how a control field can be used to control birefringence and hence enhance MOR in a Doppler broadened medium. We have shown how control laser can modify the susceptibilities and hence result significantly large MOR in frequency regions, where MOR otherwise is small. The key to large enhancement of MOR consists of utilizing EIT and also using large asymmetry in the susceptibilities at the Autler-Townes components. We have derived conditions to select frequency regions where one can obtain large MOR. The most useful regions are the probe at frequencies - where absorptions of both the circularly polarized components are negligible and dispersions of the two circularly polarized components are quite different. We have substantiated these analytical results using many numerical plots for many different parameters at different conditions.

Chapter 5

Vacuum Induced Coherences

5.1 Introduction

So far we have discussed how control laser can be used to produce the required coherence in atomic systems. However in this section we will consider a completely different situation: to create atomic coherences by the interaction of the atom with the vacuum (zero-point) fluctuations of EM field. In contrast to the single mode laser field with very large mode density, vacuum field contains all the modes of the EM spectrum with a fairly flat mode distribution, and with a very short correlation time. Hence the interaction of an atom in its excited state with vacuum results an incoherent emission - the spontaneous emission. Dicke [135] was first to report a coherent radiation by collective interaction of two-level atoms with the vacuum field, when atoms were prepared in certain specific states. Considering the entire collection of atoms as single quantum mechanical entity, he found that the individual atoms cooperate to emit radiation at a rate which is much greater than their incoherent (spontaneous) emission rate. In Chapter 6, we will discuss the effect of collective interaction in spontaneous emission in detail, in which we show that such interactions can produce *new coherences* in multilevel systems.

A single multilevel atom having closely lying states (with the energy level separation of the order of natural line width) can also produce quantum coherences in the spontaneous emission from those closely lying states. This is due to the fact that, both the decay channels are coupled via the same continuum of vacuum creating interfering path ways. The resulting coherence in the system is known as *vacuum induced coherence (VIC)*. Occurrence of this coherence was first shown by Agarwal in his excellent monograph [7]. However

some stringent conditions are required for VIC to occur, which we will discuss in detail in Sec. 5.4. In the following section we present a master equation technique which will be used to derive information about spontaneous emission.

5.2 Master Equation Formulation

As mentioned in Sec. 1.1.2, master equation technique is useful to describe the interaction of atom with a field where the atomic evolution could affect the field state and vice-versa [136]. We use the *Zwanzing projection operator technique* [137] to derive the master equation following the the method developed by Agarwal [7]. Let the density operator for the statistical states of a collection of atoms + vacuum-field coupled system be ρ_{A+F}, where A corresponds to atomic variables and F corresponds to the field variables of vacuum. In interaction picture, the operator ρ_{A+F} satisfies the Liouville Eq. (1.25)

$$\frac{\partial \rho_{A+F}(t)}{\partial t} = -\frac{i}{\hbar}\left[\tilde{\mathcal{H}}_{AF}(t), \rho_{A+F}(t)\right] = -i\mathcal{L}(t)\rho_{A+F}(t). \tag{5.1}$$

where $\mathcal{L}(t)... \equiv (1/\hbar)[\tilde{\mathcal{H}}_{AF}(t), ...]$ is a commutation operator known as Liouville operator. Here $\tilde{\mathcal{H}}_{AF}$ represents the the time dependent vacuum-atom interaction Hamiltonian. Generally our interest is to obtain useful information about either atom or field evolution. This is done by *projecting out the relevant part from ρ_{A+F} by taking trace over the irrelevant part*; e.g. $\rho_A \equiv \mathrm{Tr}_F \rho_{A+F}$. For this purpose we introduce a time independent projection operator $\wp$, such that $\wp^2 = \wp$. Let us choose $\wp \equiv \rho_F(0)\mathrm{Tr}_F$ and write the density operator ρ_{A+F} in terms of $\wp$ as

$$\rho_{A+F}(t) = \wp\rho_{A+F}(t) + (1-\wp)\rho_{A+F}(t). \tag{5.2}$$

Clearly the first term in the right hand side $\wp\rho_{A+F}$ would describe the atomic evolution and the second terms $(1-\wp)\rho_{A+F}$ would give the properties of the emitted radiation. Here we outline the derivation of master equation for ρ_A ($\wp\rho_{A+F}$).. We assume that at $t = 0$ the atom and field are uncoupled $\rho_{A+F}(0) = \rho_A(0)\rho_F(0)$. For the spontaneous emission problem, the initial state of the field is given by $\rho_F \equiv |\{0\}\rangle\langle\{0\}|$, where $|\{0\}\rangle$ represents the the vacuum of the field. Multiplying $\wp$ and $(1-\wp)$ from left hand side of Eq. (5.1), we get

$$\wp\frac{\partial \rho_{A+F}}{\partial t} = -i\wp\mathcal{L}(t)\wp\rho_{A+F}(t) - i\wp\mathcal{L}(t)(1-\wp)\rho_{A+F}(t), \tag{5.3a}$$

$$(1-\wp)\frac{\partial \rho_{A+F}}{\partial t} = -i(1-\wp)\mathcal{L}(t)\wp\rho_{A+F}(t) - i(1-\wp)\mathcal{L}(t)(1-\wp)\rho_{A+F}(t). \tag{5.3b}$$

Integrating (5.3b) formally and substituting in (5.3a) and on setting

$$\exp\left[-i(1-\wp)\int_0^\tau dt'\mathcal{L}(t')\right] \equiv U(\tau), \tag{5.4}$$

we get

$$\frac{\partial \wp\rho_{A+F}}{\partial t} = -i\wp\mathcal{L}(t)\int_0^t d\tau U(\tau)\mathcal{L}(t-\tau)\wp\rho_{A+F}(t-\tau). \tag{5.5}$$

In writing Eq. (5.5), we have used the following relations: $(1-\wp)\rho_{A+F}(0) = 0$, and also because $\mathcal{L}$ is linear in the creation ($a_{ks}^\dagger$) and annihilation (a_{ks}) operators of the vacuum field, $\wp\mathcal{L}(t)\wp = 0$. Further Born approximation is made which is due to the weak coupling of the vacuum field with the atomic transition such that to the lowest order $U(\tau) \to 1$. This would physically mean the emitted photon does not react back with the atom. This approximation, however, is not valid for atom interacting with vacuum of a high Q cavity. With the above approximation and in the long time limit we get

$$\frac{\partial \rho_A}{\partial t} = -\frac{i}{\hbar^2}\lim_{t\to\infty}\int_0^t d\tau \mathrm{Tr}_F\left[\tilde{\mathcal{H}}_{AF}(t),[\tilde{\mathcal{H}}_{AF}(t-\tau),\rho_F(0)\rho_A(t-\tau)]\right]. \tag{5.6}$$

This is a simplified form of Zwanzing's master equation. From (5.6) we note that the evolution of $\rho_A(t)$ at t would depend on its value at all previous times. However since vacuum field has very short correlation time, we make the Markoff approximation which would imply replacing $\rho_A(t-\tau)$ by $\rho_A(t)$ inside the integral of (5.6). We will derive the explicit form of master equation for the systems of our interest in Chapters 6 and 7. However, in next section we present a master equation for a typical three level system to demonstrate the origin of coherences in spontaneous emission.

5.3 Origin of VIC and The Effects

Let us consider a V system with two excited states of the $|1\rangle$ and $|2\rangle$ which decay decay to the common ground state $|g\rangle$. The total Hamiltonian that describes the atom and vacuum field system is given by

$$\mathcal{H} = \mathcal{H}_A + \mathcal{H}_F + \mathcal{H}_{AF} \tag{5.7}$$

where

$$\begin{aligned}
\mathcal{H}_A &= \hbar\omega_{1g}A_{11} + \hbar\omega_{2g}A_{22}, && (5.8)\\
\mathcal{H}_F &= \sum_{k,s} \hbar\omega_{ks} a^\dagger_{ks} a_{ks}, && (5.9)\\
\mathcal{H}_{AF} &= -\vec{d}\cdot\vec{E}_v(\vec{r}) = -(\vec{d}_{1g}A_{1g} + \vec{d}_{1g}A_{1g} + \text{H.c.})\cdot\vec{E}_v(\vec{r}); && (5.10)
\end{aligned}$$

where A_ij and $\vec{d}_{ij}$ represent projection operator and dipole operators respectively, as defined in Sec. 1.2.1. Here the quantized vacuum field $\vec{E}_v(\vec{r})$ is given by

$$\vec{E}_v(\vec{r}) = i\sum_{ks}\left(\frac{2\pi\hbar\omega_{ks}}{V}\right)^{1/2}\hat{\epsilon}_{ks}a_{ks}e^{i\vec{k}\cdot\vec{r}} + H.c., \tag{5.11}$$

where a_{ks} ($a^\dagger_{ks}$) denotes the photon annihilation (creation) operator for the k^{th} mode and polarization index s. The corresponding field polarization vector is $\hat{\epsilon}_{ks}$. The interaction Hamiltonian in the interaction picture is given by

$$\begin{aligned}
\tilde{\mathcal{H}}_{AF}(t) &= e^{i(\mathcal{H}_A+\mathcal{H}_F)t/\hbar}\,\mathcal{H}_{AF}\,e^{-i(\mathcal{H}_A+\mathcal{H}_F)t/\hbar}\\
&= -\hbar\sum_{ks}\left[a_{ks}(g_{1_{ks}}A_{1g}e^{i\omega_{1g}t} + g_{2_{ks}}A_{2g}e^{i\omega_{2g}t}) + H.c.\right], && (5.12)
\end{aligned}$$

where

$$g_{j_{ks}} = i\left(\frac{2\pi\omega_{ks}}{\hbar V}\right)^{1/2}\vec{d}_{jg}\cdot\hat{\epsilon}_{ks}e^{i\vec{k}\cdot\vec{r}} \tag{5.13}$$

is often called the vacuum Rabi coupling coefficient corresponding to $|j\rangle \leftrightarrow |g\rangle$ transition and ω_{ks} mode. In writing (5.12), we have used the RWA approximation, i.e., we have ignored terms like $a_{ks}A_{gj}$ and $a^\dagger_{ks}A_{jg}$, which can also be understood as neglecting the anti-resonant terms in the Hamiltonian. However it may be noted that using RWA on the Hamiltonian, one looses the information of the Lamb shift associated with the ground state. Therefore if one is interested to get complete information about the shifts associated with spontaneous decays, one should make RWA on the final master equation (See appendix A of [7]). Substituting Eq. (5.12) in Eq. (5.6) and using following trace algebra of field operators inside the integral of (5.6)

$$\begin{aligned}
\text{Tr}_f(\rho_f a^\dagger_{ks}a_{k's'}) = 0,\ \text{Tr}_f(\rho_f a_{ks}a^\dagger_{k's'}) = \delta_{kk'}\delta_{ss'},\\
\text{Tr}_f(\rho_f a_{ks}a_{k's'}) = \text{Tr}_f(\rho_f a^\dagger_{ks}a^\dagger_{k's'}) = 0, && (5.14)
\end{aligned}$$

we get the master equation for our system

$$\begin{aligned}\frac{\partial \rho_A}{\partial t} = & - \sum_{j=1,2} \gamma_j \left(A_{jj}\rho - 2A_{gg}\rho_{jj} + \rho A_{jj} \right) \\ & - \left[\beta \left(A_{12}\rho - 2A_{gg}\rho_{21} + \rho A_{12} \right) e^{2i\zeta t} + H.c. \right]. \end{aligned} \tag{5.15}$$

Here $\gamma_j = 2|\vec{d}_{jg}|^2\omega_{jg}^3/(3\hbar c^3)$ denotes the spontaneous decay rates from the states $|j\rangle$ to the state $|g\rangle$ and 2ζ is the separation between the excited states. It may be noted that in writing (5.15) we have dropped the Lamb shift terms associated with the spontaneous emissions. The coupling coefficient β that couples the coherence terms of the density matrix with the population terms in (5.15) has the form

$$\beta = \pi \sum_{k,s} g_{1_{ks}} g^*_{2_{ks}} \delta(\omega_0 - \omega_k); \tag{5.16}$$

where ω_0 is the atomic frequency; $\omega_{1g} \simeq \omega_{2g} \equiv \omega_0$ is assumed. From (5.15), one can write explicitly the equation for the density matrix element that represent coherence

$$\frac{\partial \rho_{12}}{\partial t} = -(\gamma_1 + \gamma_2)\rho_{12} - \beta(\rho_{11} + \rho_{22})e^{2i\zeta t}. \tag{5.17}$$

Clearly if the system is initially prepared in either of the excited states, coherence will evolve in the system only if the coupling term β is non-zero. For example, if the system is initially in state $|1\rangle$, then to lowest order in β and for $t \simeq 0$, the soultion of (5.17 gives

$$\rho_{12}(t) \equiv \frac{\beta}{2(\gamma_1 - i\zeta)}[e^{-2(\gamma_1 - i\zeta)t} - 1]. \tag{5.18}$$

Thus it is clear from (5.18) that coherence between the upper states evolve for $\beta \neq 0$. We will discuss the physical meaning of this cross coupling term β in Sec. 5.4, which puts certain constraint on the system in which VIC can occur. In the following we discuss the remarkable consequences of this coherence reported in many recent literatures.

It was first shown by Agarwal [7] that the population gets trapped in degenerate V system due to the above mentioned coherences in the decay channels. For non-degenerate V systems, Cardimona *et al* [138] showed that probe absorption at certain frequency can become zero due to VIC. Recently, there has been renewed interest in this subject particularly in the context of coherently driven systems [138, 139, 140, 141]. Harris and Imamoğlu were the first to discover the possibility of achieving lasing without population inversion in systems where two excited states were coupled to a common continuum [70, 142] (See

also [143, 144]). It has also been observed that narrowing of spontaneous emission can be obtained by making use of the VIC [139, 145]. Quantum beat has been observed in spontaneous emission which showed pronounced beat structures determined by the energy separation of the closely lying states [146, 147, 148]. The VIC also leads to cancellation of spontaneous emission [149, 150, 151]. Zhu and coworkers have experimentally demonstrated the quenching of spontaneous emission in sodium dimers [149]. Further Scully, Zhu and coworkers proposed many schemes with different configurations demonstrating the possibility of obtaining quenching of spontaneous emission [150]. It was also reported that in the presence of VIC, the resonance fluorescence [152, 153] and other spectral line shapes [141] become sensitive to the phase of the control laser. Knight and coworkers [153] have demonstrated the possibility of controlling spontaneous emission by varying the relative phase of two control lasers in a four-level system.

5.4 Condition for VIC to Occur

In the previous section we showed that VIC can occur in a typical V system via the coupling coefficient β given by Eq. (5.16) Substituting $g_{j_{ks}}$ from (5.13) in Eq. (5.16) and carrying out the summation over two orthogonal polarization modes, for a given k, we get

$$\begin{aligned} \beta &\propto \sum_s (\vec{d}_{1g} \cdot \hat{\epsilon}_{ks})(\vec{d}^{*}_{2g} \cdot \hat{\epsilon}^{*}_{ks}) \\ &\equiv \vec{d}_{1g} \cdot \vec{d}^{*}_{2g}. \end{aligned} \tag{5.19}$$

The summation over the polarization components in (5.19) are evaluated using the relation

$$\sum_s (\hat{\epsilon}_{ks})_\mu (\hat{\epsilon}^{*}_{ks})_\nu \equiv \delta_{\mu\nu} - \hat{k}_\mu \hat{k}_\nu, \tag{5.20}$$

where $\hat{k}_l$ represents the direction cosine of $\vec{k}/|\vec{k}|$ along the l^{th} Cartesian axis. From Eq. (5.19) it is clear that the condition for the VIC to occur is

$$\vec{d}_{1g} \cdot \vec{d}^{*}_{2g} \neq 0, \tag{5.21}$$

i.e., VIC can occur in an atomic system if the transition dipole matrix elements involved with the decay channels are *non-orthogonal*. Note that all the above condition is also valid for VIC to occur in Λ systems (see for example [141]).

The question arises - what are the systems for which the condition (5.21) holds ? Consider, for example, the $j = 1 \rightarrow j = 0$ transition in an atomic system. Let $|1\rangle$, $|2\rangle$ and $|g\rangle$ in the above example denote the states $|j = 1, m = 1\rangle$, $|j = 1, m = -1\rangle$ and $|j = 0, m = 0\rangle$ respectively. In this case, simple algebra shows that

$$\langle 0,0|\vec{d}|1,1\rangle \cdot \langle 1,-1|\vec{d}|0,0\rangle = -\frac{|\vec{d}|^2}{2}(\hat{x} + i\hat{y}) \cdot (\hat{x} - i\hat{y})^* = 0, \tag{5.22}$$

where d is the reduced dipole matrix element. Thus, the interference between two decay channels $|1,1\rangle \rightarrow |0,0\rangle$ and $|1,-1\rangle \rightarrow |0,0\rangle$ will not occur. Several proposals have been made to achieve the non-orthogonality in atomic dipole matrix elements [147, 148, 149, 151, 154, 155, 156]. Xia *et al* [149] have found states in sodium dimer where the spin-orbit coupling makes the dipole matrix elements to satisfy (5.21), Schmidt and Imamoğlu [154] have shown that the condition (5.21) can be met using a r.f. field, and Berman has shown this possibility using a d.c. field [151]. In another recent paper Agarwal [155] has shown that atoms when interact with an anisotropic vacuum can also show VIC, even though the transition dipole matrix elements do not satisfy (5.21).

5.5 Summary and Perspectives

In summary, we have shown: (a) how vacuum can create coherence in an atom? (b) What is the origin of this coherence? And (c) what are the conditions required for this coherence to occur? In the following chapters we will consider VIC in different situations. In Chapter 6 we will consider how radiative coupling between two V systems in free space, with transition dipole matrix elements that do not satisfy (5.21), can also produce VIC [156]. In Chapter 7 and 8, we will investigate the case of non-orthogonality and resulting coherence effects in four level atomic system. The system, we consider, consists of a singlet ground state and a singlet excited state and two closely lying intermediate states - the upper part is like a Λ system and lower part is like a V system. The motivation for selection of this particular scheme is: the coherence can be introduced in the upper Λ part of the system and its manifestation can be observed in the lower V part. Thus *the cause and effect channels are clearly distinguished*. We propose methods by which one can bypass [148] the condition (5.21) [in Chapter 7] or create states [147] that satisfy (5.21) [in Chapter 8] to bring in coherences in spontaneous emission.

Chapter 6

Vacuum Induced Coherences in Radiatively Coupled Multilevel Systems

6.1 Introduction

All the studies on VIC [138-155] discussed in the previous chapter, deal with a *single* multilevel atom or equivalently with an ensemble of non-interacting multilevel atoms - e.g., very low density atomic gas systems. However, VIC in *coupled* atomic systems has remained unexplored. In this Chapter, we consider the role of VIC in *two radiatively coupled multilevel atoms*. The average inter-atomic distance, in case of low density atomic gas systems, is much larger compared to the wavelength of the emitted radiation. However, when the inter-atomic distance becomes comparable to the wavelength, the dipole-dipole (*dd*) coupling between the atoms via vacuum gives rise to collective effects. Our usage of *dd* interaction should be understood in the sense of retarded (and complex) dipole-dipole interaction. The classic example of such collective effect is Dicke superradiance [135, 157], where the atoms in their excited state decay much faster compared to that of a single atom. The collective effects in atoms have been extensively studied [157-169]. Recently experiments have been reported to observe collective behavior with two identical atoms [158, 159]. The *dd* interaction has been shown to produce two-photon resonance [160] and frequency shifts in emission [161]. The energy exchange between two coupled systems is discussed in [162]. Many interesting features of *dd* interaction in the context of atoms interacting with a squeezed vacuum [163], and inside bandgap materials [164] have been reported. Mayer and Yeoman [165] have considered two-atom laser in the presence

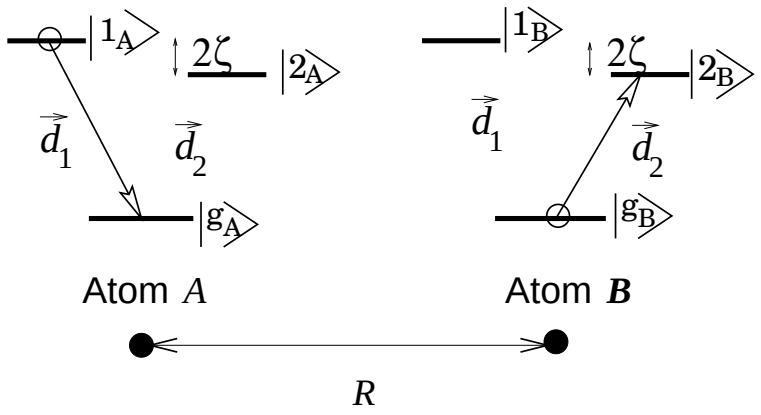

Figure 6.1: The two identical V systems under consideration. The distance between the two atoms is R. The transition dipole matrix elements $\vec{d}_1$ and $\vec{d}_2$ are chosen to be orthogonal with each other. The energy separation between the excited states is $2\hbar\zeta$. We discuss the situation where initially atom A is in excited state $|1_A\rangle$ and atom B is in ground state $|g_B\rangle$. Possibility of *dd* interaction induced excitation in the $|g_B\rangle \rightarrow |2_B\rangle$ transition is indicated.

of the atom-atom interaction. Quantum jump from two dipole interacting V-systems giving rise to new fluorescence periods has been reported by Hegerfeldt and coworkers [166]. Meystre and coworkers [167] found that the *dd* interaction leads to the occurrence of dark states in the fluorescence of two moving atoms [168]. Finally note that the local field effects in a dense media are also due to *dd* interaction [169]. All the *dd* interaction related effects can be understood as a consequence of the exchange of virtual photons between the atoms. Most of the existing literature concerns two-level atoms.

In this Chapter, we consider two identical V-systems having two closely lying excited states (as shown in Fig. 6.1). The two atoms get coupled by the exchange of radiation. We would specifically show how the radiative coupling in multilevel systems can lead to a population transfer from $|1_A\rangle$ to $|2_B\rangle$ even if the corresponding transition dipole matrix elements are orthogonal [156].

6.2 Dynamical Evolution of Two V-systems

We consider [Fig. 6.1] two identical V-systems (say A and B) in free space, having two near-degenerate excited states $|1_\mu\rangle$ and $|2_\mu\rangle$ ($\mu = A, B$) with the level separation $2\hbar\zeta$. The ground states of the atoms are represented by $|g_\mu\rangle$. Let ω_{1g} and ω_{2g} be the atomic frequen-

cies corresponding to $|1_\mu\rangle \leftrightarrow |g_\mu\rangle$ and $|2_\mu\rangle \leftrightarrow |g_\mu\rangle$ transitions respectively. Let the position vectors of the atoms be $\vec{x}_A$ and $\vec{x}_B$. Both the atoms couple with the vacuum field, which is given by

$$\vec{E}_v(\vec{x}) = \vec{E}^{(+)}(\vec{x}) + \vec{E}^{(-)}(\vec{x}); \tag{6.1}$$

where $\vec{E}^{(+)}$ ($\vec{E}^{(-)}$) represents the positive (negative) frequency part the vacuum field at $\vec{x}$ and is defined as

$$\vec{E}^{(+)}(\vec{x}) = \sum_{k,s} i \left(\frac{2\pi\hbar\omega_k}{V}\right)^{1/2} \hat{a}_{ks}\hat{\epsilon}_{ks}e^{i\vec{k}.\vec{x}}, \tag{6.2}$$

and $\vec{E}^{(-)}$ is the Hermitian conjugate of $\vec{E}^{(+)}$. Here the symbols have the usual meaning as in Eq. (5.11).

Now let us consider the following physical process: Initially atom A is taken to be in excited state $|1_A\rangle$ and the second atom in ground state $|g_B\rangle$. To highlight the effect of new interference terms, we specifically consider the case when the two transition dipole matrix elements $\vec{d}_1$ and $\vec{d}_2$ are orthogonal to each other. In the absence of atom B, the VIC cannot be created in the excited states of atom A because the transition dipole matrix elements $\vec{d}_1$ and $\vec{d}_2$ are orthogonal [see Eq. (5.21)]. However, the radiative coupling can lead to evolution of the excited state coherences. We will also show a manifestation of this coherence in the dynamical evolution of the atomic population.

The total Hamiltonian for the atoms and the field system is given by

$$\mathcal{H} = \mathcal{H}_A + \mathcal{H}_F + \mathcal{H}_{AF}, \tag{6.3}$$

where the unperturbed Hamiltonian for the atoms and field are

$$\mathcal{H}_A = \hbar \sum_{\mu=A,B} \left(\omega_{1g}\hat{\alpha}^\dagger_\mu\hat{\alpha}_\mu + \omega_{2g}\hat{\beta}^\dagger_\mu\hat{\beta}_\mu\right), \tag{6.4}$$

$$\mathcal{H}_F = \sum_{ks} \hbar\omega_{ks}\hat{a}^\dagger_{ks}\hat{a}_{ks}, \tag{6.5}$$

and the interaction Hamiltonian is

$$\begin{aligned} \mathcal{H}_{AF} &= -\vec{d}.\vec{E}_v \\ &= -\sum_{\mu=A,B}\sum_{j=1}^{2}\left[\vec{d}^{(\mu)}_{jg}\cdot\vec{E}_v(\vec{x}_\mu) + \text{H.c.}\right] \quad (\mu = A,\ B). \end{aligned} \tag{6.6}$$

The atomic transition operators introduced in (6.4), are given by

$$\begin{aligned}\hat{\alpha}_\mu &\equiv |g_\mu\rangle\langle 1_\mu|, \;\; \hat{\beta}_\mu \equiv |g_\mu\rangle\langle 2_\mu|, \\ \hat{\alpha}_\mu^\dagger &\equiv |1_\mu\rangle\langle g_\mu|, \;\; \hat{\beta}_\mu^\dagger \equiv |2_\mu\rangle\langle g_\mu|. \end{aligned} \tag{6.7}$$

Thus $\hat{\alpha}_\mu, \hat{\alpha}_\mu^\dagger$ ($\hat{\beta}_\mu, \hat{\beta}_\mu^\dagger$) represent the atomic lowering and raising operators respectively corresponding to the $|1_\mu\rangle \leftrightarrow |g_\mu\rangle$ ($|2_\mu\rangle \leftrightarrow |g_\mu\rangle$) transition. The dipole matrix elements are represented by

$$\vec{d}_{jg}^{(\mu)} = \vec{d}_j^{(\mu)} |j_\mu\rangle\langle g_\mu|. \tag{6.8}$$

For simplicity we consider a situation where the transition dipole matrix elements of atom A are parallel to the transition dipole matrix elements of atom B, i.e.,

$$\vec{d}_{1g}^{(A)} \,||\, \vec{d}_{1g}^{(B)} \;\text{ and }\; \vec{d}_{2g}^{(A)} \,||\, \vec{d}_{2g}^{(B)}. \tag{6.9}$$

We also assume that

$$\vec{d}_{1g}^{(A)} \cdot \vec{d}_{2g}^{(A)^*} = 0. \tag{6.10}$$

Thus the index μ in the right hand side of Eq. (6.8) can be dropped and the dipole matrix elements can be rewritten as

$$\vec{d}_{jg}^{(\mu)} = \vec{d}_j |j_\mu\rangle\langle g_\mu|. \tag{6.11}$$

Here we note that $\vec{d}_j$, in general, can be complex (see for example Sec. V). Using Eq. (6.11), the interaction Hamiltonian in (6.6) can be reduced to

$$\mathcal{H}_{AF} = -\sum_{\mu=A,B} \left[\left(\vec{d}_1 \hat{\alpha}_\mu^\dagger + \vec{d}_2 \hat{\beta}_\mu^\dagger \right) \cdot \vec{E}_v(\vec{x}_\mu) + \text{H.c.} \right]. \tag{6.12}$$

We work in the interaction picture by transforming (6.12) to

$$\begin{aligned}\tilde{\mathcal{H}}_{AF}(t) &= e^{\frac{i}{\hbar}(\mathcal{H}_A + \mathcal{H}_F)t} \mathcal{H}_{AF} e^{-\frac{i}{\hbar}(\mathcal{H}_A + \mathcal{H}_F)t} \\ &= -\sum_{\mu=A,B} \left[\left(\vec{d}_1 \hat{\alpha}_\mu^\dagger e^{i\omega_{1g}t} + \vec{d}_2 \hat{\beta}_\mu^\dagger e^{i\omega_{2g}t} \right) \cdot \left(\vec{E}^{(+)}(\vec{x}_\mu, t) + \vec{E}^{(-)}(\vec{x}_\mu, t) \right) + \text{H.c.} \right]; \end{aligned} \tag{6.13}$$

where,

$$\vec{E}^{(+)}(\vec{x}_\mu, t) = \sum_{k,s} i \left(\frac{2\pi\hbar\omega_k}{V} \right)^{1/2} \hat{a}_{ks} \hat{\epsilon}_{ks} e^{i(\vec{k}\cdot\vec{x}_\mu - \omega_k t)} \;\text{ and }\; \vec{E}^{(-)}(\vec{x}_\mu, t) = [\vec{E}^{(+)}(\vec{x}_\mu, t)]^\dagger. \tag{6.14}$$

Let the density operator of the combined atom-field system in the interaction picture be represented by $\rho_{A+F}(t)$ which satisfies the Liouville equation of motion

$$\frac{\partial \rho_{A+F}}{\partial t} = -\frac{i}{\hbar}\left[\tilde{\mathcal{H}}_{AF}(t), \rho_{A+F}\right]. \tag{6.15}$$

To derive useful information about the evolution of the atomic system, we derive a master equation for the reduced atomic operator by using the standard projection operator techniques [7]. We make following approximations in deriving the master equation: (a) at $t = 0$, $\rho_{A+F}(0)$ can be factorized into a product of atom [ρ_A] and field [ρ_F] density operators, i.e., $\rho_{A+F}(0) \equiv \rho_A(0)\rho_F(0)$. Furthermore, we invoke (b) the Born approximation and (c) the Markoff approximation. The Born approximation depends on the weak coupling between the vacuum and the atoms. The Markoff approximation holds because the vacuum has fairly flat density of states. Using the above approximations and tracing over the field states, the density matrix equation for the atoms becomes

$$\frac{\partial \rho_A}{\partial t} = -\frac{1}{\hbar^2}\lim_{t\to\infty}\int_0^t d\tau \mathrm{Tr}_F\left[\tilde{\mathcal{H}}_{AF}(t), [\tilde{\mathcal{H}}_{AF}(t-\tau), \rho_F(0)\rho_A]\right]. \tag{6.16}$$

The trace over the field operators inside the integral in Eq. (6.16) is calculated using the relations Eq. (5.14). One also uses the rotating wave approximation (RWA) to drop the anti-resonant terms like $\hat{\alpha}_\mu\hat{\alpha}_\mu$, $\hat{\alpha}^\dagger_\mu\hat{\alpha}^\dagger_\mu$, $\hat{\beta}_\mu\hat{\beta}_\mu$ and $\hat{\beta}^\dagger_\mu\hat{\beta}^\dagger_\mu$ in (6.16). Using the above conditions and carrying out a long algebra, we obtain the master equation for the atomic density operator

$$\begin{aligned}
\frac{\partial \rho}{\partial t} = &- \left[\left\{\gamma_1 \sum_{\mu=A,B}\left(\hat{\alpha}^\dagger_\mu\hat{\alpha}_\mu\rho - 2\hat{\alpha}_\mu\rho\hat{\alpha}^\dagger_\mu + \rho\hat{\alpha}^\dagger_\mu\hat{\alpha}_\mu\right)\right\} + 1\to 2,\ \alpha\to\beta\right] \\
&- \left[\Gamma_1\left\{(\hat{\alpha}^\dagger_A\hat{\alpha}_B\rho - 2\hat{\alpha}_B\rho\hat{\alpha}^\dagger_A + \rho\hat{\alpha}^\dagger_A\hat{\alpha}_B) + \text{H.c.}\right\} + 1\to 2,\ \alpha\to\beta\right] \\
&+ \left[\left\{i\Omega_1[\hat{\alpha}^\dagger_A\hat{\alpha}_B, \rho] + \text{H.c.}\right\} + 1\to 2,\ \alpha\to\beta\right] \\
&- \left[\left\{\Gamma_{vc}\left(\hat{\beta}^\dagger_A\hat{\alpha}_B\rho - 2\hat{\alpha}_B\rho\hat{\beta}^\dagger_A + \rho\hat{\beta}^\dagger_A\hat{\alpha}_B\right)e^{-2i\zeta t} + \text{H.c.}\right\} + A\leftrightarrow B\right] \\
&+ \left[\left\{i\Omega_{vc}[\hat{\beta}^\dagger_A\hat{\alpha}_B, \rho]e^{-2i\zeta t} + \text{H.c.}\right\} + A\leftrightarrow B\right];
\end{aligned} \tag{6.17}$$

where,

$$\begin{aligned}
\gamma_j &= \sum_{k,s}\left(\frac{2\pi\omega_k}{\hbar V}\right)\pi\,\delta(\omega_0-\omega_k)|\vec{d}_j\cdot\hat{\epsilon}_{ks}|^2,\\
\Gamma_j &= \sum_{k,s}\left(\frac{2\pi\omega_k}{\hbar V}\right)\pi\,\delta(\omega_0-\omega_k)|\vec{d}_j\cdot\hat{\epsilon}_{ks}|^2 e^{i\vec{k}\cdot\vec{R}},\\
\Omega_j &= \sum_{k,s}\left(\frac{2\pi\omega_k}{\hbar V}\right)\left(\frac{1}{\omega_0-\omega_k}-\frac{1}{\omega_0+\omega_k}\right)|\vec{d}_j\cdot\hat{\epsilon}_{ks}|^2 e^{i\vec{k}\cdot\vec{R}},\\
\Gamma_{vc} &= \sum_{k,s}\left(\frac{2\pi\omega_k}{\hbar V}\right)\pi\,\delta(\omega_0-\omega_k)(\vec{d}_2\cdot\hat{\epsilon}_{ks})(\vec{d}_1\cdot\hat{\epsilon}_{ks})^* e^{i\vec{k}\cdot\vec{R}},\\
\Omega_{vc} &= \sum_{k,s}\left(\frac{2\pi\omega_k}{\hbar V}\right)\left(\frac{1}{\omega_0-\omega_k}-\frac{1}{\omega_0+\omega_k}\right)(\vec{d}_2\cdot\hat{\epsilon}_{ks})(\vec{d}_1\cdot\hat{\epsilon}_{ks})^* e^{i\vec{k}\cdot\vec{R}}.
\end{aligned} \tag{6.18}$$

Here, $\vec{R}=\vec{x}_{_A}-\vec{x}_{_B}$. Since the states $|1_\mu\rangle$ and $|2_\mu\rangle$ are closely lying, we have set $\omega_{1g}\cong\omega_{2g}\equiv\omega_0$. The suffix A of $\rho_{_A}$ in Eq. (6.17) has been dropped for brevity. We have also dropped the Lamb shift terms associated with the spontaneous emission of the individual atoms. The summation over the polarization components is evaluated using the Eq. (5.20). Taking the limit $V\to\infty$ and replacing the summation over k by integration over the continuum of the field modes, the terms in (6.18) become

$$\begin{aligned}
\gamma_j &= \frac{2|\vec{d}_j|^2}{g\hbar}\left(\frac{\omega_0}{c}\right)^3 \quad ,\\
\Gamma_j &= \frac{1}{\hbar}\,(\vec{d}_j\cdot\mathrm{Im}\ \vec{\vec{\chi}}\cdot\vec{d}_j^{\,*}) \quad , \quad \Omega_j=\frac{1}{\hbar}\,(\vec{d}_j\cdot\mathrm{Re}\ \vec{\vec{\chi}}\cdot\vec{d}_j^{\,*}),\\
\Gamma_{vc} &= \frac{1}{\hbar}\,(\vec{d}_2\cdot\mathrm{Im}\ \vec{\vec{\chi}}\cdot\vec{d}_1^{\,*}) \quad , \quad \Omega_{vc}=\frac{1}{\hbar}\,(\vec{d}_2\cdot\mathrm{Re}\ \vec{\vec{\chi}}\cdot\vec{d}_1^{\,*});
\end{aligned} \tag{6.19}$$

where $\vec{\vec{\chi}}$ is a tensor whose components are given by

$$\begin{aligned}
\chi_{\mu\nu}(\vec{x}_{_A},\vec{x}_{_B},\omega_0) &\equiv \left(k_0^2\delta_{\mu\nu}+\frac{\partial^2}{\partial x_{_{A\,\mu}}\partial x_{_{A\,\nu}}}\right)\frac{e^{ik_0R}}{R}\\
&\equiv \left[\delta_{\mu\nu}\left(\frac{k_0^2}{R}+\frac{ik_0}{R^2}-\frac{1}{R^3}\right)-R_\mu R_\nu\left(\frac{k_0^2}{R^3}+\frac{3ik_0}{R^4}-\frac{3}{R^5}\right)\right]e^{ik_0R},
\end{aligned} \tag{6.20}$$

where $k_0=\omega_0/c$ and $R=|\vec{x}_{_A}-\vec{x}_{_B}|$.

6.3 Interpretation of Different Terms in The Master Equation

The $2\gamma_j$ in Eq. (6.19) represents the single atom spontaneous decay rate from the state $|j\rangle$ to the state $|g\rangle$. Rest of the coefficients in (6.17) are related to the coupling between the two V-

systems. This coupling is produced by the exchange of a photon between the two systems. The dipole-dipole interaction manifests itself through the tensor $\vec{\vec{\chi}}$ defined by Eq. (6.20). The tensor $\vec{\vec{\chi}}_{\alpha\beta}\ (\vec{x}_{_A}, \vec{x}_{_B}, \omega)$ has the following meaning: It represents the α^{th} component of the electric field at the point $\vec{x}_{_A}$, produced by an oscillating dipole of unit strength along the direction β and located at the point $\vec{x}_{_B}$ [170]. In the limit $c \to \infty$ ($k_0 \to 0$), it reduces to the static dipole-dipole interaction. Γ_j and Ω_j represent the *dd* couplings which are related to the decay and level shift of the collective atomic states. These coefficients couple a pair of parallel dipoles and are well known [7], particularly in the context of collective effects in two level atoms. *The new coherence terms Γ_{vc} and Ω_{vc} are the dipole-dipole cross coupling coefficients, which couple a pair of orthogonal dipoles*. The meaning of such terms can be clearly understood by calculating the evolution of the population in the state $|g_{_A}, 2_{_B}\rangle$, given the initial condition $|1_{_A}, g_{_B}\rangle$. From the master equation (6.17), one can show that at $t \approx 0$,

$$\frac{\partial}{\partial t}\langle 1_{_A}, g_{_B}|\rho|g_{_A}, 2_{_B}\rangle = -(\Gamma^*_{vc} + i\Omega^*_{vc})e^{2i\zeta t}, \tag{6.21}$$

and hence

$$\begin{aligned}\frac{\partial}{\partial t}\langle g_{_A}, 2_{_B}|\rho|g_{_A}, 2_{_B}\rangle &= -(\Gamma_{vc} - i\Omega_{vc})e^{-2i\zeta t}\langle 1_{_A}, g_{_B}|\rho|g_{_A}, 2_{_B}\rangle \\ &\quad -(\Gamma^*_{vc} + i\Omega^*_{vc})e^{2i\zeta t}\langle g_{_A}, 2_{_B}|\rho|1_{_A}, g_{_B}\rangle \\ &= -2|\Gamma_{vc} - i\Omega_{vc}|^2\left(\frac{\sin 2\zeta t}{2\zeta}\right).\end{aligned} \tag{6.22}$$

Thus to the lowest order in Γ_{vc} and Ω_{vc}, we obtain

$$\langle g_{_A}, 2_{_B}|\rho|g_{_A}, 2_{_B}\rangle \approx 4|\Gamma_{vc} + i\Omega_{vc}|^2\left(\frac{\sin^2\zeta t}{4\zeta^2}\right). \tag{6.23}$$

Therefore the radiative process, in which atom A in the excited state $|1_{_A}\rangle$ loses its excitation which in turn excites atom B to the state $|2_{_B}\rangle$, is possible only because of Γ_{vc} and Ω_{vc} terms in the master equation (6.17). Note further that such terms start becoming insignificant as $2\hbar\zeta$ - the energy separation between the two excited states increases. Such interference terms occur in the master equation even when the transition dipole matrix elements $\vec{d}_1$ and $\vec{d}_2$ are orthogonal to each other. Such contributions come from the second term in Eq. (6.20). In the rest of the paper, we study in detail the various consequences of these interference terms which could be large and could significantly contribute to the dynamics of the system when the atomic separation is smaller than λ.

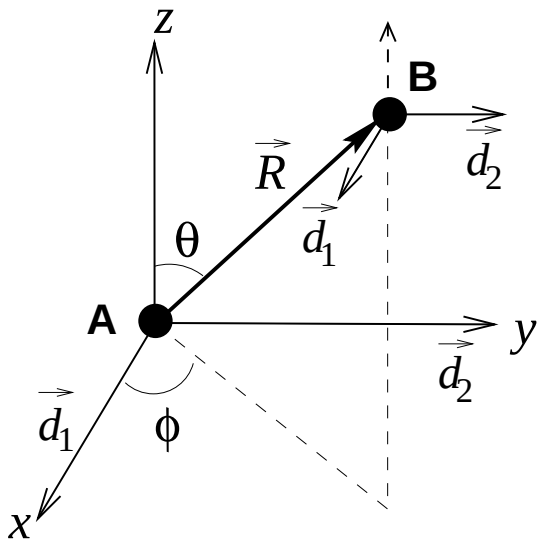

Figure 6.2: The geometry under consideration where the dipole matrix elements $\vec{d}_1$ and $\vec{d}_2$ are taken to be real and aligned along the x and y directions respectively.

Let us consider a geometry where atom A is placed at the origin of a Cartesian coordinate system and the position vector of atom B is $\vec{R}$ (as shown in Fig. 6.2). $\vec{R}$ makes an angle θ with the z axis. Let us assume $\vec{d_1} = \hat{x}d$ and $\vec{d_2} = \hat{y}d$. All the radiative coupling terms in the master equation can be written down explicitly as

$$\begin{aligned}
\Gamma_1 &= \frac{|d|^2}{\hbar}\mathrm{Im}\ \chi_{xx} = \frac{3\gamma}{2}(P_i - \sin^2\theta\cos^2\phi\, Q_i), \qquad \Omega_1 = \frac{|d|^2}{\hbar}\mathrm{Re}\ \chi_{xx} = \frac{3\gamma}{2}(P_r - \sin^2\theta\cos^2\phi\, Q_r),\\
\Gamma_2 &= \frac{|d|^2}{\hbar}\mathrm{Im}\ \chi_{yy} = \frac{3\gamma}{2}(P_i - \sin^2\theta\sin^2\phi\, Q_i), \qquad \Omega_2 = \frac{|d|^2}{\hbar}\mathrm{Re}\ \chi_{yy} = \frac{3\gamma}{2}(P_r - \sin^2\theta\sin^2\phi\, Q_r)\\
\Gamma_{vc} &= \frac{|d|^2}{\hbar}\mathrm{Im}\ \chi_{yx} = -\frac{3\gamma}{2}\sin^2\theta\sin\phi\cos\phi\, Q_i, \qquad \Omega_{vc} = \frac{|d|^2}{\hbar}\mathrm{Re}\ \chi_{yx} = -\frac{3\gamma}{2}\sin^2\theta\sin\phi\cos\phi\, Q_r;
\end{aligned} \tag{6.24}$$

where ϕ is defined as in the Fig. 6.2, and

$$\begin{aligned}
P_r &= \frac{\cos\xi}{\xi} - \frac{\sin\xi}{\xi^2} - \frac{\cos\xi}{\xi^3} \quad , \quad Q_r = \frac{\cos\xi}{\xi} - 3\frac{\sin\xi}{\xi^2} - 3\frac{\cos\xi}{\xi^3},\\
P_i &= \frac{\sin\xi}{\xi} + \frac{\cos\xi}{\xi^2} - \frac{\sin\xi}{\xi^3} \quad , \quad Q_i = \frac{\sin\xi}{\xi} + 3\frac{\cos\xi}{\xi^2} - 3\frac{\sin\xi}{\xi^3};\ \xi = k_0 R.
\end{aligned} \tag{6.25}$$

In the following, we examine the behavior of the cross coupling coefficients responsible for the new coherence effects in different geometries. In Fig. 6.3 we plot these coefficients as a function of the distance between the two atoms. In Fig. 6.3(a) we have plotted Γ_1 and Γ_{vc}, and in Fig. 6.3(b) we plot Ω_1 and Ω_{vc}, for comparison. Clearly, the values of the cross

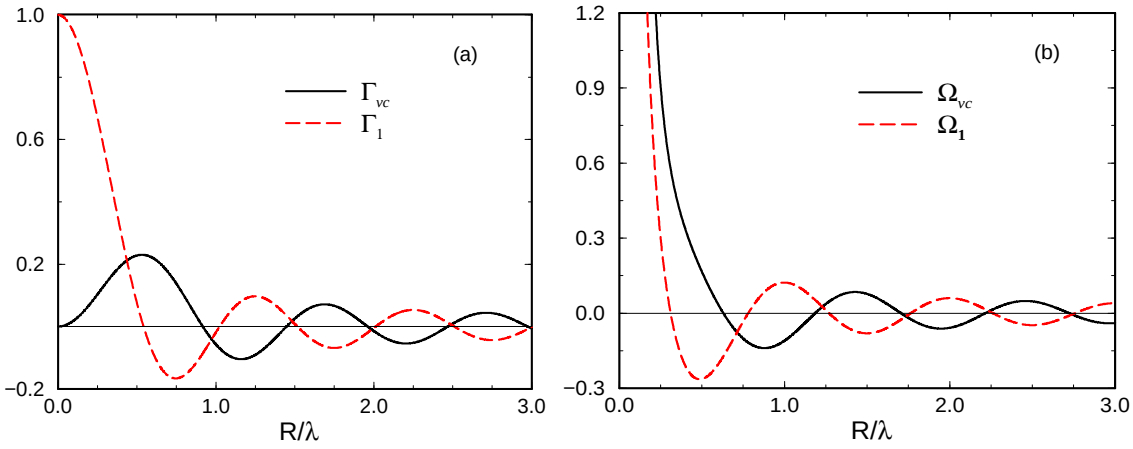

Figure 6.3: Plots of *dd*-coupling coefficients as a function of the atomic separation. Here $\theta = \pi/2$, i.e. both the atoms lie on the xy-plane and $\phi = \pi/4$. The new coherence terms Γ_{vc}, Ω_{vc} are comparable to Γ_j, Ω_j. All the coefficients are scaled with γ.

coupling coefficients are comparable with the Γ_j and Ω_j values. The value of Ω_{vc} becomes significantly large for $R < \lambda/2$. However for $R \to 0$, the terms Ω_j, Ω_{vc} diverge, whereas the terms $\Gamma_j, \Gamma_{vc} \to 1$.

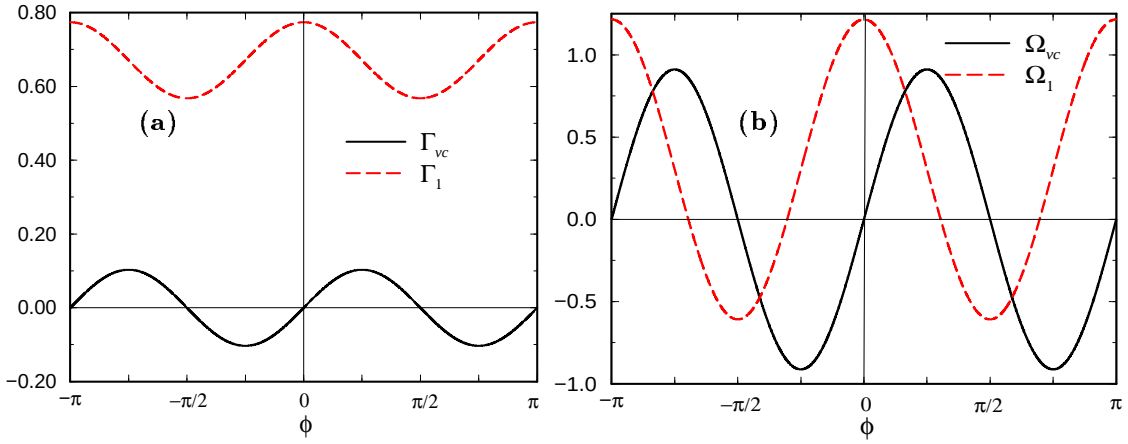

Figure 6.4: The *dd*-coupling terms as a function of the azimuthal angle ϕ. Here $\theta = \pi/2$ and the atomic separation is taken to be $\lambda/4$. All coefficients are scaled with γ.

Further, in Fig. 6.4 we examine the atomic position dependences of these coefficients. We have plotted the coupling coefficients as a function of ϕ. Here we have fixed $\theta = \pi/2$; i.e., both the atoms are lying in the xy-plane. Again for a comparison, we have plotted Γ_1 and Γ_{vc} in Fig. 6.4(a), and Ω_1 and Ω_{vc} in Fig. 6.4(b). We observe the following special cases:

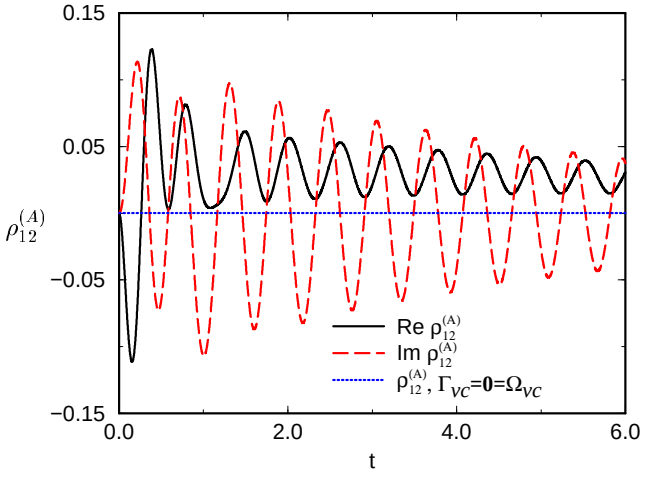

Figure 6.5: Time evolution of the coherence in the excited states of atom A with atom B being in $|g_{_B}\rangle$. The coherence evolves only for non-zero values of Γ_{vc} and Ω_{vc}. Large oscillations are seen in $\rho_{12}^{(A)}$ which is decided by $\Omega_j,\ \Omega_{vc}$, and ζ. The parameters used are $\theta = \pi/2,\ \phi = \pi/4,\ R = \lambda/2\pi$ and $2\zeta = 3\gamma$.

Case I: If $\theta = n\pi$, then $\Gamma_{vc} = \Omega_{vc} = 0$; i.e., if $\vec{R}$ is perpendicular to the plane containing $\vec{d}_1$ and $\vec{d}_2$, the interference terms in the master equation vanish.
Case II: When $\phi = n\pi/2$, the coherence terms $\Gamma_{vc} = \Omega_{vc} = 0$; i.e. when the second atom is placed in a position such that $\vec{R}$ is along one of the dipoles $\vec{d}_1$ or $\vec{d}_2$, then again the interference terms drop out. Thus the interference effects in the radiatively coupled systems are sensitive to the geometry.

6.4 Numerical Results

In this section we present the numerical results that demonstrate the effect of the interference terms on the dynamics of the radiatively coupled multilevel systems. We use fifth order Runge-Kutta method for the numerical solution of the master equation (6.17). For numerical solutions we use the initial condition that at $t = 0$, the first atom is in excited state $|1_{_A}\rangle$ and the second atom is in the ground state $|g_{_B}\rangle$.

In Fig. 6.5, we have plotted the density matrix element $\rho_{12}^{(A)} \equiv \langle 1_{_A}|\langle g_{_B}|\rho(t)|2_{_A}\rangle|g_{_B}\rangle$ which represents the coherence in the excited states of atom A when atom B is in ground state $|g_{_B}\rangle$. It is clear from Fig. 6.5 that the interference terms $\Gamma_{vc},\ \Omega_{vc}$ in the master equation

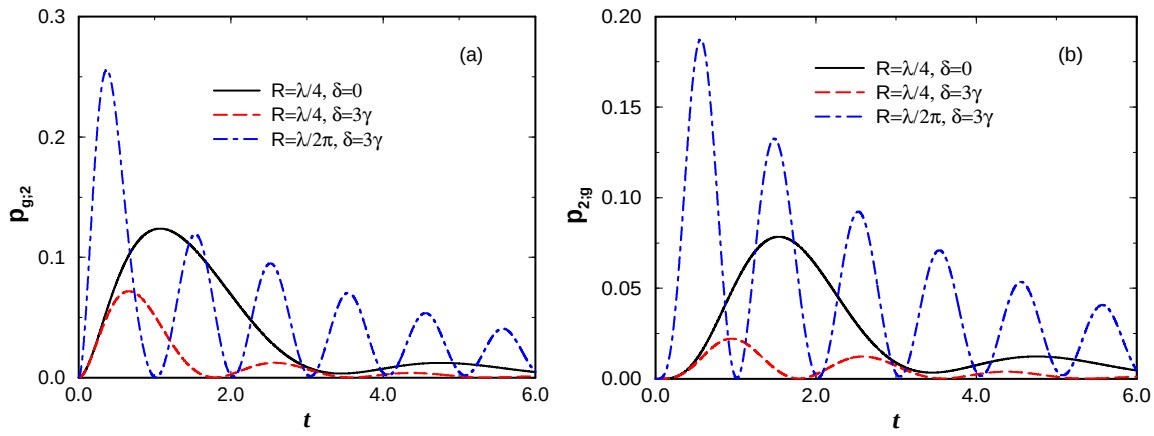

Figure 6.6: The time evolution of (a) $p_{g;2}$ and (b) $p_{2;g}$ are plotted for different parameters with the initial condition that atom A is in state $|1_A\rangle$ and atom B in $|g_B\rangle$. In both cases $\theta = \pi/2$ and $\phi = \pi/4$. The values of other parameters are shown as legends.

result in finite coherence in atom A. Otherwise, when $\Gamma_{vc} = \Omega_{vc} = 0$, such coherences vanish. It is important to note that this coherence is produced by the radiative coupling between two atoms even when the dipole matrix elements $\vec{d}_1$ and $\vec{d}_2$ are orthogonal.

In Figs. 6.6 and 6.7, we plot the probabilities that atom A is in state $|i_A\rangle$ and atom B is in $|j_B\rangle$, which we denote by $p_{i;j} \equiv \langle i_A|\langle j_B|\rho(t)|i_A\rangle|j_B\rangle$. In Fig. 6.6(a), we present $p_{g;2}(t)$ that represents the simultaneous probability of atom A being deexcited to state $|g_A\rangle$ and atom B being excited to the state $|2_B\rangle$. Fig. 6.6(b) is the plot of $p_{2;g}(t)$ that represents the probability that the atom A is excited to state $|2_A\rangle$ with atom B being in $|g_B\rangle$. Obviously both $p_{g;2}$ and $p_{2;g}$ become zero if $\Gamma_{vc} = \Omega_{vc} = 0$. It is observed that smaller is the atomic separation, larger is the excitation probability. For atomic separation $R = \lambda/2\pi$, the excitation probabilities are very large, e.g., more than 25% of the population in atom B could be excited to state $|2_B\rangle$ at $t \sim 0.3/\gamma$ (Fig. 6.6(a)) and, similarly in atom A, about 18.5% population could be excited to state $|2_A\rangle$ at $t \sim 0.5/\gamma$. Thus significant amount of energy transfer can take place between the states $|1_A\rangle$ and $|2_B\rangle$, though the corresponding transition dipoles are orthogonal to each other. Note that the initial evolution of $p_{2;g}$ is much slower compared to the evolution of $p_{g;2}$. This can be understood as follows: The excitation of atom B to the state $|2_B\rangle$ can be caused by a single photon transfer from A to B [the process $|1_A, g_B\rangle \rightarrow |g_A, 2_B\rangle$], whereas the excitation of atom A to the state $|2_A\rangle$ occurs only through atom B and this involves a net transfer of two photons [processes $|1_A, g_B\rangle \rightarrow |g_A, 2_B\rangle \rightarrow |2_A, g_B\rangle$ or

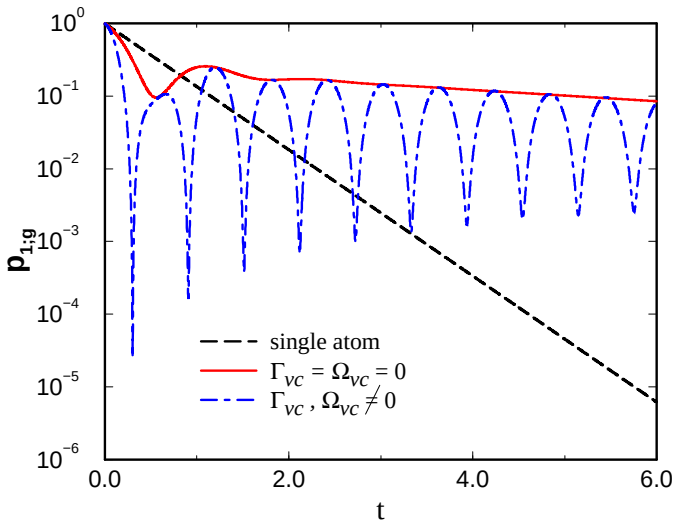

Figure 6.7: Plot of the probability that both atoms remain in their initial states. This probability is plotted on a logarithmic scale as a function of time in linear scale. The parameters used are $\theta = \pi/2,\ \phi = \pi/4,\ R = \lambda/4$ and $\zeta = 0$.

$|1_A, g_B\rangle \rightarrow |g_A, 1_B\rangle \rightarrow |2_A, g_B\rangle$]. The oscillatory character of $p_{g;2}$ and $p_{2;g}$ comes from non-vanishing ζ and from the *dd*-coupling coefficients Ω_j and Ω_{vc}. The excitation probabilities are seen to be larger for degenerate excited states ($\zeta = 0$) compared to that with finite separation between the excited states. For very large ζ ($>> \gamma$), this interference effect disappears.

In Fig. 6.7, we present a comparative study of the probability that atoms remain in their initial states, i.e. $p_{1;g}$, in the presence and absence of the *dd*-coupling terms. The probability of atom A staying in $|1_A\rangle$ decays exponentially in the absence of atom B. However, in the presence of the second atom, the nature of its decay is significantly modified - large oscillations are seen in $p_{1;g}$ in the presence of the new coherence terms, which is evident from Fig. 6.7. The origin of this oscillation is attributed to the large values of Ω_{vc}.

6.5 Two V-systems with magnetic sub-levels in the presence of a magnetic field

In this section we consider the new coherence effects in two V-systems with m-degenerate magnetic sub-levels as excited states. The system could be, for example, a ^{40}Ca system - where $4\ ^1P_1$ degenerate sublevels would correspond to the excited states $|1_\mu\rangle \equiv |j =$

$1, m = 1\rangle$ and $|2_\mu\rangle \equiv |j = 1, m = -1\rangle$, and the $4\,{}^1S_0$ state would correspond to the ground state $|g_\mu\rangle$. In this case the dipole matrix elements $\vec{d_1}$ and $\vec{d_2}$ are complex and orthogonal to each other, and are given by

$$\vec{d_1} = -d\hat{\epsilon}_-,\ \vec{d_2} = d\hat{\epsilon}_+;\ \hat{\epsilon}_\pm = \frac{\hat{x} \pm i\hat{y}}{\sqrt{2}}, \tag{6.26}$$

where d is the reduced dipole matrix element. The magnetic field produces a Zeeman splitting 2ζ and fixes the quantization axis (z axis in our case). The geometry can be taken to be the same as in Fig. 6.2. However in the present case, $\vec{d_1}$ and $\vec{d_2}$ being complex dipoles, they are not fixed along the real axes unlike in Fig. 6.2. Using Eq. (6.19), the *dd* coupling coefficients for this scheme can be obtained

$$\begin{aligned}
\Gamma_1 &= \Gamma_2 = \frac{|d|^2}{2\hbar}\mathrm{Im}\,(\chi_{xx} + \chi_{yy}) \equiv \frac{3\gamma}{4}(2P_i - \sin^2\theta Q_i), \\
\Omega_1 &= \Omega_2 = \frac{|d|^2}{2\hbar}\mathrm{Re}\,(\chi_{xx} + \chi_{yy}) \equiv \frac{3\gamma}{4}(2P_r - \sin^2\theta Q_r), \\
\Gamma_{vc} &= -\frac{|d|^2}{2\hbar}\left[\mathrm{Im}\,(\chi_{xx} - \chi_{yy}) + i\ \mathrm{Im}\,(\chi_{xy} + \chi_{yx})\right] \equiv \frac{3\gamma}{4}\sin^2\theta e^{2i\phi}Q_i, \\
\Omega_{vc} &= -\frac{|d|^2}{2\hbar}\left[\mathrm{Re}\,(\chi_{xx} - \chi_{yy}) + i\ \mathrm{Re}\,(\chi_{xy} + \chi_{yx})\right] \equiv \frac{3\gamma}{4}\sin^2\theta e^{2i\phi}Q_r.
\end{aligned} \tag{6.27}$$

The Ps′ and Qs′ are as defined in Eq. (6.25). In deriving (6.27), we have used the fact that $\chi_{xy} = \chi_{yx}$. It may be noted that Γ_i and Ω_i are real, and are independent of the azimuthal angle, whereas Γ_{vc} and Ω_{vc} are complex and are functions of ϕ. For $\theta = n\pi$, the coherence terms disappear in Eq. (6.17). Thus if $\vec{R}$ is perpendicular to the plane containing both the dipoles, i.e. both atoms lie on the quantization axis (z-axis), the coherence effects vanish.

The solutions of the master equation can be recalculated using the above coefficients and the analog of all the results presented in Sec. IV can be produced for the present system. For completeness, we present the numerical plot that shows the excitation probability $p_{g;2}$ with the initial condition $p_{1;g}(t = 0) = 1$. The time evolution of $p_{g;2}$ is similar to the one in the case of real dipoles (cf. Fig. 6.6(a)).

It may further be noted that $p_{g;2}$ is independent of ϕ though Γ_{vc} and Ω_{vc} are functions of ϕ. This is because $p_{g;2}$ is a function of the absolute values of Γ_{vc} and Ω_{vc}. - which can be shown from (6.23) and (6.27): to the lowest order in Γ_{vc} and Ω_{vc},

$$p_{g;2} \approx 4\left(|\Gamma_{vc}|^2 + |\Omega_{vc}|^2\right)\left(\frac{\sin^2\zeta t}{4\zeta^2}\right). \tag{6.28}$$

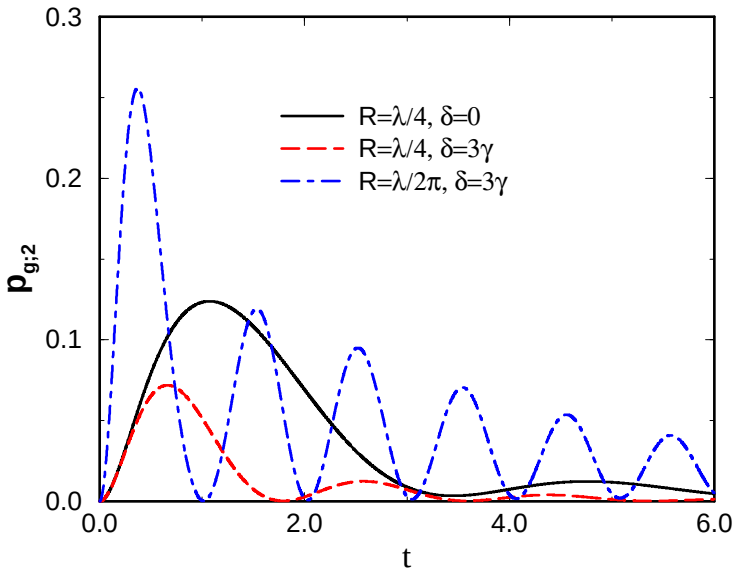

Figure 6.8: The time evolution of the probability $p_{g;2}$ when the dipoles $\vec{d}_1$ and $\vec{d}_2$ are complex. All the parameters are same as in Fig. 6.6.

We now discuss how the new coherence effect can be monitored experimentally for the above mentioned system. The dipole transitions $|1_\mu\rangle \leftrightarrow |g_\mu\rangle$, in the system described above, involve photons having σ_+ polarization. Thus the emission from $|1_\mu\rangle \rightarrow |g_\mu\rangle$ does not contain any field component in σ_- polarization. On the other hand, the emission from $|2_\mu\rangle \rightarrow |g_\mu\rangle$ would contain σ_- component. Thus the signal that one has to look for is - the intensity of the emitted photon from $|2_\mu\rangle$ levels in σ_- polarization, which would a be measure of the total excitation probability to $|2_\mu\rangle$ states and hence would confirm the occurrence of VIC. Another possibility to probe the population in $|2_\mu\rangle$ will be to excite it with a circularly polarized radiation to a fourth state $6\ ^1S_0$ and to monitor the fluorescence from $6\ ^1S_0$.

6.6 Summary

We have shown that the radiative coupling between the multilevel atoms with near-degenerate transitions can produce *new interference effects* which are especially important when the distance between two dipoles is less than a wavelength. We have demonstrated this possibility by considering two identical V-systems such that the pair of transition dipole matrix elements in each system are orthogonal to each other in both the atoms. Such interference

effects are especially significant in the energy transfer studies. The choice of orthogonal dipole matrix elements enables us to specially isolate the effects of the vacuum induced coherences in the radiative coupling between multilevel atoms with nearly degenerate transitions. We have presented detailed numerical results to bring out the role of multi-atom multilevel interference effects.

Chapter 7

Cavity-Vacuum Induced Coherences from Preselection of Polarization

7.1 Introduction

It is already clear that the vacuum field in free space, interacting with an atomic system, can create coherence subject to the condition that atomic transition dipoles satisfy the Eq. (5.21). From Eq. (5.19) one understands that the origin of the condition (5.21) is because spontaneous emission occurs in two orthogonal modes of polarization. It is desirable to examine how the condition (5.21) can be *bypassed*. This could be possible if we *preselect* the polarization mode - then we do not need the condition (5.21) for interference to occur in spontaneous emission. In order to preselect the polarization, we consider the problem of spontaneous emission in a mode selective cavity. It is of course known that the cavity can provide a good way to manipulate the spontaneous emission from an excited atom [171]. We demonstrate the possibility of restoring quantum interference effects in spontaneous emission of an excited atom inside a cavity with its modes selected *a priori*, and thus avoid the condition (5.21). A possible configuration is shown in Fig. 7.1.

7.2 Dynamics of a Four Level System in a Cavity

We consider a two-mode cavity containing a four-level atomic scheme with say, two near-degenerate Zeeman split magnetic sub-levels $|1\rangle \equiv |j = 1, m = 1\rangle$ and $|2\rangle \equiv |j = 1, m = -1\rangle$ as its intermediate states (shown in Fig. 7.2). The "a-mode" ("b-mode") couples $|e\rangle \leftrightarrow$

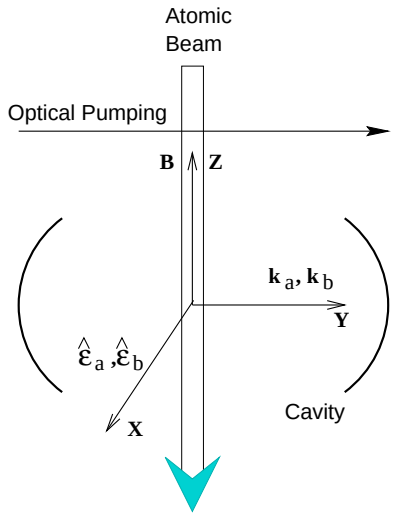

Figure 7.1: A possible configuration for the preselection of polarizations of the cavity modes that can give rise to new coherences. The propagation vectors of the cavity modes $\vec{k}_a, \vec{k}_b$ are along the Y-direction and cavity polarizations $\hat{\epsilon}_a, \hat{\epsilon}_b$ are along the X-direction, with the quantization axis (Z-direction) fixed by the direction of the magnetic field $\vec{B}$.

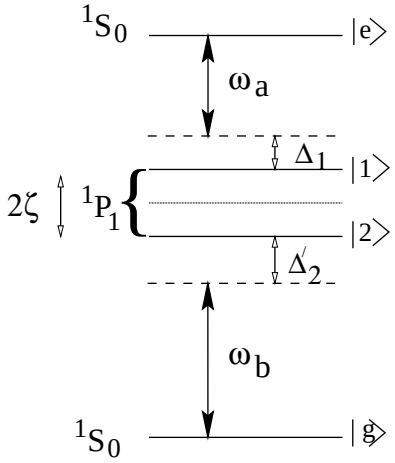

Figure 7.2: A four-level model scheme (say of ^{40}Ca) with closely lying intermediate levels $|1\rangle \equiv |j = 1, m = 1\rangle$ and $|2\rangle \equiv |j = 1, m = -1\rangle$. Here ω_a (ω_b) is the frequency of the cavity field coupling $|e\rangle$ to $|1\rangle$ and $|2\rangle$ ($|1\rangle$ and $|2\rangle$ to the state $|g\rangle$). 2ζ is the spacing between intermediate levels and the various detunings are defined by $\Delta_j = \omega_{ej} - \omega_a$, $\Delta'_j = \omega_{jg} - \omega_b$.

$|j\rangle$ ($|j\rangle \leftrightarrow |g\rangle$) transitions (for $j = 1, 2$). The scheme could be ^{40}Ca cascade, as shown by the symbols in the left hand side of the figure. The total Hamiltonian for the atomic system and the cavity fields is [see 5.7]

$$\mathcal{H} = \mathcal{H}_A + \mathcal{H}_F + \mathcal{H}_{AF}, \tag{7.1}$$

where,

$$\begin{aligned} \mathcal{H}_A &= \hbar(\omega_{eg}A_{ee} + \omega_{1g}A_{11} + \omega_{2g}A_{22}), \\ \mathcal{H}_F &= \hbar(\omega_a a^\dagger a + \omega_b b^\dagger b), \\ \mathcal{H}_{AF} &= -\vec{d}.\vec{E}_{cav} \\ &= -i\hbar\sum_{j=1}^{2}\left(G_{je}a^\dagger A_{je} + G_{gj}b^\dagger A_{gj}\right) + \text{H.c.}\,. \end{aligned} \tag{7.2}$$

Here A_{ij} and ω_{ij} are the atomic operators and the atomic transition frequencies as defined in Sec. 1.2. And E_{cav} is the quantized two mode cavity field given by

$$\vec{E}_{cav}(\vec{r}) = \left[i\left(\frac{2\pi\hbar\omega_a}{V}\right)^{1/2}\hat{\epsilon}_a\, a e^{i\vec{k}_a.\vec{r}} + a \to b\right] + \text{H.c.}. \tag{7.3}$$

Here a, b ($a^\dagger, b^\dagger$) are annihilation (creation) operators for the cavity field modes with frequencies ω_a and ω_b respectively. The atom-cavity mode coupling constants are given by

$$G_{je} = \left(\frac{2\pi\hbar\omega_a}{V}\right)^{1/2}\frac{\vec{d}_{je}.\hat{\epsilon}_a}{\hbar},\;\; G_{gj} = \left(\frac{2\pi\hbar\omega_b}{V}\right)^{1/2}\frac{\vec{d}_{gj}.\hat{\epsilon}_b}{\hbar}, \tag{7.4}$$

with V being the cavity volume and $\hat{\epsilon}_a$ and $\hat{\epsilon}_b$ being the polarizations of the cavity modes. We work in the interaction picture. The Hamiltonian in the interaction picture is given by

$$\begin{aligned} \tilde{\mathcal{H}}_{AF}(t) &= e^{\frac{i}{\hbar}(\mathcal{H}_A+\mathcal{H}_F)t}\mathcal{H}_{AF}e^{-\frac{i}{\hbar}(\mathcal{H}_A+\mathcal{H}_F)t} \\ &= -i\hbar\sum_{j=1}^{2}\left(G_{je}a^\dagger A_{je}e^{-i\Delta_j t} + G_{gj}b^\dagger A_{gj}e^{-i\Delta'_j t}\right) + \text{H.c.},\;\; j = 1, 2; \end{aligned} \tag{7.5}$$

where, $\Delta_j = \omega_{ej} - \omega_a$ ($\Delta'_j = \omega_{jg} - \omega_b$) is the cavity mode detuning from the $|e\rangle \leftrightarrow |j\rangle$ ($|j\rangle \leftrightarrow |g\rangle$) transition. The above Hamiltonian describes the reversible interactions between the atom and the cavity field. However we should also take into account the irreversible processes due to coupling of the cavity field with the outside world via cavity mirrors. We denote the leakage rates of the photons in the cavity modes by κ_a and κ_b. At optical frequencies we can neglect the thermal photons. We further work in the bad cavity limit.

The following density matrix equation in the interaction picture for the combined atom-field system contains two parts: (a) coherent evolution described by the Liouvillian $\mathcal{L}$, and (b) the field relaxation part described by $\mathcal{L}_F$ [172]:

$$\frac{\partial \rho_{A+F}}{\partial t} = (\mathcal{L} + \mathcal{L}_F)\rho_{A+F}, \tag{7.6}$$

where,

$$\begin{aligned} \mathcal{L}\rho_{A+F} = & - \frac{i}{\hbar}\left[\tilde{\mathcal{H}}_{AF}(t), \rho_{A+F}\right], \\ \mathcal{L}_F\rho_{A+F} = & - \kappa_a(a^\dagger a\rho_{A+F} - 2a\rho a^\dagger + \rho_{A+F}a^\dagger a) \\ & - \kappa_b(b^\dagger b\rho_{A+F} - 2b\rho b^\dagger + \rho_{A+F}b^\dagger b). \end{aligned} \tag{7.7}$$

To get useful information about the evolution of the atomic system, we derive the Master equation for the reduced atomic operator by approximately eliminating the cavity field using the standard projection operator techniques [7, 172]. In the following, we outline some of the important steps. We rewrite Eq. (7.6) as

$$\frac{\partial \tilde{\rho}_{A+F}}{\partial t} = \tilde{\mathcal{L}}(t)\tilde{\rho}_{A+F}(t), \tag{7.8}$$

by transforming to a new frame with the transformations,

$$\tilde{\rho}_{A+F} \equiv e^{-\mathcal{L}_F t}\rho_{A+F}, \;\; \tilde{\mathcal{L}} \equiv e^{-\mathcal{L}_F t}\mathcal{L}e^{\mathcal{L}_F t}. \tag{7.9}$$

We define the projection operator to be $\wp... \equiv \rho_F(0)Tr_F...$ and write Eq. (7.8) as,

$$\frac{\partial \tilde{\rho}_{A+F}}{\partial t} = \tilde{\mathcal{L}}\wp\tilde{\rho}_{A+F} + \tilde{\mathcal{L}}(1-\wp)\tilde{\rho}_{A+F}. \tag{7.10}$$

The assumptions that we make are (a) at $t = 0$, $\rho_{A+F}(0)$ can be factorised into a product of atom and cavity field density operators, (b) the photons emitted can not react back with the atom i.e., we use the Born approximation and (c) the Markoff approximation $G^2\kappa^{-1} \ll \kappa$ (G refers to vacuum Rabi frequencies) which ensures that the system has a short memory. Using (7.9) and the above approximations and tracing over the field states Eq. (7.10) reduces to,

$$\frac{\partial \rho_A}{\partial t} = -\frac{1}{\hbar^2}\lim_{t\to\infty}\int_0^t d\tau Tr_F\left[\tilde{\mathcal{H}}_{AF}(t), e^{\mathcal{L}_F\tau}[\tilde{\mathcal{H}}_{AF}(t-\tau), \rho_F(0)\rho_A]\right]. \tag{7.11}$$

For convenience, $\tilde{\rho_A}$ is replaced by ρ_A in (7.11) and in subsequent calculations.

The trace over the field operators inside the integral is calculated using the following relations. For arbitrary field operators A and B, simple trace algebra and the definition of adjoints give

$$\begin{aligned} Tr_F\left[Ae^{\mathcal{L}_F\tau}B\rho_F(0)\right] &= \langle A(\tau)B\rangle, \\ Tr_F\left[Ae^{\mathcal{L}_F\tau}\rho_F(0)B\right] &= \langle BA(\tau)\rangle. \end{aligned} \tag{7.12}$$

Further, the time correlations for the cavity fields in the absence of the interaction with the atom are known to be

$$\begin{aligned} \langle aa^\dagger(\tau)\rangle = \langle a(\tau)a^\dagger\rangle &= e^{-\kappa_a\tau}, \\ \langle bb^\dagger(\tau)\rangle = \langle b(\tau)b^\dagger\rangle &= e^{-\kappa_b\tau}, \end{aligned} \tag{7.13}$$

with all other second order correlation functions being zero.

Substituting the complete Hamiltonian from Eq. (7.5) in (7.11) and using the relations (7.12), the trace inside the integral is expressed in terms of field correlations. Further using (7.13) and evaluating the integral in Eq. (7.11), we obtain the master equation for the atomic density operator as

$$\begin{aligned} \frac{\partial\rho_A}{\partial t} = & - i(\delta_1+\delta_2)[A_{ee},\rho_A] - i[(\delta_1'A_{11}+\delta_2'A_{22}),\rho_A] \\ & - \left\{\Gamma_1(A_{ee}\rho_A - 2A_{11}\rho_{ee}+\rho_A A_{ee}) + \Gamma_1'(A_{11}\rho_A - 2A_{gg}\rho_{11}+\rho_A A_{11}) + 1\to 2\right\} \\ & + \left\{2G_{1e}G_{2e}^*\frac{\kappa_a+i\zeta}{(\kappa_a+i\Delta_2)(\kappa_a-i\Delta_1)}A_{12}\rho_{ee}e^{2i\zeta t}+h.c.\right\} \\ & + \left\{2G_{g1}G_{g2}^*\frac{\kappa_b-i\zeta}{(\kappa_b+i\Delta_2')(\kappa_b-i\Delta_1')}A_{gg}\rho_{12}e^{-2i\zeta t}+h.c.\right\} \\ & - \left\{G_{g1}^*G_{g2}e^{2i\zeta t}\left(\frac{1}{\kappa_b-i\Delta_2'}A_{12}\rho_A+\frac{1}{\kappa_b+i\Delta_1'}\rho_A A_{12}\right)+h.c.\right\} \end{aligned} \tag{7.14}$$

where,

$$\begin{aligned} \Gamma_j &= |G_{je}|^2\kappa_a/(\kappa_a^2+\Delta_j^2),\ \Gamma_j' = |G_{gj}|^2\kappa_b/(\kappa_b^2+\Delta_j'^2),\ \zeta=(\omega_{1g}-\omega_{2g})/2, \\ \delta_j &= |G_{je}|^2\Delta_j/(\kappa_a^2+\Delta_j^2),\ \delta_j' = |G_{gj}|^2\Delta_j'/(\kappa_b^2+\Delta_j'^2),\ j=1,2\,. \end{aligned} \tag{7.15}$$

Here Γ and Γ''s represent various decay constants from different levels and δ and δ''s are the frequency shifts of atomic levels resulting from interaction with the vacuum field in a detuned cavity. This is the key equation of this chapter and will be used in the subsequent analysis to study the coherence effects induced by the cavity.

To understand the meaning of various terms in the Master equation (7.14) we write the equations explicitly for the density matrix elements:

$$\begin{aligned}
\frac{\partial \rho_{ee}}{\partial t} &= -2(\Gamma_1+\Gamma_2)\rho_{ee}, \\
\frac{\partial \rho_{11}}{\partial t} &= -2\Gamma_1'\rho_{11} + 2\Gamma_1\rho_{ee} - \eta\,\frac{G_{g1}^* G_{g2}}{\kappa_b - i\Delta_2'}\rho_{21}e^{2i\zeta t} - \eta\,\frac{G_{g1}G_{g2}^*}{\kappa_b + i\Delta_2'}\rho_{12}e^{-2i\zeta t}, \\
\frac{\partial \rho_{12}}{\partial t} &= -\left(\Gamma_1'+\Gamma_2'+i(\delta_1'-\delta_2')\right)\rho_{12} + 2\eta\, G_{1e}G_{2e}^*\frac{\kappa_a+i\zeta}{(\kappa_a+i\Delta_2)(\kappa_a-i\Delta_1)}\rho_{ee}e^{2i\zeta t} \\
&\quad -\eta\, G_{g1}^* G_{g2}\left(\frac{\rho_{22}}{\kappa_b - i\Delta_2'} + \frac{\rho_{11}}{\kappa_b + i\Delta_1'}\right)e^{2i\zeta t}, \\
\frac{\partial \rho_{gg}}{\partial t} &= 2\Gamma_1'\rho_{11} + 2\Gamma_2'\rho_{22} + 2\eta\, G_{g1}G_{g2}^*\frac{\kappa_b - i\zeta}{(\kappa_b+i\Delta_2')(\kappa_b - i\Delta_1')}\rho_{12}e^{-2i\zeta t} \\
&\quad +2\eta\, G_{g1}^* G_{g2}\frac{\kappa_b+i\zeta}{(\kappa_b - i\Delta_2')(\kappa_b+i\Delta_1')}\rho_{21}e^{2i\zeta t}.
\end{aligned} \tag{7.16}$$

Equation for $\dot{\rho}_{22}$ is the same as for $\dot{\rho}_{11}$ with $1 \leftrightarrow 2$ and $\zeta \to -\zeta$. Note the presence of oscillating components in (7.16). If ζ is large compared to damping constants Γ's or detunings δ's, then these exponentials averaged out to zero (shown explicitly in the discussion following Eq. (7.20) leading to

$$\begin{aligned}
\frac{\partial \rho_{ee}}{\partial t} &= -2(\Gamma_1+\Gamma_2)\rho_{ee}, \\
\frac{\partial \rho_{11}}{\partial t} &= -2\Gamma_1'\rho_{11} + 2\Gamma_1\rho_{ee}, \\
\frac{\partial \rho_{12}}{\partial t} &= -\left(\Gamma_1'+\Gamma_2'+i(\delta_1'-\delta_2')\right)\rho_{12}, \\
\frac{\partial \rho_{gg}}{\partial t} &= 2\Gamma_1'\rho_{11} + 2\Gamma_2'\rho_{22}.
\end{aligned} \tag{7.17}$$

These equations can be compared with the equations for emission in free space. Under the initial condition that the atom is in the state $|e\rangle$, equations (7.17) admit simple solutions:

$$\begin{aligned}
\rho_{ee}(t) &= \exp[-2(\Gamma_1+\Gamma_2)t], \\
\rho_{11}(t) &= \frac{\Gamma_1}{\Gamma_1+\Gamma_2-\Gamma_1'}\left(\exp[-2\Gamma_1' t] - \exp[-2(\Gamma_1'+\Gamma_2')t]\right), \\
\rho_{gg}(t) &= 1 - \rho_{ee} - \rho_{11}(t) - \rho_{22}(t),
\end{aligned} \tag{7.18}$$

and $\rho_{22}(t)$ is same as $\rho_{11}(t)$ with $1 \leftrightarrow 2$.

For ζ comparable to Γ's and Δ's, the exponential terms are important. The dynamical equations involve coupling of populations to coherences and vice-versa. Such couplings

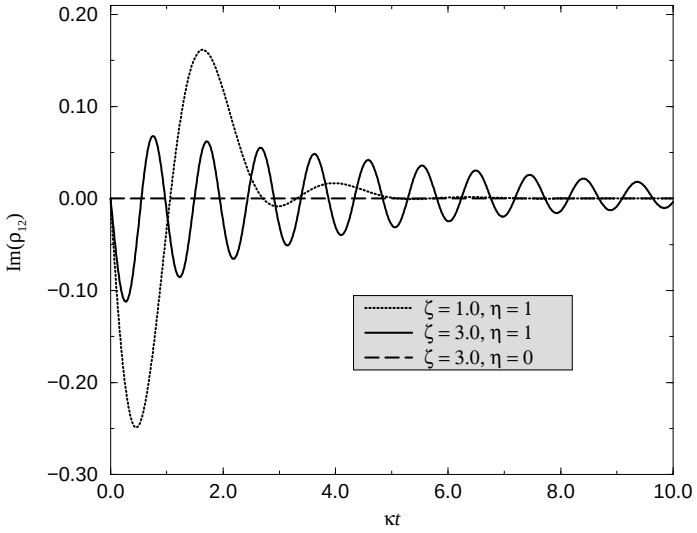

Figure 7.3: The time evolution of coherence between the intermediate states is plotted. All frequencies are scaled with $\kappa_a = \kappa_b = \kappa$. We choose $G_{je} \equiv G_{gj} = \kappa$, $\Delta_1' = -\Delta_2' = \zeta = -\Delta_1 = \Delta_2$. For $\eta = 0$, no coherence is produced, and for $\eta = 1$, as ζ increases, the frequency of oscillation increases but the amplitude of coherence decreases.

give rise to new coherence effects. Accordingly, we have introduced an interference parameter η in Eqs. (7.16), so that $\eta = 1(= 0)$ would refer to the presence (absence) of coherence effects.

7.3 Cavity Induced Intermediate State Coherence

It is clear from Eq. (7.16) that, for $\eta = 0$, the coherence between the intermediate levels is never established; i.e., $\rho_{ij} = 0$ for all times. When η is unity, there is a two-fold possibility for the coherence to evolve - (a) the second term in the equation for $\dot{\rho}_{12}$ causes evolution of coherence due to coupling of the states $|1\rangle$ and $|2\rangle$ to the excited state by the cavity vacuum field "a" and (b) the third term that arises from the coupling of $|1\rangle$ and $|2\rangle$ to the state $|g\rangle$ by the cavity vacuum field "b". The resulting evolution of coherence is shown in Fig. 7.3. For degenerate intermediate levels $|j\rangle$ $(j = 1, 2)$, and ω_a (ω_b) in resonance with $|e\rangle \rightarrow |j\rangle$ ($|j\rangle \rightarrow |g\rangle$) transition, no such oscillation is seen - though coherence evolves.

7.4 Quantum Beats in Atomic Populations

For $\eta = 1$, the populations in Eq. (7.16) can be obtained analytically. For simplicity, assume that $\Gamma_i \equiv \Gamma_i' \equiv \Gamma$, $G_{ie} \equiv G_{gi} \equiv G$, $\kappa_a \equiv \kappa_b = \kappa$ and the cavity field $\omega_a\,(\omega_b)$ is tuned to the center of the two intermediate states and the excited (ground) state. Then, the solution of Eq. (7.16) is found to be

$$\begin{aligned}
\rho_{ii}(t) = & - \left(1+\frac{2|\alpha|^2}{\Gamma^2+f^2}\right)e^{-4\Gamma t} + \left(1+\frac{|\alpha|^2}{f^2}\right)e^{-2\Gamma t} \\
& - \frac{2|\alpha|^2}{\Gamma^2+f^2}e^{-2\Gamma t}\left[\left(\frac{\Gamma^2}{f^2}-1\right)\,\cos(2ft)+\frac{2\Gamma}{f}\,\sin(2ft)\right], i=1,2; \qquad (7.19)\\
\rho_{gg}(t) = & \quad 1 \quad -\rho_{ee}(t)-2\rho_{ii}(t).
\end{aligned}$$

Here, the parameter $\alpha = GG^*/(\kappa + i\zeta)$ corresponds to the cross terms in Eq. (7.16). It can therefore be seen that for $|\alpha| = 0$, Eq. (7.19) reduces to Eq. (7.18). The argument of the trigonometric functions in Eq. (7.19) gives the beat frequency

$$2f = 2\left[(\delta'+\zeta)^2 - |\alpha|^2\right]^{1/2}. \qquad (7.20)$$

The condition for the beats to occur is $(\delta'+\zeta)^2 > |\alpha|^2$. For various values of ζ, we show the time dependence of ρ_{ii} and ρ_{gg} in Fig. 7.4 assuming $|G|$ to be of the order of κ. If the intermediate levels are degenerate ($\zeta = 0$), then f is purely imaginary and therefore the trigonometric functions in Eq. (7.19) change to hyperbolic functions - ceasing the oscillations in the populations. Similarly, for $\zeta \ll \kappa$, f is imaginary and hence there is no beating. However, for $\zeta \sim \kappa$, the beating in population is prominently seen. An increase in ζ leads to increase in the beat frequency. For ζ very large compared to κ, the beat frequency $2f$ is much larger than κ - leading to fast oscillations, the average of which results in Eq. (7.18).

Further we note that for $\zeta \sim 3\kappa$, the ground state population decreases for a small time interval implying a population transfer to the intermediate levels. It should be borne in mind that, we work in the low-Q cavity limit where cavity vacuum is not strong enough to cause the vacuum field Rabi oscillation [21, 173]. To interpret the decrease in population, we go back to Eq. (7.14). The fourth line of Eq. (7.14) suggests that the ground state population couples the intermediate state coherences via $G_{g1}G_{g2}^*$ (and $G_{g1}^*G_{g2}$); e.g., an emission followed by absorption of the same photon on a different transition. The corresponding transitions would correspond to $|1\rangle \rightarrow |g\rangle \rightarrow |2\rangle$ (and $|2\rangle \rightarrow |g\rangle \rightarrow |1\rangle$). The various transitions of $G_{ij}G_{il}^*$ type and various interference paths are illustrated in Fig. 7.5. In particular

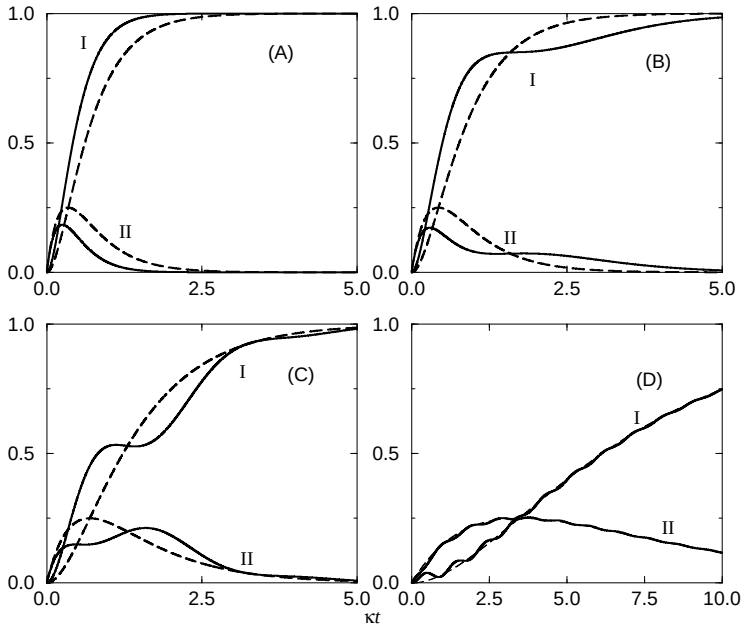

Figure 7.4: The time dependence of the populations in the ground state ρ_{gg} (represented by I) and the intermediate states $\rho_{11}(=\rho_{22})$ (represented by II). The dashed lines represent $\eta = 0$ where we see no oscillation. The solid lines represent $\eta = 1$. The plots for various values of ζ: (A) $\zeta = 0$ - no beat structure is seen, (B) $\zeta = 0.5\kappa$, (C) $\zeta = 1.0\kappa$ and (D) $\zeta = 3.0\kappa$ - where the population in the ground state decreases during $t \sim \kappa^{-1}$.

from Fig. 7.5(B), one understands the decrease in the ground state population.

7.5 Origin of Cavity Induced Coherences

In this section we examine the question - what leads to such coherences which otherwise do not occur. It is clear from Eq. (7.16) that, the coherence terms are related to matrix elements like

$$G_{g1}G^*_{g2} = \left(\frac{2\pi\omega_b}{\hbar V}\right)(\vec{d}_{g1}.\hat{\epsilon}_b)(\vec{d}^*_{g2}.\hat{\epsilon}^*_b). \tag{7.21}$$

For the chosen geometry of Fig. 7.1, Eq. (7.21) reduces to

$$G_{g1}G^*_{g2} = \left(\frac{2\pi\omega_b}{\hbar V}\right)(\vec{d}_{g1})_x(\vec{d}^*_{g2})_x. \tag{7.22}$$

The later is non-vanishing; as for $\sigma_\pm$ transitions, $\vec{d}_{g1} \equiv -\frac{d}{\sqrt{2}}(\hat{x} + i\hat{y})$, $\vec{d}_{g2} = \frac{d}{\sqrt{2}}(\hat{x} - i\hat{y})$ [see Eq. (3.7)]. Note further that if polarization cannot be preselected, then we have to sum Eq.

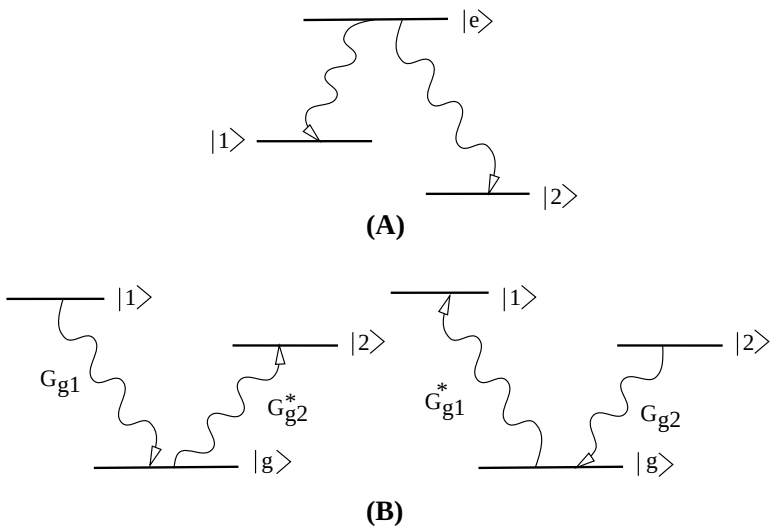

Figure 7.5: The various interference paths are shown by considering upper and lower transitions. (A) The upper Λ like part: both transitions share a single reservoir of cavity vacuum - contributing to the coherence between the states $|1\rangle$ and $|2\rangle$. (B) The lower V like part: to the lowest order interaction, photons emitted by $|1\rangle \leftrightarrow |g\rangle$ transition can be absorbed by $|g\rangle \leftrightarrow |2\rangle$ transition and vice versa - explaining the decrease in population of state $|g\rangle$.

(7.21) over the two possible polarization modes leading to [see Eq. (5.19)]

$$\begin{aligned} \sum_{pol} G_{g1}G^{*}_{g2} &= \left(\frac{2\pi\omega_b}{\hbar V}\right)\sum_{pol}(\vec{d}_{g1}.\hat{\epsilon}_b)(\vec{d}^{*}_{g2}.\hat{\epsilon}^{*}_b) \\ &= \left(\frac{2\pi\omega_b}{\hbar V}\right)(\vec{d}_{g1}.\vec{d}^{*}_{g2}). \end{aligned} \tag{7.23}$$

Under these conditions the coherence term can survive only if the dipole matrix elements are non-orthogonal. It is thus clear that, in order to see the interferences or beats at 2ζ, one has to make a preselection of polarization so that coherence between $|1\rangle$ and $|2\rangle$ can be produced by spontaneous emission. Note that this is different from the usual quantum beat spectroscopy [174, 175, 176] where coherence is produced by excitation with an *external field of appropriate band width*.

7.6 Summary

To summarize, we have shown: (a) how the preselection of polarization leads to certain types of interference effects which otherwise are missing unless the dipole matrix elements

are non-orthogonal; (b) how the preselection of polarization can be achieved in a cavity. We demonstrate this in the context of a four level atomic system in a bimodal cavity in the limit of a bad cavity. We show that the new coherences evolve, resulting quantum beats in the atomic populations. Recently Swain and co-workers [177] have used the cavity preselection to observe many coherence effects at finite temperature.

Chapter 8

Laser Field Induced Quantum Beats in Correlations in Cascade Emission

8.1 Introduction

It is well known [178, 179] that V-system can exhibit quantum beats in fluorescence if initially the system is prepared such that there is coherence between excited states. It is also known that quantum beats are sensitive to whether one considers a system with upper state coherence or a system with lower state coherence. For example, a Λ-system with initial coherence between two lower states does not lead to quantum beats [178]. One could thus inquire the possibility of beats in a four level system as shown in Fig. 8.1; if the system is initially prepared in the excited state $|e\rangle$. The upper part of this system is like a Λ-system and lower part like a V-system. Clearly quantum beats at the frequency separation between the levels $|1\rangle$ and $|2\rangle$ will occur if the process of spontaneous emission from $|e\rangle$ to $|1\rangle$ and $|2\rangle$ can *create coherence* between states $|1\rangle$ and $|2\rangle$. The quantum beat will occur in fluorescence arising from transitions $|1\rangle, |2\rangle$ to $|g\rangle$. No quantum beat will occur in fluorescence arising from the transitions $|e\rangle$ to $|1\rangle$, $|2\rangle$. However this coherence in the spontaneous emission can be created only if the transition dipole matrix elements $\vec{d}_{e1}$ and $\vec{d}_{e2}$ are non-orthogonal (see condition (5.21)). As noted earlier, most of the naturally occurring systems [e.g., Eq. (5.22)] do not satisfy (5.21). Thus a typical atomic scheme shown in Fig. 8.1 will not display quantum beats in fluorescence if *initially* the atom is prepared in the state $|e\rangle$. Hence one has to explore appropriate ways to satisfy (5.21).

In this Chapter, we consider the possibility of manipulating energy levels using laser

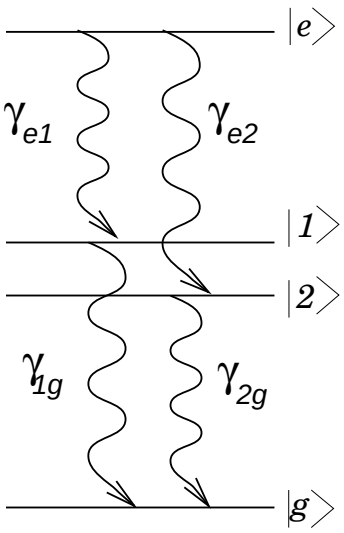

Figure 8.1: A four level atom with closely lying intermediate levels $|1\rangle$ and $|2\rangle$; a combination of Λ like (upper part) and V like (lower part) systems. The spontaneous emission from $|e\rangle$ can create coherence between $|1\rangle$ and $|2\rangle$, if system is initially at $|e\rangle$ and transition dipoles $\vec{d}_{e1}$ and $\vec{d}_{e2}$ are non-orthogonal, and hence quantum beats can be seen in fluorescence. Here γ_{ab} represent the spontaneous decay rates.

fields and thereby satisfying the condition (5.21) in a system as shown in Fig. 8.2 [147]. Here the laser fields mix the energy levels and make the dipole matrix elements dependent on the strength and frequency of the laser field. As a result of the new coherence created by the laser, quantum beat occurs in the intensity correlation between the two spontaneously emitted photons in the cascade emission.

8.2 The System and its Dynamics

We consider the scheme shown in Fig. 8.2. This scheme, for example, could refer to levels in Rb atom. The levels $|\alpha\rangle$ and $|\beta\rangle$ are coherently driven with a frequency close to $|\alpha\rangle \leftrightarrow |\beta\rangle$ transition frequency. Let $G = \vec{d}_{\alpha\beta} \cdot \vec{E}_l/\hbar$ be the Rabi frequency of the laser field E_l, driving the transition $|\alpha\rangle \leftrightarrow |\beta\rangle$. The interaction with the laser frequency ω_l is contained in the Hamiltonian defined by

$$\mathcal{H} \equiv \hbar\omega_{eg} A_{ee} + \hbar\omega_{\alpha g} A_{\alpha\alpha} + \hbar\omega_{\beta g} A_{\beta\beta} - \hbar G(A_{\beta\alpha} e^{-i\omega_l t} + h.c.). \tag{8.1}$$

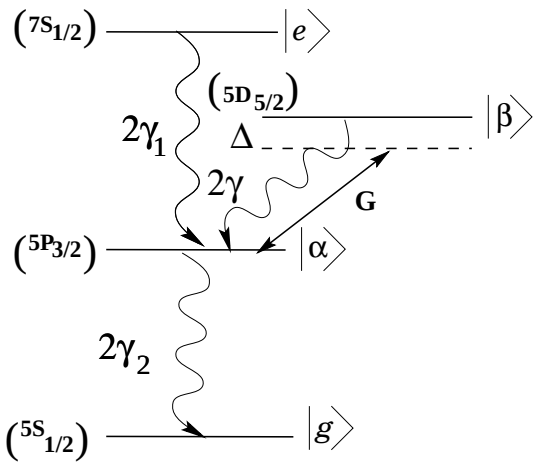

Figure 8.2: A scheme to realize VIC in a system shown in Fig. 8.1. Here laser field mixes the levels $|\alpha\rangle$ and $|\beta\rangle$ to make the transition dipole matrix elements non-orthogonal. Symbols in left hand side are relevant energy levels of *Rb* atom.

Here A_{ij} and ω_{ij} have the same meaning as in Sec. 1.2. Let $2\gamma_i$'s ($i = 1, 2$) represent rates of spontaneous emissions as shown in the Fig. 8.1. Then the density matrix equation, including these decays of the system, is [see e.g., Eq. (1.55) for a lambda system]

$$\frac{\partial \rho}{\partial t} = -\frac{i}{\hbar}[\mathcal{H}, \rho] - \gamma_1\{A_{ee}, \rho\} - \gamma_2\{A_{\alpha\alpha}, \rho\} - \gamma\{A_{\beta\beta}, \rho\} + 2\gamma_1\rho_{ee}A_{\alpha\alpha} + 2\gamma_2\rho_{\alpha\alpha}A_{gg} + 2\gamma\rho_{\beta\beta}A_{\alpha\alpha}. \tag{8.2}$$

On introducing a canonical transformation

$$\begin{aligned} \tilde{\rho}_{e\alpha} &\rightarrow \rho_{e\alpha}e^{i\omega_{e\alpha}t},\ \tilde{\rho}_{eg} \rightarrow \rho_{eg}e^{i\omega_{eg}t},\ \tilde{\rho}_{e\beta} \rightarrow \rho_{e\beta}e^{i(\omega_{e\alpha}-\omega_l)t}, \\ \tilde{\rho}_{\alpha g} &\rightarrow \rho_{\alpha g}e^{i\omega_{\alpha g}t},\ \tilde{\rho}_{\alpha\beta} \rightarrow \rho_{\alpha\beta}e^{i\omega_l t},\ \tilde{\rho}_{g\beta} \rightarrow \rho_{g\beta}e^{i(\omega_{g\beta}-\omega_l)t}, \\ \text{and } \tilde{\rho}_{aa} &\rightarrow \rho_{aa};\ for\ a = e, \alpha, \beta, g\,, \end{aligned} \tag{8.3}$$

Eq. (8.2) reduces to

$$\dot{\tilde{\rho}} \equiv -\frac{i}{\hbar}[\mathcal{H}_{\text{eff}}, \tilde{\rho}] - \gamma_1\{A_{ee}, \tilde{\rho}\} - \gamma_2\{A_{\alpha\alpha}, \tilde{\rho}\} - \gamma\{A_{\beta\beta}, \tilde{\rho}\} + 2\gamma_1\tilde{\rho}_{ee}A_{\alpha\alpha} + 2\gamma_2\tilde{\rho}_{\alpha\alpha}A_{gg} + 2\gamma\tilde{\rho}_{\beta\beta}A_{\alpha\alpha}; \tag{8.4}$$

where the effective Hamiltonian is

$$\mathcal{H}_{\text{eff}} \equiv \hbar\Delta A_{\beta\beta} - \hbar G(A_{\beta\alpha} + A_{\alpha\beta}) \tag{8.5}$$

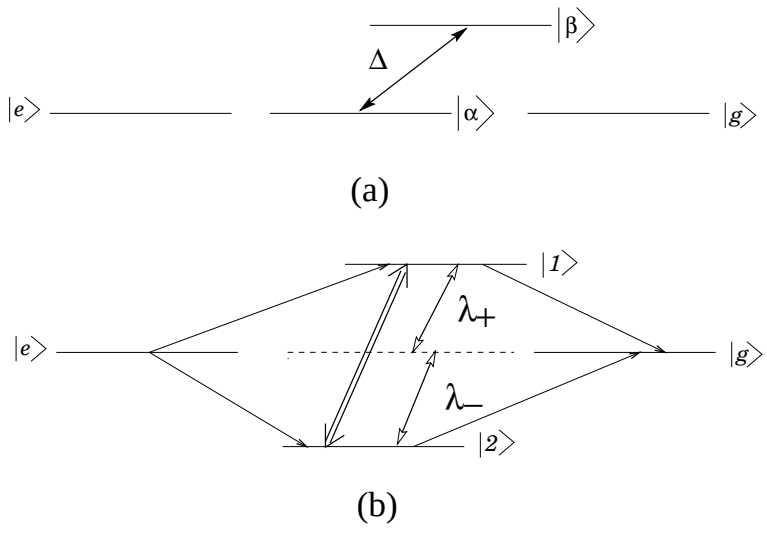

Figure 8.3: (a) The various unperturbed energy levels of the effective Hamiltonian in Eq. (8.5) with $G = 0$. (b) The new eigenstates after mixing of energy levels by the laser field. The various decay paths to $|g\rangle$ is shown by the arrows. $\lambda_\pm$ are the eigenvalues of the effective Hamiltonian $\mathcal{H}_{\text{eff}}$.

with $\Delta = \omega_{\alpha\beta} - \omega_l$ being the laser detuning. The different unperturbed energy levels will now appear as shown in the Fig. 8.3(a). The levels α and β are mixed by the laser field - the eigenstates of $\mathcal{H}_{\text{eff}}$ are given by

$$\begin{pmatrix} |1\rangle \\ |2\rangle \end{pmatrix} \equiv \begin{pmatrix} \cos\theta & \sin\theta \\ -\sin\theta & \cos\theta \end{pmatrix} \begin{pmatrix} |\beta\rangle \\ |\alpha\rangle \end{pmatrix} \tag{8.6}$$

with eigenvalues

$$\lambda\pm = \frac{\Delta \pm \sqrt{\Delta^2 + 4G^2}}{2}, \quad \tan\theta = \frac{\Delta - \sqrt{\Delta^2 + 4G^2}}{2G}. \tag{8.7}$$

Thus $\mathcal{H}_{\text{eff}}$ can also be written as

$$\mathcal{H}_{\text{eff}} = \hbar\lambda_+|1\rangle\langle 1| + \hbar\lambda_-|2\rangle\langle 2|. \tag{8.8}$$

Thus in the dressed state picture the system in Fig. 8.2 equivalent to Fig. 8.1 with the intermediate states determined by Eq. (8.6).

8.3 Beat in Photon Correlation in Cascade Emission

In the following we evaluate the two photon correlation [136] function $\mathcal{G}^{(2)}(\vec{r}_1, t; \vec{r}_2, t+\tau)$ for detecting a photon from the transition $|e\rangle \rightarrow |\alpha\rangle$ at space-time $(\vec{r}_1, t_1)$ and another photon from the transition $|\alpha\rangle \rightarrow |g\rangle$ at $(\vec{r}_2, t+\tau)$. We assume that transition frequencies $\omega_{e\alpha}$ and $\omega_{\alpha g}$ are widely different. The frequency of emitted photon is affected by the laser driving the transition $|\alpha\rangle \leftrightarrow |\beta\rangle$. We further assume that this change in frequency is much smaller than $|\omega_{e\alpha} - \omega_{\alpha g}|$. Note that we do not spectrally resolve fluorescence and such correlations in two photon cascade emission have been extensively studied [180, 181, 182, 183, 184]. Aspect and coworkers carried out classic experiments on two photon correlations in the context of Bell's inequalities [181]. Interference in the cascade correlation has been investigated using dispersive material [184].

The correlation function $\mathcal{G}^{(2)}(\vec{r}_1, t; \vec{r}_2, t+\tau)$ is defined by the joint probability of detecting two photons at two different space-time points $(\vec{r}_1, t)$ and $(\vec{r}_2, t+\tau)$ and is given by

$$\mathcal{G}^{(2)}(\vec{r}_1, t; \vec{r}_2, t+\tau) = \langle \vec{E}_v^-(\vec{r}_1, t)\vec{E}_v^-(\vec{r}_2, t+\tau)\vec{E}_v^+(\vec{r}_2, t+\tau)\vec{E}_v^+(\vec{r}_1, t)\rangle; \tag{8.9}$$

where $\vec{E}_v^+$ ($\vec{E}_v^-$) is the positive (negative) frequency part of the spontaneously emitted quantized-radiation field. In the far field zone approximation, i.e., if the distance between the atom and detector is much larger than the inter-atomic distance, then the radiation field can be expressed in terms of dipole moment operators (see Sec. 7 of [7]) as

$$\vec{E}_v^+(\vec{r}_i, t) \sim -\vec{\mathcal{A}}_i A_{\alpha e}(t - r_i/c) - \vec{\mathcal{B}}_i A_{g\alpha}(t - r_i/c); \tag{8.10}$$

where $\vec{\mathcal{A}}_i$ and $\vec{\mathcal{B}}_i$ are uninteresting constants that depend upon various dipole matrix elements, position of the detectors, the directions of observation, frequencies of transitions. Using the expression of the far field (8.10) the two photon correlation function (8.9) can be written as

$$\mathcal{G}^{(2)}(\vec{r}_1, t; \vec{r}_2, t+\tau) \equiv \mathcal{G}_0^{(2)}\langle A_{e\alpha}(t)A_{\alpha g}(t+\tau)A_{g\alpha}(t+\tau)A_{\alpha e}(t)\rangle, \tag{8.11}$$

where, $\mathcal{G}_0^{(2)}$ is a function of $\mathcal{A}_i$ and $\mathcal{B}_i$. In Eq. (8.11) the dipole operators are denoted as $A_{\alpha\beta} = |\alpha\rangle\langle\beta|$.

We will calculate the two photon correlation function (8.11) from first principles using the master equation 8.4 and the quantum regression theorem [185]. Here, our model consists of (a) the spontaneous emission events $|e\rangle \rightarrow |\alpha\rangle$, $|\alpha\rangle \rightarrow |g\rangle$; (b) the coherent field

interacting on the transition $|\alpha\rangle \leftrightarrow |\beta\rangle$, as shown in Fig. 8.2. The correlation function (8.11) can be calculated using the Eq. (8.4). In order to apply quantum regression theorem we need most general solution of (8.4) in the form of evolution from some time t to a later time $t+\tau$. Clearly, one can write (8.4) as

$$\dot{\tilde{\rho}} = L\tilde{\rho}, \tag{8.12}$$

where L is Liouville operator. Therefore the formal solution of (8.12) can be obtained as

$$\tilde{\rho}(t+\tau) \equiv e^{L\tau}\tilde{\rho}(t), \tag{8.13}$$

$$\tilde{\rho}_{pq}(t+\tau) \equiv \sum_{mn} \xi_{pqmn}(\tau)\tilde{\rho}_{mn}(t), \tag{8.14}$$

with

$$\xi_{pqmn}(\tau) \equiv \left(e^{L\tau}\right)_{pqmn}. \tag{8.15}$$

From (8.15) we have

$$\langle A_{qp}(t+\tau)\rangle \equiv \sum_{mn} \xi_{pqmn}(\tau)\langle A_{nm}(t)\rangle, \tag{8.16}$$

and hence

$$\begin{aligned} \langle A_{e\alpha}(t)A_{\alpha\alpha}(t+\tau)A_{\alpha e}(t)\rangle &= \sum_{mn} \xi_{\alpha\alpha mn}(\tau)\ \langle A_{e\alpha}(t)A_{nm}(t)A_{\alpha e}(t)\rangle \\ &= \sum_{mn} \xi_{\alpha\alpha mn}(\tau)\ \langle A_{ee}(t)\rangle \delta_{n\alpha}\delta_{m\alpha}. \end{aligned} \tag{8.17}$$

Thus $\mathcal{G}^{(2)}$ becomes

$$\mathcal{G}^{(2)} = \mathcal{G}_0^{(2)}\ \langle A_{ee}(t)\rangle\ \xi_{\alpha\alpha\alpha\alpha}(\tau) \equiv \mathcal{G}_0^{(2)}\ e^{-2\gamma_1 t}\ \xi_{\alpha\alpha\alpha\alpha}(\tau). \tag{8.18}$$

The function $\xi_{\alpha\alpha\alpha\alpha}(\tau)$ contains all the information about the *dynamics of the intermediate state* $|\alpha\rangle$. Physically it represents *the probability of finding the atom at* $t = \tau$ *in the state* $|\alpha\rangle$ *given that it was in the state* $|\alpha\rangle$ *at time t=0*. The quantum beat structure of $\mathcal{G}^{(2)}$ (if any) is determined by the function $\xi_{\alpha\alpha\alpha\alpha}$. We have calculated this function using the solution of (8.4) which has a complicated form, and hence we do not present complete solution. However, in absence of any decays of the system ($\gamma_i = 0$) the function $\xi_{\alpha\alpha\alpha\alpha}$ is given by

$$\xi_{\alpha\alpha\alpha\alpha}(\tau) = \frac{1}{2}\left[1 + \cos(2G\tau)\right]; \tag{8.19}$$

which shows oscillatory behavior of the correlation function. We display the results in Figs. 8.4 and 8.5 for both resonant and off-resonant lasers (taking $\gamma_1 = \gamma_2 = \gamma = 1$). These figures clearly show the quantum beat structure in the cascade correlation function.

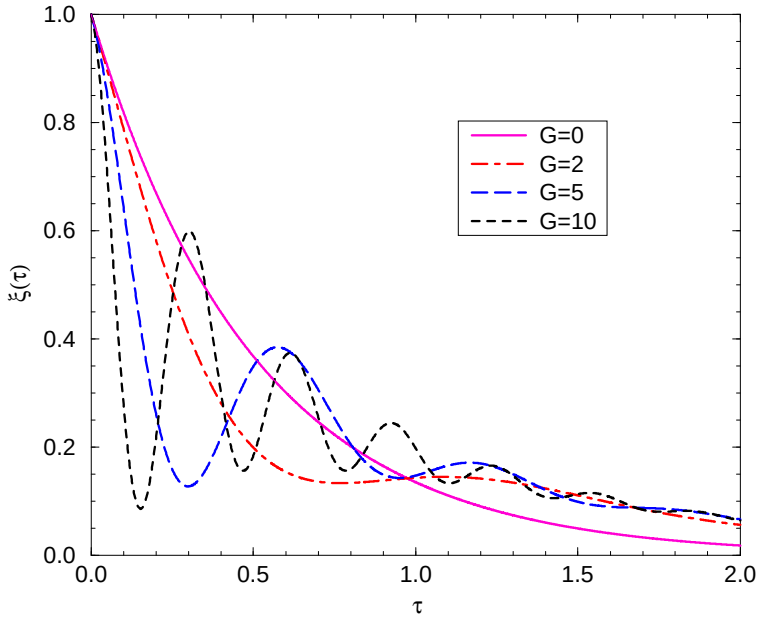

Figure 8.4: Plot of $\xi(\tau) \equiv \xi_{\alpha\alpha\alpha\alpha}(\tau)$ [Eq. (8.5)] for upper photon of the cascade system being detected at t and lower photon being detected at $t + \tau$ with the resonant coupling laser on the $|\alpha\rangle \leftrightarrow |\beta\rangle$ transition. All γ's are taken to be unity.

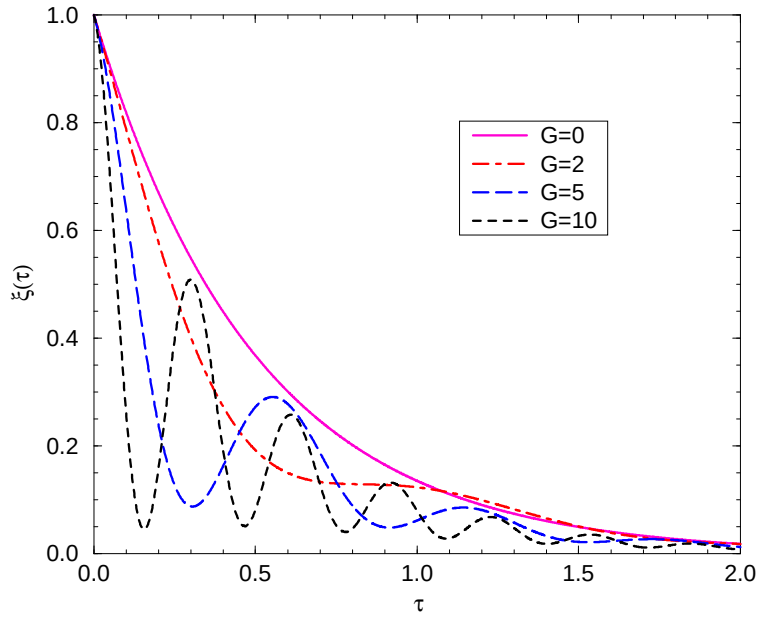

Figure 8.5: Plot of $\xi(\tau)$ with laser detuning $\Delta = 3$. The correlation amplitude decreases compared to the case where coupling laser is in resonance.

8.4 Evolution of Coherence and the Physical Interpretation

We next present a physical picture for the interpretation of the above beat structure. We work in terms of the eigenstates of $\mathcal{H}_{\rm eff}$ which are displayed in Fig. 8.3(b). The equations that govern the dynamics in the dressed state basis (for $\Delta = 0$ and $G \neq 0$) are determined as

$$\begin{aligned}
\dot{\rho}_{e1} &= -\frac{1}{2}(2\gamma_1+\gamma_2+\gamma-2iG)\rho_{e1}-\frac{1}{2}(\gamma-\gamma_2)\rho_{e2},\\
\dot{\rho}_{e2} &= -\frac{1}{2}(2\gamma_1+\gamma_2+\gamma+2iG)\rho_{e2}-\frac{1}{2}(\gamma-\gamma_2)\rho_{e1},\\
\dot{\rho}_{11} &= -\frac{1}{2}(2\gamma_2+\gamma)\rho_{11}+\gamma_1\rho_{ee}+\frac{\gamma}{2}\rho_{22}+\frac{\gamma_2}{2}(\rho_{12}+\rho_{21}),\\
\dot{\rho}_{12} &= -\frac{1}{2}(2\gamma_2+3\gamma+4iG)\rho_{12}-\gamma_1\rho_{ee}-\frac{1}{2}(2\gamma-\gamma_2)(\rho_{22}+\rho_{11})-\frac{\gamma}{2}\rho_{21},\\
\dot{\rho}_{1g} &= -\frac{1}{2}(\gamma_2+\gamma+2iG)\rho_{1g}-\frac{1}{2}(\gamma-\gamma_2)\rho_{2g},\\
\dot{\rho}_{2g} &= -\frac{1}{2}(\gamma+\gamma_2-2iG)\rho_{2g}-\frac{1}{2}(\gamma-\gamma_2)\rho_{1g},\\
\dot{\rho}_{22} &= -\frac{1}{2}(2\gamma_2+\gamma)\rho_{22}+\gamma_1\rho_{ee}+\frac{\gamma}{2}\rho_{11}+\frac{\gamma_2}{2}(\rho_{12}+\rho_{21}),\\
\dot{\rho}_{gg} &= \frac{\gamma_2}{2}(\rho_{22}-\rho_{12}-\rho_{21}+\rho_{11}).
\end{aligned} \tag{8.20}$$

The density matrix equations show how the diagonal and off diagonal elements remain coupled via various spontaneous emission coefficients. These couplings give rise to various interferences. In Fig. 8.3(b) we also display the two pathways for cascade emission viz $|e\rangle \rightarrow |1\rangle \rightarrow |g\rangle$ and $|e\rangle \rightarrow |2\rangle \rightarrow |g\rangle$. The laser field has mixed the levels $|\alpha\rangle$ and $|\beta\rangle$. This mixing makes the transition dipole matrix elements between $|e\rangle \leftrightarrow |1\rangle$ and $|e\rangle \leftrightarrow |2\rangle$ nonorthogonal as shown below:

$$\begin{aligned}
\vec{d}_{e1}.\vec{d}^{*}_{e2} &= \langle i|\vec{d}|(\cos\theta|\beta\rangle+\sin\theta|\alpha\rangle).[(-\sin\theta\langle\beta|+\cos\theta\langle\alpha|)|\vec{d}|e\rangle]\\
&= \sin\theta\cos\theta\vec{d}_{e\alpha}.\vec{d}_{\alpha e}\\
&= \sin\theta\cos\theta|\vec{d}_{e\alpha}|^2 \neq 0.
\end{aligned} \tag{8.21}$$

The occurrence of beat in the photon correlations shown in the previous section will depend on the coherence between $|1\rangle$ and $|2\rangle$. In Fig. 8.6 we show that the coherence ρ_{12} indeed develops in time, given that the atom was initially in the state $|e\rangle$.

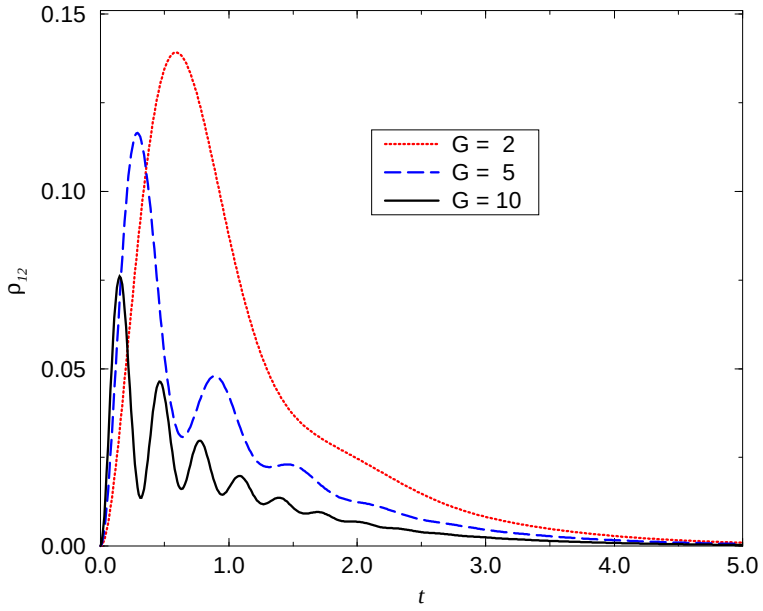

Figure 8.6: The evolution of the coherence ρ_{12} is shown for various values of the Rabi frequency of a resonant laser; which otherwise is zero in absence of the laser field.

8.5 Summary

To summarize, we have demonstrated the possibility of laser field induced quantum beats in two-photon correlations in cascade emission - which, otherwise, is an exponentially decaying function. The laser field, which couples the intermediate state of the cascade system with a fourth state, mixes the energy levels. Thus the transition dipole matrix elements depend on the strength and frequency of the laser field. The modified transition dipole matrix elements are shown to satisfy the condition (5.21) causing VIC to occur in the system. This coherence between the two intermediate levels is crucial for the production of quantum beats. The frequency of quantum beat depends on the intensity and frequency of the laser field.

Conclusions and Future Outlook

In conclusion, this thesis reports novel optical phenomena occurring in atomic medium using external laser fields. It also reports possibility of creating *new* coherences in spontaneous emission and discusses interesting consequences. The main underlying theme of this thesis is *atomic coherences*. The new findings are described with analytical results and are substantiated by presenting extensive numerical results. In the following we present a brief summary of important conclusions of each chapter and discuss some future outlook of the problems.

In Chapter 2, we have shown how anisotropy can be induced in an initially isotropic atomic medium by a magnetic field (called as magneto-optical rotation (MOR)) or a laser field. This results in rotation of plane of polarization of a probe field passing through the medium. This study gave rise to the interesting possibility - coherent control of the polarization rotation caused by magnetic field using a laser field. In Chapter 3, we have discussed laser field induced birefringence and hence rotation of plane of polarization of a probe field passing through the medium. Also we have shown that using a strong control laser we can achieve large enhancement of the MOR. By suitably choosing the control laser parameters, we have shown that *new probe frequency regions* are created to obtain large MOR, where the rotations, otherwise, are very small. This work is followed by a more general study of coherent control of MOR in an inhomogeneously broadened medium in Chapter 4. In this chapter we have made detailed analysis of the conditions under which one can achieve large enhancement of MOR. We demonstrated that an interplay between the magnetic field and laser field can be used to obtain significantly large MOR, which gives rise to possibility of using it as a *magneto-optical switch*. Further investigations are needed on different interesting possibilities such as using the control field induced enhancements to measure small magnetic fields.

In Chapter 5, we have introduced coherences in spontaneous emission, that is induced

by an incoherent (vacuum) field, known as vacuum induced coherence (VIC). We have discussed the origin of such coherences and shown that certain stringent conditions are required for such coherences to occur in atomic systems. In Chapter 6, we have reported VIC in radiatively coupled multilevel multi-atom systems. We have shown that the radiative coupling between the dipoles can produce *new* interference effects, which are especially important when the distance between two dipoles is less than a wavelength. We have especially chosen the transition dipole matrix elements of the atomic systems such that they do not meet the condition for VIC to occur. This choice has enabled us to isolate the effects of the VIC in the radiative coupling between multilevel atoms. We have done detailed analysis of this effect both analytically and numerically. Nevertheless further investigations are needed to study the consequences of this new coherence effect; to give an example, it would be interesting to investigate the role of the new coherence in the context of superradiance in the multilevel atoms. Further in Chapter 7, we have examined the possibility of bypassing the stringent requirement for VIC to occur. We have demonstrated that preselection of polarization of cavity vacuum can lead to *new* interference effects in spontaneous emission, which otherwise do not occur unless the transition dipole matrix elements of the atom satisfy the stringent condition. We have reported this possibility in the context of a four-level atomic system in a bimodal cavity in the limit of a bad cavity. We have shown that as a result of the new coherence, quantum beat occurs in the atomic populations. This study has led to further investigations on the effect of the new coherence at finite temperature by many other researchers. However it would be interesting to investigate this coherence effect by preselecting the polarization in a good cavities, where one would expect an enhanced coherence effect. Finally in Chapter 8, we have examined restoration of VIC using a laser field. We have demonstrated that the laser field mixes the atomic energy levels, and thus makes the transition dipole matrix elements dependent on the strength and frequency of the laser field. This modified transition dipole matrix elements are shown to meet the condition for VIC to occur in the system. We have also demonstrated the possibility of laser field induced quantum beats in two-photon correlations in cascade emission. The emission spectrum of such a system would be interesting to examine, which is also expected to show the effect of such laser induced coherences.

References

[1] M. Plank, Verh. dt. phys. Ges. **2**, 202 (1900); *ibid* 237 (1900).

[2] A. Einsten, Phys. Z **18**, 121 (1917); for English translation and discussions on Ref.[1,2] see D. ter Haar in *The old quantum theory*, Pergamon, Oxford (1967).

[3] R. Loudon, *The Quantum Theorey of Light*, 2nd Edition (Claredon Press, Oxford, 1997).

[4] J. D. Jackson, *Classical Electrodynamics* (Wiley, New York, 1962).

[5] R. W. Boyd, *Nonlinear Optics* (Academic Press, 1992).

[6] P. A. M. Dirac, *The Principles of Quantum Mechanics* (Oxford University Press, 1958).

[7] G. S. Agarwal, *Quantum Statistical Theories of Spontaneous Emission and their relation to other approaches*, Springer-Verlag, Berlin (1974).

[8] M. Sargent, M. O. Scully, and W. Lamb, *Laser Physics* (Addison-Wesley Publishing Co., Massachusetts, 1974), pg. 15.

[9] C. Cohen-Tannoudji, B. Diu and F. Laloë, *Quantum Mechanics, Vol. 2* (John Wiley and Sons, 1977) Pg. 1307.

[10] W. H. Louisell, *Quantum Statistical Properties of Radiation*, (John Wiley and Sons, 1973), see Appendix J.

[11] J. J. Sakurai, *Modern Quantum Mechanics* (Addisopn-Wesley Publishing Co., California, 1982)

[12] C. Chen-Tannoudji, J. Dupont-Roc, and G. Grynberg, *Atom-Photon Interactions* (John Wiley and Sons, New York, 1992).

[13] I.I. Rabi, Phys. Rev. A **51**, 652 (1937).

[14] F. Bloch, Phys. Rev. **70**, 460 (1946).

[15] L. Allen and J. H. Eberly, *Optical Resonance and Two-level Atoms* (John Wiley and Sons, 1975).

[16] P. L. Knight and P. W. Milloni, Phys. Rep. **66**, 21 (1980); S. Swain, in *Advances in Atomic and Molecular Physics*, Eds. D. R. Bates and B. Bederson, Vol. 16, pg. 159 (1980).

[17] B. R. Mollow, Phys. Rev. **188**, 1969 (1969).

[18] W. Hartig, W. Rasmussen, R. Schieder, and H. Walther, Z. Phys. A **278**, 205 (1976); R. E. Grove, F. Y. Wu, and S. Ezekiel, Phys. Rev. A **15**, 227 (1977).

[19] B. R. Mollow, Phys. Rev. A **5**, 2217 (1972); for experiment see F. Y. Wu, S. Ezekiel, M. ducloy, and B. R. Mollow, Phys. Rev. Lett.**38**, 1077 (1977).

[20] C. Cohen-Tannoudji and S. Reynaud, J. Phys. B **10**, 345 (1977); For an exellent review see: C. Cohen-Tannoudji in *Frontiers in in Laser Physics*, eds. R. Balian, S. Haroche and S. Liberman (North-Holland, Amsterdam, 1977) Vol. I.

[21] E. T. Jaynes and F. W. Cummings, Proc. IEEE **1**, 89 (1963).

[22] F. W. Cummings, Phys. Rev. **140**, 1051 (1965); J. H. Eberly, N. B. Narozhny, and J. J. Sanchez-Mondragon, Phys. Rev. Lett.**44**, 1323 (1980).

[23] L. Mandel, Opt. Lett. **4**, 205 (1979); R. Sort and L. Mandel, Phys. Rev. Lett. **51**, 384 (1983).

[24] H. J. Kimble, D. Dagenais and L. Mandel, Phys. Rev. Lett.**39**, 691 (1977).

[25] H. J. Charmichael, A. S. Lane, and D. F. Walls, Phys. Rev. Lett.**58**, 2539 (1987).

[26] Theoretical prediction was given in D. F. Walls and P. Zoller, Phys. Rev. Lett.**47**, 709 (1981); recent experimetal observation [Z. H. Lu, S. Bali, and J. E. Thomas, Phys. Rev. Lett.**81**, 3635 (1998)] confirmed the prediction.

[27] G. S. Agarwal, Progress in Optics, vol. 11, 1 (1973), ed. E. Wolf (Amsterdam: Narthe Holland).

[28] Y. Zhu, Q. Wu, A. Lezama, D. J. Gauthier, and T. W. Mossberg, Phys. Rev. A**41**, 6574 (1990); for theory see: G. S. Agarwal, Y. Zhu, D. J. Gauthier, and T. W. Mossberg, J. Opt. Soc. Am. B **8**, 1136 (1991).

[29] R. W. Boyd, M. G. Raymer, P. Narum, and D. J. Harter, Phys. Rev. A**24**, 411 (1981); G. S. Agarwal and R. W. Boyd, Phys. Rev. A**38**, 4019 (1988).

[30] G. S. Agarwal and W. Harshwardhan, Phys. Rev. A**50**, R4465 (1994).

[31] G. Algetta, A. Gozzini, L. Moi, and G. Orriols, Nuovo Cimento B **36**, 5 (1976).

[32] R. M. Whitley and C. R. Stroud, Phys. Rev. A**14**, 1498 (1976).

[33] H. R. Grey, R. M. Whitley, and C. R. Stroud, Opt. Lett. **3**, 218 (1978).

[34] P. L. Knight, M. A. Lauder, and B. J. dalton, Phys. Rep. **190**, 1 (1990); E. Arimondo, in *Progress in Optics* vol. XXXV, ed. E. Wolf (Elsvier, Amsterdam, 1996), p. 256.

[35] E. Arimondo and G. Orriols, Lett. Nuovo Cemento **17**, 333 (1976).

[36] J. D. Stettler, C. M. Bowden, N. M. Witrol, and J. H. Eberly, Phys. Lett. A **73**, 171 (1979).

[37] P. L. Knight, Comm. At. Mol. Phys. **15**, 193 (1984).

[38] I. V. Jyotsna and G. S. Agarwal, Phys. Rev. A**53**, 1690 (1996).

[39] J. R. Morris and B. W. Shore, Phys. Rev. A**27**, 906 (1983); V. S. Smirnov, A. M. Tumaikin, and V. I. Yudin, Sov. JETP **69**, 913 (1989).

[40] V. S. Smirnov, A. M. Tumaikin, and V. I. Yudin, Sov. Phys. JETP **69**, 913 (1989); V. Milner and Y. Prior, Phys. Rev. Lett.**80**, 940 (1998).

[41] F. Renzoni, A. Lindner, and E. Arimondo, Phys. Rev. A**60**, 450 (1999).

[42] W. Harshwardhan and G. S. Agarwal, Phys. Rev. A**53**, 1812 (1996).

[43] R. E. Tench, B. W. Peuse, P. R. Hemmer, J. E. thomas, S. Ezekiel, C. C. Leiby Jr., R. H. Picard, and C. R. Wills, J. Phys. Colloq. **42**, C8-45 (1981); J. E. thomas, P. R. Hemmer, S. Ezekiel, C. C. Leiby Jr., R. H. Picard, and C. R. Wills, Phys. Rev. Lett.**48**, 867 (1982).

[44] A. Aspect, E. Arimondo, R. Kaiser, N. Vensteenkiste, and C. Cohen-Tannoudji, Phys. Rev. Lett.**61**, 826 (1988).

[45] W. Harshawardhan and G. S. Agarwal, Phys. Rev. A **58**, 598 (1998).

[46] U. Fano, Phys. Rev. **124**, 1866 (1961); U. Fano and J. W. Cooper, Phys. Rev. **137**, 1364 (1965).

[47] K. J. Boller, A. Immamoğlu, and S. E. Harris, Phys. Rev. Lett.**66**, 2539 (1991); J. E. Field, K. H. Hann, and S. E. Harris, *ibid* **67**, 3062 (1991).

[48] G. S. Agarwal, Phys. Rev. A**55**, 2467 (1997).

[49] S. H. Autler and C. H. Townes, Phys. Rev. **100**, 707 (1955).

[50] J. H. Hertz, K. Koffman, W. Brunner, H. Paul, G. Ritcher, and H. Steudel, Phys. Lett. A **26**, 156 (1968).

[51] Y. Li and M. Xiao, Phys. Rev. A**51**, 4959 (1995).

[52] M. Xiao, Y. Li, S. Jin, and J. G. Banacloche, Phys. Rev. Lett.**74**, 666 (1995); J. G. Banacloche, Y. Li, S. Jin, and M. Xiao, Phys. Rev. A**51**, 576 (1995); Y. Li and M. Xiao, Phys. Rev. A**51**, R2730 (1995).

[53] R. R. Moseley, S. Shepherd, D. J. Fulton, B. D. Sinclair, and M. H. Dunn, Phys. Rev. Lett.**74**, 670 (1995); S. Shepherd, D. J. Fulton, and M. H. Dunn, Phys. Rev. A**54**, 5394 (1996).

[54] G. S. Agarwal, Phys. Rev. A**51**, R2711 (1995).

[55] S. E. Harris, Phys. Rev. Lett.**77**, 5357 (1996).

[56] S. A. Hopkin, E. Usadi, H. X. Chen, and A. V. Durrant, Opt. Commun. **138**, 185 (1997); A. V. Durrant, H. X. Chen, S. A. Hopkin, and J. A. Vaccaro, *ibid* **151**, 136 (1998).

[57] Y. Zhao, C. Wu, B. S. Han, M. S. Kim, and E. Awad, Phys. Rev. Lett.**79**, 641 (1997); B. S. Han and M. S. Shariar, Opt. Lett. **22**, 1138 (1997); K. Yamamoto, K. Ichimura, and N. Gemma, Phys. Rev. A**58**, 2460 (1998); K. Ichimura, K. Yamamoto, and N. Gemma, *ibid* **58**, 4116 (1998).

[58] D. J. Fulton, S. Shepherd, R. R. Moseley, B. D. Sinclair and M. H. Dunn, Phys. Rev. A**52**, 2302 (1995); J. R. Boon, E. Zekou, D. McGloin, and M. H. Dunn, Phys. Rev. A**59**, 4675 (1999).

[59] M. J. Werner and A. Imamoğlu, Phys. Rev. A**61**, R011801 (2000); C. L. Bentley Jr., J. Liu, Y. Liao, Phys. Rev. A**61**, 023811 (2000).

[60] E. A. Korsunsky, N. Leinfellner, A. Huss, S. Baluschev and L. windholz, Phys. Rev. A**59**, 2302 (1999).

[61] Y. Chen, C. Lin, and I. A. Yu, Phys. Rev. A**61**, 053805 (2000); D. McGloin, M. H. Dunn, and D. J. Fulton, Phys. Rev. A**62**, 053802 (2000).

[62] S. E. Harris, Phys. Rev. Lett.**70**, 552 (1993); R. Grobe, F. T. Hioe, and J. H. Eberly, Phys. Rev. Lett.**73**, 3183 (1994); and this idea is extended to quantum regime to show matching of photon statistics in G. S. Agarwal, Phys. Rev. Lett.**71**, 1351 (1993).

[63] A. Kasapi, Phys. Rev. Lett.**77**, 5357 (1996).

[64] H. Y. Ling, Y. Li, and M. Xiao, Phys. Rev. A**57**, 1338 (1998); M. Mitsunaga and N. Imoto, Phys. Rev. A**59**, 4773 (1999).

[65] G. S. Agarwal and W. Harshawardhan, Phys. Rev. Lett.**77**, 1039 (1996); this has been recently demonstrated experimentally: D. Wang, J. Y. Gao, J. H. Xu, G. C. La Rocca, and F. Bassani (*to be published*).

[66] S. E. Harris and Y. Yamamoto, Phys. Rev. Lett.**81**, 3611 (1998).

[67] M. Yan, E. G. Rickey, and Y. Zhu, (*to be published*).

[68] S. E. Harris, Phys. Today **50(7)**, 36 (1997); J. Marangos, J. Mod. Optics **45**, 471 (1998).

[69] O. Kocharovskaya and Ya. I. Khanin, Sov. Phys. JETP Lett. **48**, 630 (1988).

[70] S. E. Harris, Phys. Rev. Lett.**62**, 1033 (1989).

[71] A. Imamoğlu and S. E. Harris, Opt. Lett. **14**, 1344 (1989).

[72] M. O. Scully, S. -Y. Zhu, and A. Gavridiles, Phys. Rev. Lett.**62**, 2813 (1989).

[73] G. S. Agarwal, S. Ravi, and J. Cooper, Phys. Rev. A**41**, 4721 (1990); A. Imamoğlu, J. E. Field, and S. E. Harris, Phys. Rev. Lett.**66**, 1154 (1991);

[74] S. E. Fry, X. Li, D. Nikonov, G. G. Padmabandu, M. O. Scully, V. A. Smith, K. F. Tittel, C. Wang, R. S. Wilkinson, and S. -Y. Zhu, Phys. Rev. Lett.**70**, 3235 (1993); A. Nottelman, C. Peters, and W. Lange, Phys. Rev. Lett.**70**, 1783 (1993).

[75] A. S. Zibrov, M. D. Lukin, D. E. Nikonov, L. Hollberg, M. O. Scully, V. L. Velichansky, and H. G. Robinson, Phys. Rev. Lett.**75**, 1499 (1995).

[76] G. G. Padmabandu, G. R. Welch, I. N. Shubin, E. S. Fry, D. E. Nikonov, M. D. Lukin, and M. O. Scully, Phys. Rev. Lett.**76**, 2053 (1996).

[77] G. S. Agarwal, Phys. Rev. A**44**, R28 (1991).

[78] G. S. Agarwal, Phys. Rev. Lett.**67**, 980 (1991).

[79] S. Menon and G. S. Agarwal, Phys. Rev. A**59**, 740 (1999).

[80] O. Kocharovskaya, Phys. Rep. **219**, 175 (1992); P. Mandel, Contemporary Phys. **34**, 235 (1993).

[81] S. P. Tewari and G. S. Agarwal, Phys. Rev. Lett.**56**, 1811 (1986); *ibid* **66**, 1797 (1991).

[82] S. E. Harris, J. E. Field, and A. Imamoğlu, Phys. Rev. Lett.**64**, 1107 (1990).

[83] G. S. Agarwal and S. P. Tewari, Phys. Rev. Lett.**70**, 1417 (1993).

[84] K. Hakuta, L. Marmet, and B. P. Stoicheff, Phys. Rev. Lett.**66**, 596 (1991); Phys. Rev. A**45**, 5152 (1992).

[85] G. Z. Zhang, K. Hakuta, and B. P. Stoicheff, Phys. Rev. Lett.**71**, 3099 (1993); G. Z. Zhang, M. Kasturagwa, K. Hakuta, R.I. Thompson, and B. P. Stoicheff, Phys. Rev. A**52**, 1594 (1993).

[86] M. Jain, G. Y. Gin, and S. E. Harris, Opt. Lett. **18**, 998 (1993).

[87] M. Jain, H. Xia, G. Y. Yin, A. J. Merriam, and S. E. Harris, Phys. Rev. Lett.**77**, 4326 (1996); for a non-perturbative theory see: W. Harshwardhan and G. S. Agarwal, Phys. Rev. A**58**, 598 (1998).

[88] H. Schmidt and A. Imamoğlu, Opt. Lett. **21**, 1936 (1996).

[89] M. D. Lukin, P. R. Hemmer, M. Löffler, and M. O. Scully, Phys. Rev. Lett.**81**, 2675 (1998).

[90] M. O. Scully, Phys. Rev. Lett.**67**, 1855 (1991).

[91] A. S. Zibrov, M. D. Lukin, L. Hollberg, D. E. Nikonov, M. O. Scully, H. G. Robinson, L. V. Velichansky, Phys. Rev. Lett.**76**, 3935 (1996).

[92] S. E. Harris, Opt. Lett. **19**, 2018 (1994).

[93] O. A. Kocharovskaya, P. Mandel, and M. O. Scully, Phys. Rev. Lett.**74**, 2451 (1995); M. Löffler, D. E. Nikonov, O. A. Kocharovskaya, and M. O. Scully, Phys. Rev. A**56**, 5014 (1997).

[94] L.V. Hau, S. E. Harris, Z. Dutton and C. H. Behroozi, Nature (London) **397**, 549 (1999).

[95] M. M. Kash, V. A. Sautenkov, A. S. Zibrov, L. Hollberg, G. R. Welch, M. D. Lukin, Y. Rostovtev, E. S. Fry, and M. O. Scully, Phys. Rev. Lett.**82**, 5229 (1999).

[96] D. Budker, D. F. Kimball, S. M. Rochester, and V. V. Yashchuk, Phys. Rev. Lett.**83**, 1767 (1999).

[97] M. D. Lukin, S. F. Yelin, and M. Fleischhauer, Phys. Rev. Lett.**84**, 4232 (2000); M. Fleischhauer and M. D. Lukin, Phys. Rev. Lett.**84**, 5094 (2000).

[98] O. A. Kocharovskaya, Y. Rostovtsev and M. O. Scully, Phys. Rev. Lett.**86**, 621 (2000); Y. Rostovtsev and M. O. Scully, quant-ph/0001058.

[99] S. E. Harris and L. V. Hau, Phys. Rev. Lett.**82**, 4611 (1999).

[100] D. F. Phillips, A. Fleischhauer, A. Mair, R. Walsworth, and M. D. Lukin, Phys. Rev. Lett.**86**, 783 (2001).

[101] C. Liu, Z. Dutton, C. H. Behroozi, and L. V. Hau, Nature **409**, 490 (2001).

[102] S. Chu and S. Wong, Phys. Rev. Lett.**48**, 738 (1982); M. W. Mitchell and R. Y. Chiao, Am. J. Phys. **66**, 14 (1998).

[103] A. M. Steinberg and R. Y. Chiao, Phys. Rev. A**49**, 2017 (1994); E. Bolda, J. C. Garrison, and R. Y. Chiao, Phys. Rev. A**49**, 2938 (1994).

[104] L. J. Wang, A. Kuzmich, and A. Dogariu, Nature **406**, 277 (2000). A. Dogariu, A. Kuzmich, and L. J. Wang, physics/0012060 (to be published in Phys. Rev. A).

[105] M. Faraday, Phil. Trans. R. Soc. **XIX**, 1 (1846).

[106] D. A. Van Baak, Am. J. Phys. **64**, 724 (1996).

[107] D. S. Kliger, J. W. Lewis, and C. E. Randall, "*Polarized light in optics and spectroscopy*" (Academics Press, 1990).

[108] J-P Connerade, J. Phys. B **16**, 399 (1983); J-P Connerade, T. A. Stavrakas, and M. A. Baig, *Synchrotron Radiation Sources and their Applications*, ed. G. N. Greaves and I. H. Munro (Edinburgh: SUSSP Publications, Edinburgh University, 1989), p. 310; X. H. He and J-P Connerade, J. Phys. B **26**, L255 (1993).

[109] W. Gawlik, J. Kowalski, R. Neumann, H. B. weigemann, and K. Winkler, J. Phys. B **12**, 3873 (1979); X. Chen, V. L. Telegdi, and A. Weis, Opt. Commun. **74**, 301 (1990); E. Pfleghaar, J. Wurster, S. I. Kanorsky, and A. Weis, *ibid* **99**, 303 (1993); A. J. Wary, D. J. Heading, and J-P Connerade, J. Phys. B **27**, 2229 (1994).

[110] For extensive discussion on MOR and many interesting applications see: J-P. Connerade, *Highly Excited Atoms*, (Cambridge University Press, 1998).

[111] G. S. Agarwal, P. Anantha Lakshmi, J-P Connerade, and S. West, J. Phys. B **30**, 5971 (1997).

[112] P. Jungner, T. Fellman, B. Stahlberg, and M. Lindberg, Opt. Commun. **73**, 38 (1989); K. H. Drake and W. Lange, *ibid*, **66**, 315 (1988).

[113] P. Avan and C. Cohen-Tannoudji, J. Physique Lett. **36**, L85 (1975); S. Giraud-Cotton, V. P. Kaftandjian, and L. Klein, Phys. Rev A **32**, 2211 (1985); F. Schuller, M. J. D. MacPherson, and D. N. Stacey, Opt. Commun. **71**, 61 (1989).

[114] For a recent review of MOR with laser sources see: W. Gawlik, in "*Modern Nonlinear Optics*", ed. M. Evans, and S. Kielich, Advances in Chemical Physics Series vol. LXXXV, Part 3 (Wiley, New York, 1994).

[115] M. O. Scully and M. Fleischhhauer, Phys. Rev. Lett.**69**, 1360 (1992); Phys. Rev. A**49**, 1973 (1994); M. Fleischhhauer, A. B. Matsko, and M. O. Scully, Phys. Rev. A**62**, 013808 (2000).

[116] V. A. Sautenkov, M. D. Lukin, C. J. Bednar, I. Novikova, E. Mikhailov, M. Fleischhauer, V. L. Velichansky, G. R. Welch, and M. O. Scully, Phys. Rev. A **62**, 023810 (2000); I. Novikova, A. B. Matsko, V. A. Sautenkov, V. L. Velichansky, G. R. Welch, and M. O. Scully, Opt. Lett. **25**, 1651 (2000).

[117] D. Budker, V. Yashchuk, and M. Zolotorev, Phys. Rev. Lett. **81**, 5788 (1998); D. Budker, D. F. Kimball, S. M. Rochester, and V. V. Yashchuk, Phys. Rev. Lett.**85**, 2088 (2000); D. Budker, D. F. Kimball, S. M. Rochester, V. V. Yashchuk, and M. Zolotorev, Phys. Rev. A**62**, 043403 (2000).

[118] M. Yamamoto and S. Murayama, J. Opt. Soc. Am. **69**, 781 (1979).

[119] F. Schuller, R. B. Warrington, K. P. Zetie, M. J. D. Macpherson, and D. N. Stacey, Opt. Commn. **93**, 169 (1992).

[120] W. Harpper, Prog. Quantum Electron. **1**, 53 (1970).

[121] A. M. Bonch-Bruevich, N. N. Kostin, and V. A. Khodovoi, JETP Lett. **3**, 279 (1966).

[122] P. F. Liao and G. C. Bjorklund, Phys. Rev. Lett.**36**, 584 (1976); Phys. Rev. A**15**, 2009 (1977).

[123] C. Wieman and T. W. Hänsch, Phys. Rev. Lett.**36**, 1170 (1976); R. Teets, R. Feinberg, T. W. Hänsch and A. L. Schawlow, Phys. Rev. Lett.**37**, 683 (1976).

[124] Yu. Heller, V. F. Lukinykh, A. K. Popov, and V. V. Slabko, Phys. Lett. **82A**, 4 (1981); see also S. Cavalieri, M. Matera, F. S. Pavone, J. Zhang, P. Lambropoulos, and T. Nakajima, Phys. Rev. A**47**, 4219 (1993).

[125] B. Ståhlberg, P. Jungner, T. Fellman, K.-A. Suominen, and S. Stenholm, Opt. Commun. **77**, 147 (1990); K.-A. Suominen, S. Stenholm, B. Ståhlberg, J. Opt. Soc. America B **8**, 1899 (1991).

[126] F. S. Pavone, G. Bianchini, F. S. Cataliotti, T. W. Hänsch, M. Inguscio, Opt. Lett. **22**, 736 (1997).

[127] S. Wielandy and A. L. Gaeta, Phys. Rev. Lett. **81**, 3359 (1998).

[128] A. D. Cronin, R. B. Warrington, S. K. Lamoreaux, and E. N. Forston, Phys. Rev. Lett.**80**, 3719 (1998).

[129] A. K. Patnaik and G. S. Agarwal, Opt. Commun. **179**, 97 (2000).

[130] A. K. Patnaik and G. S. Agarwal, in *Frontiers of Laser Physics and Quantum Optics*, Eds. Z. Xu, S. Xie, S. -Y. Zhu, M. O. Scully (Springer-Verlag, Germany), pg. 403.

[131] A. K. Patnaik and G. S. Agarwal, Submitted to Phys. Rev. A.

[132] G. Vemuri and G. S. Agarwal, Phys. Rev. A**53**, 1060 (1996); G. Vemuri, G. S. Agarwal and B. D. N. Rao, *ibid*, 2842 (1996).

[133] W. Demtröder, *Laser Spectroscopy* (Springer, Berlin, 1986).

[134] M. Abbramowich and I. A. Stegun, *Hand Book of Mathematical Functions*, (Dover Publication, NY, 1972), pg. 279.

[135] R. H. Dicke, Phys. Rev. **93**, 99 (1954).

[136] L. Mandel and E. Wolf, *Optical Coherences and Quantum Optics*, Cambridge Univ. Press (1995).

[137] R. W. Zwanzing, in *Lectures in Theoretical Physics*, Vol.III, Ed. W. E. Brittin (John Wiley, New York, 1961).

[138] D. A. Cardimona, M. G. Raymer, and C. R. Stroud Jr., J. Phys. B **15**, 55 (1982).

[139] P. Zhou, and S. Swain, Phys. Rev. Lett. **77**, 3995 (1996); Phys. Rev. A **56**, 3011 (1997).

[140] S. Menon, and G. S. Agarwal, Phys. Rev. A **61**, 013807 (2000).

[141] S. Menon, and G. S. Agarwal, Phys. Rev. A **57**, 4014 (1998); J. Javanainen, Europhys. Lett. **17**, 407 (1992).

[142] A. Imamoğlu, Phys. Rev. A **40**, 2835 (1989).

[143] P. Zhou, and S. Swain, Phys. Rev. Lett. **78**, 832 (1997).

[144] E. Paspalakis, S. -Q. Gong, and P. L. Knight, Opt. Commun. **152**, 293 (1998); S. -Q. Gong, E. Paspalakis, and P. L. Knight, J. Mod. Opt. **45**, 2433 (1998).

[145] C. H. Keitel, Phys. Rev. Lett. **83**, 1307 (1999).

[146] G. C. Hegerfeldt, and M. B. Plenio, Phys. Rev. A **46**, 373 (1992); *ibid*, **47**, 2186 (1993); T. P. Altenmüller, Z. Physik D **34**, 157 (1995).

[147] A. K. Patnaik, and G. S. Agarwal, J. Mod. Opt. **45**, 2131 (1998).

[148] A. K. Patnaik, and G. S. Agarwal, Phys. Rev. A **59**, 3015 (1999).

[149] H. R. Xia, C. Y. Ye, and S. Y. Zhu, Phys. Rev. Lett. **77**, 1032 (1996); An intutive physical picture is given in: G. S. Agarwal, Phys. Rev. A **55**, 2457 (1997).

[150] S. Y. Zhu, R. C. F. Chan, and C. P. Lee, Phys. Rev. A **52**, 710 (1995); S. Y. Zhu, and M. O. Scully, Phys. Rev. Lett. **76**, 388 (1996); H. Lee, P. Polynkin, M. O. Scully, and S. Y. Zhu, Phys. Rev. A **55**, 4454 (1997); H. Huang, S. -Y. Zhu, and M. S. Zubairy, Phys. Rev. A **55**, 744 (1997); F. Li, S. -Y. Zhu, *ibid*, **59**, 2330 (1999).

[151] P. R. Berman, Phys. Rev. A **58**, 4886 (1998).

[152] M. A. G. Martinez, P. R. Herczfeld, C. Samuels, L. M. Narducci, and C. H. Keitel, Phys. Rev. A **55**, 4483 (1997).

[153] E. Paspalakis, and P. L. Knight, Phys. Rev. Lett. **81**, 293 (1998); E. Paspalakis, C. H. Keitel, and P. L. Knight, Phys. Rev. A **58**,

[154] H. Schmidt and A. Imamoğlu, Opt. Commun. **131**, 333 (1996)

[155] G. S. Agarwal, Phys. Rev. Lett. **84**, 5500 (2000).

[156] G. S. Agarwal and A. K. Patnaik, to be published in Phys. Rev. A(April, 2001).

[157] For an excellent review on the subject, see: M. Gross and S. Haroche, Phys. Rep. **93**, 303 (1982).

[158] R. G. DeVoe, and R. G. Brewer, Phys. Rev. Lett. **76**, 2049 (1996); the theory is discussed in: R. G. Brewer, Phys. Rev. Lett. **77**, 5153 (1996).

[159] P. Mataloni, E. De Angelis, and F. De Martini, Phys. Rev. Lett. P. Mataloni, E. De Angelis, and F. De Martini, Phys. Rev. Lett. **85**, 1420 (2000).

[160] G. V. Varda and G. S. Agarwal, Phys. Rev. A **45**, 6721 (1992).

[161] G. V. Varda and G. S. Agarwal, Phys. Rev. A **44**, 7626 (1991); D. F. V. James, Phys. Rev. A **47**, 1336 (1993).

[162] Two 2-level atoms inside cavity is considered in: G. S. Agarwal, and S. Dutta Gupta, Phys. Rev. A **57**, 667 (1998); excitation exchange between atoms (atomic separation $\leq \lambda/2$) giving rise to self interference of a single photon is discussed in: H. T. Dung and K. Ujihara, Phys. Rev. A **59**, 2524 (1999); Phys. Rev. Lett. 84, 254 (2000); energy exchange leading to modification in spontaneous emission in a mono-layer is reported in: P. T. Worthing, R. M. Amos, and W. L. Barnes, Phys. Rev. A **59**, 865 (1999).

[163] Z. Ficek, Phys. Rev. A **44**, 7759 (1991); Z. Ficek and R. Tanaś, Opt. Commun. **153**, 245 (1998).

[164] G. Kurizki, Phys. Rev. A **42**, 2915 (1990); S. John and T. Quang, Phys. Rev. A **52**, 4083 (1995); S. Bay, P. Lambropoulos, and K. Molmer, Opt. Commun. **132**, 257 (1996).

[165] G. M. Meyer, and G. Yeoman, Phys. Rev. Lett. **79**, 2650 (1997); G. Yeoman, and G. M. Meyer, Phys. Rev. A **58**, 2518 (1998); Similar situation in free space is discussed in T. Rudlph, and Z. Ficek, Phys. Rev. A **58**, 748 (1998).

[166] A. Beige and G. C. Hegerfeldt, Phys. Rev. A **59**, 2385 (1999); S. U. Addicks, A. Beige, M. Dakna, and G. C. Hegerfeldt, quant-ph/0002093 and references there in.

[167] G. Lenz and P. Meystre, Phys. Rev. A **48**, 3365 (1993); E. V. Goldstein P. Pax, and P. Meystre, Phys. Rev. A **53**, 2604 (1996); G. J. Yang, O. Zobay, and P. Meystre, Phys. Rev. A **59**, 4012 (1999);

[168] Static dd interaction has been important in earlier studies on collisional transfer of excitation from one atom to the other, e.g. see: W. R. Green, M. D. Wright, J. F. Young, and S. E. Harris, Phys. Rev. Lett. **43**, 120 (1979).

[169] M. E. Crenshaw, M. Scalora, and C. M. Bowden, Phys. Rev. Lett. **68**, 911 (1992); C. M. Bowden and J. P. Dowling, Phys. Rev. A **47**, 1247 (1993); M. E. Crenshaw and C. M. Bowden, Phys. Rev. Lett. **85**, 1851 (2000).

[170] M. Born and E. Wolf, *Principles of Optics, 7th Edition* (Cambridge University Press, 1999), Sec. 2.3.3.

[171] For an excellent review and references on theories and experiments on cavity induced changes of spontaneous emission, see S. Haroche, and D. Kleppner, Phys. Today **42**(1), 24 (1989). For more recent reviews on this subject, see J.J. Childs, Kyungwon An., R.R. Dasari, and M.S. Feld in "*Cavity Quantum Electrodynamics*", ed. P.R. Berman (Academic Press, 1993), p. 325.

[172] See the appendix in R.K. Bullough, Hyperfine Interaction **37**, 71 (1987).

[173] G.S. Agarwal, J. Opt. Soc. Am. B**2**, 480 (1985); H.I. Yoo and J.H. Eberly, Phys. Rep. **118**, 239 (1985).

[174] Y.R. Shen, *The Principles of Non-linear Optics*, (John Wiley & Sons, Inc., 1984), chap.13.

[175] M. O. Scully and M. S. Zubairy, *quantum Optics*, (Cambridge Univ. Press, Cabridge, 1996).

[176] B. M. Garraway, and P. L. Knight, Phys. Rev. A **54**, 3592 (1996).

[177] P. Zhou and S. Swain, Opt. Commun. **179**, 267 (2000); P. Zhou, S. Swain and L. You, quant-ph/0004001; see also G.-X. Li, Opt. Commun. **184**, 397 (2000).

[178] R. M. Herman, H. Grotch, R. Kornblith, and J. H. Eberly, Phys. Rev. A**11**, 1389 (1975).

[179] W. W. Chow, M. O. Scully, and J. O. Stoner Jr., Phys. Rev. A**11**, 1380 (1975); M. O. Scully, Phys. Rev. Lett.**55**, 2802 (1985).

[180] C. A. Kocher and E. D. Commins, Phys. Rev. Lett.**18**, 575 (1967); G. H. Nussbaum and F. M. Pipkin, *ibid.* **19**, 1089 (1967); C. A. Kocher, Ann. of Phys. (N.Y.) **65**, 1 (1971).

[181] A. Aspect, P. Grangier, and G. Roger, Phys. Rev. Lett.**47**, 460 (1981); P. Grangier, P., G. Roger, G., and A. Aspect, Europhys. Lett. **1**, 173 (1986); see also S. J. Freedman and J.

F. Clauser, Phys. Rev. Lett.**28**, 938 (1972); E.S. Fry and R. C. Thompson, *ibid.*, **37**, 465 (1976).

[182] H. Huang and J. H. Eberly, J. Mod. Optics **40**, 915 (1993).

[183] G. M. Meyer, G. S. Agarwal, H. Huang, and M. O. Scully, '*Electron Theory and Quantum Electrodynamics - 100 years later*", edited by J. P. Dowling (Plennum Press, 1997)

[184] H. Huang and G. S. Agarwal, J. Mod. Optics **42**, 465 (1995); M. O. Scully, U. W. Rathe, C. Su, and G. S. Agarwal, Opt. Commun. **136**, 39 (1997).

[185] M. Lax, Phys. Rev. **172**, 350 (1968).

List of Publications

I. Papers in Journals and Books:

1. *Laser-field-induced quantum beats in correlations in cascade emission*, Anil K. Patnaik and G. S. Agarwal, J. Mod. Opt. **45**, 2131-2138 (1998).

2. *Cavity-induced coherence effects in spontaneous emissions from preselection of polarization*, Anil K. Patnaik and G. S. Agarwal, Phys. Rev. A **59**, 3015-3020 (1999).

3. *Laser Field Induced Birefringence and Enhancement of Magneto-Optical Rotation*, Anil K. Patnaik and G. S. Agarwal, Opt. Commun. **179**, 195-211 (2000).

4. *Controlling Magneto Optical Rotation via Quantum Coherences*, Anil K. Patnaik and G. S. Agarwal, in Frontiers of Laser Physics and Quantum Optics, Eds. Z. Xu, S. Xie, S.-Y. Zhu, M. O. Scully, pp. 403-407, (Springer, Berlin, 2000).

5. *Vacuum Induced Coherences in Radiatively Coupled Multilevel Systems*, G. S. Agarwal and Anil K. Patnaik, Phys. Rev. A **63**, 043805 (2001).

6. *Coherent control of Magneto-optical Rotation*, Anil K. Patnaik and G. S. Agarwal, Submitted to Phys. Rev. A.

II. In Proceedings/Abstracts of International and National Conferences:

1. *Laser field induced quantum beats in two photon correlations*, Anil K. Patnaik, Pg. 210, Proc. National Laser Symposium 1997, held at Physical Research Laboratory, Ahmedabad (India), 10-12 December (1997).

2. *Quantum coherence: source of beat in photon correlations*, Anil K. Patnaik, Pg. 25, Abstracts of Seminar on Physics with Cooled and Trapped atoms and Ions 1998, held at Bhabha Atomic Research Center, Mumbai (India), 5-6 March (1998).

3. *Quantum coherences from polarization pre-selection of cavity vacuum*, Anil K. Patnaik, Pg. 86, Proc. National Laser Symposium 1998, held at Indian Institute of Technology, Kanpur (India), 14-16 December (1998).

4. *Controlling magneto optical rotation via quantum coherences*, Anil K. Patnaik and G. S. Agarwal, in Proc. International Conference on Laser Physics and Quantum Optics 1999, held at Shanghai (China), 25-28 August (1999).

5. *Field Induced Anisotropy and Magneto Optical Switch*, Anil K. Patnaik, Proc. National Laser Symposium 1999, held at University of Hydrabad (India), 15-17 December (1999).

6. *Coherent Control of Birefringence*, Anil K. Patnaik and G. S. Agarwal, QThD 79, Proc. Inetrnational Quantum Electronic Conference (CLEO/Europe-IQEC 2000), held at Nice (France), 10-15 September (2000).

7. *Vacuum Induced Coherences in Radiatively Coupled Multilevel Systems*, G. S. Agarwal and Anil K. Patnaik, Pg. 47, Proc. International Conference on Perspectives in Theoretical Physics, held at Physical Research Laboratory, Ahmedabad (India), 8-12 January (2001).